

## Επιστημονικό Υπόβαθρο

---

Παραδοτέο 3.2 (έκδοση 1.0)

31/5/2018



# Literature Review on Smart Water Technologies

## 1 Introduction

### 1.1 Water Distribution Challenges

Water distribution systems are faced with a number of challenges, such as aging infrastructures, decreased water resources, population growth, reduced financial capabilities and lack of investment, climate change, extreme events, as well as pollution and contamination events due to accidents and malicious attacks. Due to the water-energy-food nexus [1], when the quantity and quality of water is disrupted, this can have a cascading effect on the food chain, on energy production as well as on health.

The drinking water industry is highly decentralized; for instance, in the USA, where there are more than 150,000 public water systems serving more than 300 million consumers. Aging infrastructure is a challenge for these utilities; the USA Environmental Protection Agency (EPA) estimated that, for the period 2011–2030, more than \$380 billion will be invested for infrastructure improvement [2]. As a consequence of having aging infrastructure, is the increase of hydraulic failures such as leakages, pipe bursts, malfunctioning valves and pumps. In addition, quality failures can occur, e.g. due to malfunctions in the disinfection system or due to the infiltration of contaminants from pipe cracks and joints. These failures can downgrade the water supply quantity and quality and can cause serious problems in health, safety and security, local economy, as well as in the operation of society [3].

To add an economic perspective, the cost of water which lost worldwide due to leakages, metering errors and non-billed consumption, was estimated at \$15 billion per year [4]; every day it is estimated that more than 45 million m<sup>3</sup> of treated water is lost due to leakages in developing countries, which could have served 200 million consumers, and in addition, almost 30 million m<sup>3</sup> is consumed but not billed [4].

Maintaining water quality within the regulations specified by the World Health Organization (WHO) [5], the European Commission [6], or the U.S. Environmental Protection Agency (EPA) [7], is an important challenge faced by water utilities which supply water to consumers through drinking water distribution networks. However, guaranteeing a high level of water quality, continuously, is not an easy task, as faults may occur in the system which affect quality. For instance, where hydraulic faults may downgrade the water delivery service, they may cause quality faults. These quality faults, which may be due to the injection of certain chemical, biological or radioactive substance within the water, will travel along the flow of water, and depending on the substance, it may cause significant damage.

In most of the world, disinfectants such as chlorine are used in prescribed concentrations to maintain the drinking water quality, by preventing bacteria growth and neutralizing chemical agents [8]. According to the WHO, a free chlorine residual concentration must exist in drinking water distribution systems, with minimum target concentration 0.2  $\frac{mg}{L}$  at the point of delivery and 0.5  $\frac{mg}{L}$  for high-risk circumstances [5]. It is common practice to supply water with a few tenths of a milligram per litre of chlorine residual.

In most countries, by law, water providers are required to control and monitor water quality and hydraulic states, to guarantee the delivery of adequate disinfected water to all consumers. To satisfy this, water providers collect hydraulic and quality data at various locations in the network (either manually or by using sensors) and control the system appropriately through a series of hydraulic and quality actuators. Through this, water providers are able to detect faults related to the hydraulic dynamics (pressures, flows) or quality dynamics (such as disinfectant and contaminant concentration).

Hydraulic faults, such as leakages, pipe bursts, malfunctioning pumps and valves, may interrupt water consumption or may deteriorate water quality, due to contaminant infiltration in the system. Most frequently, water contamination faults in water distribution systems are due to natural or accidental events. When accidental contamination failures occur, these can have a dramatic effect on the society. For instance, in Milwaukee (USA) in 1993, a large-scale contamination event occurred which was caused due to a problem in the water filtration. This triggered an outbreak of cryptosporidiosis infecting 403,000 consumers of which 4,400 were hospitalized and in addition, 50 deaths were associated with the event [9]. Another example was in Nokia (Finland), in November 2007, 450 m<sup>3</sup> of waste-water were injected by accident into the town's water distribution system, causing an outbreak of gastroenteritis. As a result, thousands were infected, hundreds were hospitalized, and the authorities imposed a complete ban on all water usage for 12 weeks [10]. As shown in Figure 1, simulation modeling of the event demonstrated that the contamination affected a significant part of the city [11]). Another large-scale contamination event was in West Virginia (USA), in 2014, in which an industrial solvent, contaminated 15% of the drinking water, affecting more than 300,000 consumers; the incidence was declared by U.S. President Obama as a "federal disaster" [12].

To provide a high-quality of service, modern water utilities have established monitoring and control processes. For monitoring, utility operators may use sensors installed within the water distribution system, as well as manual sampling with utility employees, to determine the occurrence of events which may affect the normal operation of the system. By controlling the system actuators (such as pumps, valves), water utilities are able to supply sufficient quantity of water of good quality to consumers, while maintaining low pressures in order to reduce background leakages, reduce energy usage as well as reconfigure the system appropriately when an event occurs in order to reduce its impact. For example, Pressure Reduction Valves (PRV) are typically installed in the DMA inflow pipes in order to regulate and reduce the pressure within the DMA [13]. Furthermore, utility operators need to determinate the inputs to the hydraulic actuators (valves and pumps) as well as to the quality actuators (e.g. chlorine booster disinfection), in order to maximize efficiency and improve the system safety. They also need to estimate the quantity of water which will be demanded by the consumers, and take all appropriate actions to guarantee the continuous supply of drinking water. Moreover, utilities must make long-term planning ahead, to guarantee that the appropriate infrastructure is in place, in parallel with the development of the urban environment.

Due to their vital role in the society and the economy, water systems are considered as critical infrastructures [14], along with power and telecommunications systems. Various terrorist and criminal threats or attacks on water infrastructures has been recorded in the last decades [15], and some of the most notable cases are provided below:

- In 1976, a biologist in Germany threatened to contaminate water supplies with Anthrax, unless he was paid \$8.5 million.
- In 1984, followers of the Indian guru Rajneeshee contaminated water and food supplies with biological agents in The Dalles, Oregon, USA, to serve their political agenda. The followers gained access to the town's water system maps, and tried to inject contaminants to water tanks [16].

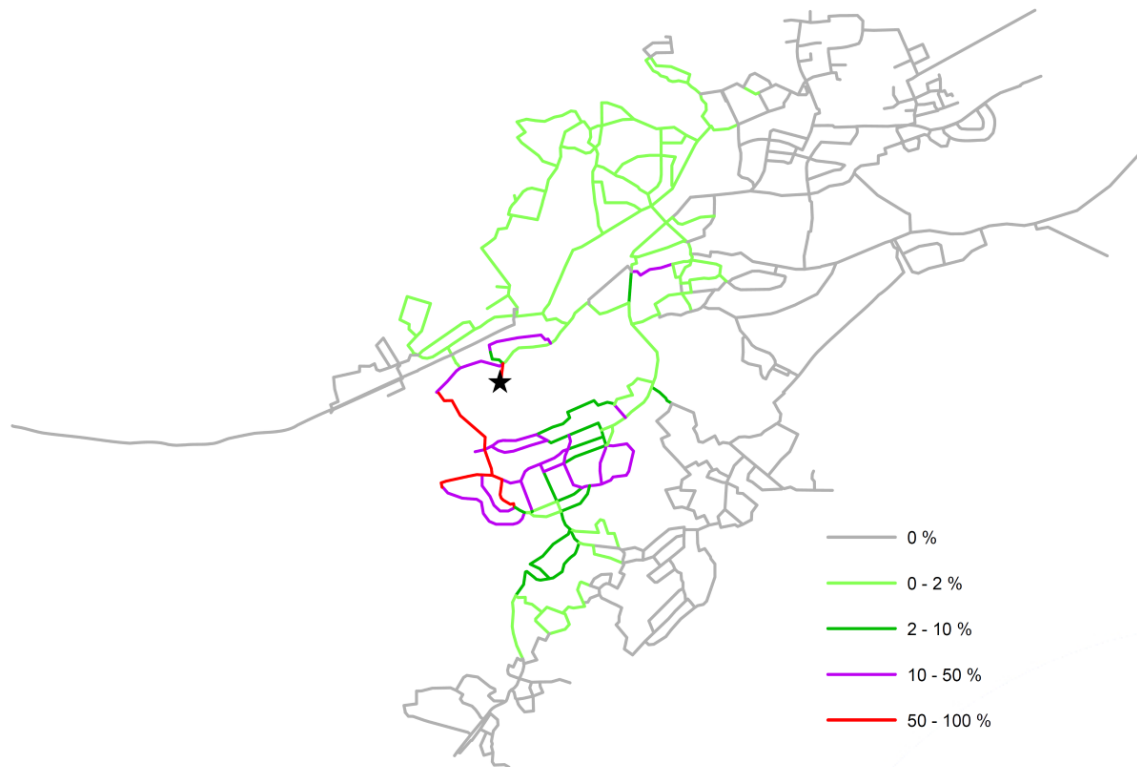


Figure 1: Simulated extend of contamination event in Nokia, Finland (29 November 2007, 21:00). The injection point of the contaminant is indicated with a star. The pipe color corresponds to the estimated percentage of waste-water in each pipe for that specific time instance.

- In 2000, a cyber-attack on a waste-water management system in Queensland, Australia, caused the release of millions of sewage to parks and contaminated rivers.
- In 2003, the Al-Qaida called for the poisoning of drinking water in American and Western cities.

A rising challenge in water utilities is security of their cyber-physical elements [17]. For instance, utilities may use sensors and actuators which are connected to the internet, or are connected to elements which may be connected to the internet. These elements may be exposed to malicious attacks, such as unauthorized actuator control as well as creating fake sensor measurements. In addition to these, the rise of cyber-attacks on industrial systems, as it was in the case of Stuxnet, could cause a number of attacks (denial-of-service, eavesdropping and deception) which may deteriorate the operation or even cause system failure.

## 1.2 ICT for water management

Water utilities, in their effort to improve management of their systems, are exploring the use of new methodologies and technologies, which will allow them to reduce energy usage and water loss. For instance, water utilities can monitor their water distribution system using *Supervisory Control And Data Acquisition* (SCADA) systems, gathering measurements from sensors installed throughout

the system, and controlling actuators [18]. In addition to automated SCADA system operations, a number of monitoring and control events may still be conducted manually, such as the collection of water samples for laboratory analysis, or the manual closing/opening of a valve, at various locations and times. In addition, water utilities may utilize *Geographic Information Systems* (GIS) for modelling the network structure, and may maintain databases with consumer, laboratory and maintenance reports. Furthermore, hydraulic models of the system may be available for simulating the behavior of the system under various conditions.

Typically water utilities monitor the minimum night flow in different parts of their network, such as in *District Metered Areas* (DMA) (i.e. a sub-network of which the water inflow is measured), and trained operators compare these minimum night-flow measurement with historical data, to determine the occurrence of leakages[19].

Currently, a number of water utilities explore the use of wireless metering technologies, such as *Automatic Metered Readers* (AMR) and *Advanced Metering Infrastructure* (AMI), for measuring water consumption and communicating this information to the water utility. At the moment, AMRs and AMIs are promoted mainly for real-time billing purposes, as well as and for alerting consumers when their consumption increases significantly. However, these technologies can be further exploited to address future needs, such as real-time state-estimation, water demand management, water loss management, forecasting, event management and others [20].

In addition to periodic consumer demands collected for billing purposes, water utilities may monitor various sensors measuring water quality and hydraulics, as well as various types of information such as alarms, battery voltage levels, server and telephone-center logs, which produce a large volume of data which is growing as time passes. For some applications, such as control or event detection, this information should be available locally and in real-time, whereas in other cases, this information should be stored for further analysis or for billing purposes.

### 1.3 Towards Smart Water Networks

The potential of using information and communication technologies, as well as monitoring and control technologies, for water management, has cultivated the vision of *Smart Water Networks* [21, 22], in analogy to the *Smart Grid* concept advocated for Power Systems [23, 24]. Smart Water Network (SWN) is a general term which describes the envisioned new generation of water distribution networks, building upon the state of art in information, communication, sensing, control technologies and research results, in order to improve the efficiency, reliability and security of the system, allowing self-monitoring and self-healing. These systems will be able to acquire and process large volume of data from within the water network, as well as from external sources, analyze the information and automate a significant part of monitoring and control, while achieving the operational requirements involving energy efficiency and operational costs. Sensor measurements and models will be linked and software/hardware can be used to process their measurements in order to achieve different objectives.

In specific, sensors installed in the system can measure hydraulic parameters such as water-levels in tanks, flows and pressures, while other sensors can measure quality parameters such as disinfection residuals, pH, temperature, conductivity[25].

Sensors in SWNs will vary in cost and accuracy, may measure general characteristics (e.g. ORP, Free Chlorine) or specific contaminants using biosensors, they may have external ownership (e.g. consumer-owned), and may have minimal energy requirements (e.g. using energy harvesting).

Smart water utilities will also be able to integrate the database measurements with other available heterogeneous data, in order to extract new and useful knowledge. For instance, consumer reports through the call centers and through the social media, as well as measurements from *Internet-of-Things* (IoT) devices, could be integrated with event detection algorithms to determine the existence of an abnormal system status.

The large volume of heterogeneous data produced during the operation of a SWN, either from sensors or from models, originating from within the network or from outside the network, may be described as “Big Data”, and can be analyzed using big-data architectures and distributed algorithms [26, 27]. The key idea of big-data processing is that it is not feasible or efficient to process and analyze these data on a single computational unit, but rather to employ scalable solutions by exploiting the synergy of parallel and distributed computing, distributed databases, as well as parallel and distributed algorithms. Therefore, a challenge for the water industry is how to process (with respect to the available hardware) and analyze (with respect to the available algorithms) the large volume of data produced during the operation of a water system.

A definition which summarizes the SWN, as described in this book, is the following: *Smart Water Networks* refers to the use of sensing and communication technologies, along with intelligent algorithms for modelling, simulation, control, optimization and big-data analytics, for the purpose of enhancing efficiency and improving security, reliability, resilience, quality and robustness of drinking water distribution systems, as well as to minimize the impact of unforeseen events.

## 1.4 The SmartWater2020 Project

Around 15-25% of the drinking water in Europe flowing through the water networks is lost and is not priced due to leaks, thefts and damages. This entails a huge financial cost to water distribution organizations. This phenomenon has a particular impact on islands of the Mediterranean, such as Cyprus and Crete, due to water scarcity and high desalination costs. The project *SmartWater2020*, “Intelligent Water Distribution Networks for Reducing Loss”, is being funded by the INTERREG V-A “Greece-Cyprus 2014-2020” Cooperation Programme to develop smart technologies capable of helping water authorities in Crete (Greece) and Cyprus, to improve their water distribution system’s monitoring and control capabilities which in turn can help reduce water losses.

The project activities involve the installation of innovative technologies such as sensors, valves, and meters in water supply systems, their interconnection with an innovative smart water monitoring software for early detection of leakage and water quality problems, as well as the development of a pioneering pressure control system to reduce water losses.

As part of the project, a thorough needs assessment was conducted in order to extract the needs the industrial organizations participating in the SmartWater2020 project: the Water Board of Limassol (Cyprus), the Water Board of Larnaca (Cyprus), the Municipal Water Supply and Sewerage Company Malevizi (Greece) and the Water Development Department, Ministry of Agriculture, Rural Development and Environment (Cyprus). Based on the survey conducted among the partners, the following smart water case studies have been identified to be investigated within the scope of the project:

- Reduction of telemetry cost: this involves the use of innovative algorithmic tools for compressing and reconstructing big volumes of streaming data, as well as the experimentation with long-range and short-range wireless communication technologies.
- Improve ability in detecting and isolating leakages: this involves the use of pressure sensors and hydraulic models, in order to detect whether water pressures are outside the expected bounds, along with advanced algorithms for the uncertainty-aware detection and localization of extreme events.
- Enhance capabilities in estimating water quality conditions within the network: This involves the integration of water quality sensors with state estimators, in order to estimate quality parameters in areas which are not monitored by sensors.

- Reduce background leakages through pressure control: This involves solving the optimization and control problem of deciding the most appropriate valve settings in order to reduce the overall and worst-case pressures within the DMAs.
- Automated topology mapping through mobile sensors: This involves the experimental design of a mobile sensor which will propagate within a testbed in order to map its unknown or partially known structure.

## 1.5 Structure of report

This report presents the key enabling algorithmic methodologies and industrial technologies towards building efficient SWNs, while being aligned with the objectives of the SmartWater2020 project. The report is organized as follows:

- Section 2 introduces the innovative networking and communication technologies to be exploited by our proposed SWN, including both short-range and long-range technologies.
- Section 3 explores well-established software tools that are used for water distribution modelling and simulation, covering the EPANET ecosystem and beyond.
- Section 4 is described data acquisition and processing methods. Specifically, introduces the ways to manage and analyze data produced by the sensors or the models of the networks.
- Section 5 presents several approaches for early extreme, leakage and quality detection of events that can be occur at any phase and time of the SWN infrastructure's operation.
- Section 6 explores state estimation and control in water distribution networks by presenting: leakage risk estimation as a proactive managements strategy, hydraulic and quality dynamics, and quality and pressure controls.
- Section 7 presents the discussion and concluding remarks of the report.

## 2 Networking & Communication Technologies

The realization of smart water networks relies on heterogeneous network architectures that interconnect the physical space (e.g., water distribution network) with the operational center for supporting all respective decision making processes. A typical architecture for such a network backbone is presented in Fig. 2, highlighting different types of connectivity and roles in the network; sensor nodes deployed within the field of interest, network server for collecting and processing water-relevant data towards dedicated services (e.g. water network administration, on-site inspection, and water model data extraction), and gateways which act as the communication bridges between the sensor nodes and the network server. Sensor nodes can exchange communication for

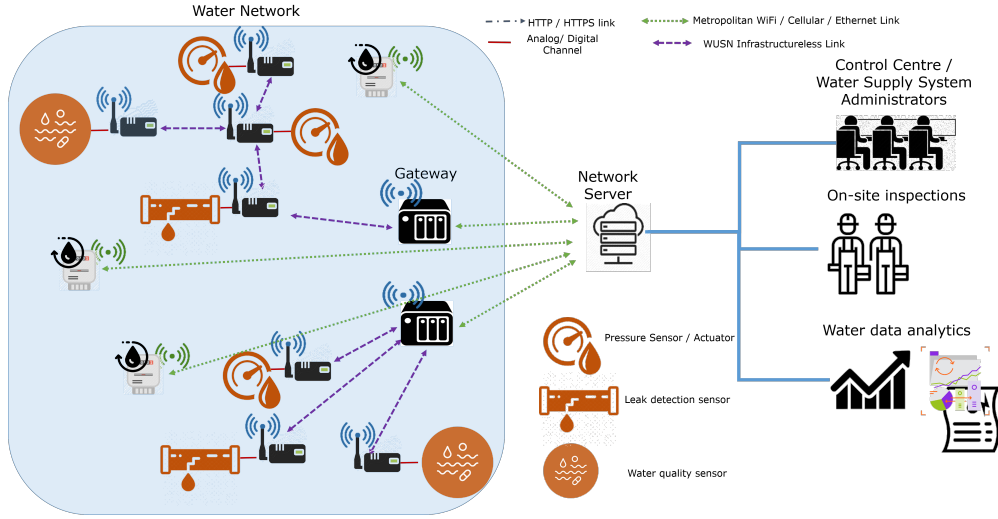


Figure 2: The network architecture for realizing smart water networks.

network management and data relaying through underground links, while the data collected on the gateways can in turn be collected through underground-to-aboveground communication links. The architecture additionally considers command and control information originated from the network server/gateways to the sensor nodes. Considering this heterogeneous architecture, in the following paragraphs we will elaborate on the communication challenges for underground environments and the enabling wireless technologies that can serve as the backbone for interconnecting the water network infrastructure.

### 2.1 Communication challenges in underground environments

Despite its potential advantages EM-based underground communication is challenged by numerous issues, which are not typically met in conventional, over-the-air deployments. Ambient and environmental aspects, such as temperature, weather, moisture, burial depth have often a profound impact on the connectivity of the network.

The key factor for defining the characteristics of the EM-based underground channel is the propagation medium, i.e. soil or air. Specifically, when the deployment considers soil as the main propagation medium (e.g., on the outer surface of a water pipeline) the path loss behaviour is dictated by [28]:

- the soil categorization (i.e. topsoil, referring to the first 30cm of soil, or subsoil, referring to the 30-100cm region);

- the volumetric water content (VWC), defined as the quantity of water in the soil, depending both on the spatial (i.e. deployment region) as well as temporal (i.e., season) characteristics;
- the texture of the soil, dictated by the portion of air, bound water, free water and bulk soil;

The co-existence of these environmental factors signifies EM large-scale propagation phenomena. Specifically, EM-waves encounter much higher attenuation in soil compared to air, with a direct impact on the effective transmission range; for instance theoretical and empirical studies indicate that when the 2.4GHz frequency is employed the transmission range does not exceed 0.5m. In addition, depending on the soil categorization (topsoil or subsoil) the ground surface may cause reflective EM-waves, with positive or negative effects on the communication. Typically, the respective communication channel adopts the principles of a two-path model, wherein reflection effects offer constructive interference, while the existence of unpredictable obstacles (e.g., rocks) cause EM waves to refract and scatter, thereby introducing multi-path fading in the communication channel. The temporal behavior of the soil-based EM underground communication can be captured by the properties of a Rayleigh distribution, considering that each path in the underground channel is Rayleigh distributed and that the envelope of the signal from each path is modeled as an independent Rayleigh distributed random variable.

The use of EM-based communications for underground monitoring is complemented by over-the-air ad-hoc, and infrastructure-based networks. In these architectures, two additional types of links than underground-to-underground links (UG2UG) are formulated, namely: (a) aboveground-to-underground (AG2UG), and (b) underground-to-aboveground (UG2AG). Empirical studies [29, 30] on the performance of the resulting heterogeneous networks considering a relatively small depth (< 40cm) indicate that both AG2UG and UG2GA links are highly unsymmetrical, due to the soil-air/air-soil interface and the multi-path effects from the soil surface. In addition, a variation of  $\sim 30\%$  in the VWC level can cause a degradation of  $\sim 70\%$  and  $80\%$  for UG2AG and AG2UG links, respectively, thereby highlighting that the varying temporal characteristics (in terms of seasonal and geospatial attributes) affect profoundly the UG2AG and AG2UG links. Notably, in terms of connectivity [31, 32], these behavioral attributes in AG2UG, UG2AG, and UG2UG links result into different levels of transmission range for each channel type.

Shifting towards underground deployments using the air as the propagation medium (e.g., within water pipes, or manholes for water and wastewater facilities), the EM-based communications face in general less challenges than the soil-based communications. Even so, the propagation characteristics of EM waves are significantly different from those of the terrestrial wireless channels, due to the restrictions caused by the structures of the underground facilities. Depending on whether the type of deployment is within a tunnel- of a room-and-pillar type of environment, two respective channel models can be adopted [33, 34]: (a) the multi-mode model, which can completely characterize natural wave propagation in both near and far regions of the source for the tunnel environment, and (b) the multi-mode model combined with the shadow fading model for the room-and-pillar environment. Different operational parameters (e.g., frequency, size of infrastructure, relative positioning of transceivers) have different impact on each channel type. Table 1 enlists the empirical observations made for each channel type (tunnel or room-and-pillar).

The discussion thus far highlights that the environment typically met in water infrastructures is far from ideal for EM-based communications. Nevertheless, the advent of wireless sensors capable of realizing the backbone of smart water networks would not be possible without the essential low-power transceivers that allow short- or long-range communication and data transmission at low and moderate rates. In the following paragraphs we provide an overview of both short- and long-range enabling EM-based communication technologies, with a dedicated emphasis on the respective wireless standards.

Table 1: The impact of different parameters on the tunnel and room-and-pillar environment for EM-based underground communications.

	Operational Frequency	Size of Room / Tunnel	Antenna Position	Electrical Parameters
Tunnel	As frequency increases the signal attenuation decreases $\Rightarrow$ the length of the fast fluctuating region is increased	Larger tunnels prolong fast fluctuating region • Wide-low tunnel: the horizontal polarized antenna is preferred $\longleftrightarrow$ Narrow-high tunnel: the vertical polarized antenna is preferred	TX antenna placed near the tunnel center: position of RX antenna does not affect the signal (significant attenuation's of RX power) $\longleftrightarrow$ TX antenna placed near the tunnel walls: small attenuation if RX antenna is placed at center, significant attenuation if RX antenna is placed near walls	Electrical parameters of tunnel air can be considered the same as those of normal air $\Rightarrow$ no influence on signal propagation
Room-and-pillar	Similar effects as in the tunnel environment with smaller influence. Nevertheless, compared to tunnel environments, extra multipath fading is caused by the pillars $\Rightarrow$ higher path loss is experienced by the waves spreading in the room.			

## 2.2 Short-range Enabling Technologies

The de-facto enabling technology for short-range wireless communications is the IEEE standard for Low-Rate Personal Area Networks (IEEE 802.15.4) [35], extensively employed for numerous Wireless Sensor Networks applications, ranging from environmental and structural health monitoring, to health care, industrial automation, and, more recently, Smart City scenarios. From the perspective of the OSI reference model, IEEE 802.15.4 specifies the PHY and MAC layers, defining among others the topology and network roles for WSN; the operational ranges of frequency and respective spectrum handling, modulation, and bit rate; the operational modes at the MAC sub-layer including timing aspects; the interactions between different layers and different nodes (service primitives).

Specifically, depending on the national and international spectrum regulations, IEEE 802.15.4 defines 6 operational frequency bands: (a) 868 MHz (Europe), (b) 915 MHz (USA), (c) 779 MHz (China), (d) 950 MHz (Japan), (e) 2.4 GHz world-wide, (f) UWB, both in sub-GHz and 3-10 GHz. Depending on the operational frequency the spread spectrum technique is also defined, ranging from Direct Sequence Spread Spectrum (DSSS) to Parallel Sequence Spread Spectrum (PSSS) and Chirp Spread Spectrum (CSS). Figure 3 summarizes the technical characteristics of the resulting PHY specifications [36].

Band (MHz)	Region	Number of Channels	Modulation	Data Rate (Kbps)	Support
868 - 868.6	Europe	1	BPSK	20	<b>Mandatory</b>
			ASK	250	Optional
			O-QPSK	100	
779-787	China	8	MPSK	250	<b>Mandatory</b>
			P-QPSK		
902 - 928	USA	10	BPSK	40	<b>Mandatory</b>
			ASK	250	Optional
			O-QPSK	100	
950-956	Japan	22	BSPK	20	<b>Mandatory</b>
			GFSK	100	
2400 - 2483.5	Worldwide	16	<b>O-QPSK (DSSS)</b>	250	<b>Mandatory</b>
		14	CSS		1000
249.6 - 749.6 (UWB sub-GHz)	Worldwide	1	BPM and BPSK	110 – 27400 (Varying w.r.t. chip rate)	Optional
3244 - 4724 (UWB low band)		4	BPM and BPSK	110 – 27400 (Varying w.r.t. chip rate)	Optional
5944 - 10234 (UWB high band)		11	BPM and BPSK	110 – 27400 (Varying w.r.t. chip rate)	Optional

Figure 3: The IEEE 802.15.4 specifications for the PHY layer (adapted from [36]).

The standard additionally defines two types of network topologies, namely star and peer-to-peer. Star topologies have one *PAN coordinator*, and define the many-to-one communication pattern. On the other hand, peer-to-peer topologies dictate the many-to-many communication mode and as such support more than one PAN coordinators. The role of the PAN coordinator is to act as primary controller of the network, by controlling the association of nodes as well as initiating, terminating, or routing communications. In addition, to allow for very low-cost low-complexity devices, IEEE 802.15.4 defines Reduced Function Device (RFD) and Full Function Device (FFD). RFDs implement

a subset of the IEEE 802.15.4-defined primitives and cannot act as coordinator. FFDs have a full implementation of IEEE 802.15.4 and can adopt any role in the network.

The MAC specification for the IEEE 802.15.4 defines the topology construction by the means of passive / active channel scanning and energy detection; the association / de-association of the devices to a specific network; the synchronization of all devices to network beacons, whenever applicable. Driven by the diversity of the application scenarios, the MAC specification provides two main operational modes: (a) non-beacon enabled, (b) beacon-enabled. The non-beacon enabled mode employs the CSMA /CA mechanism for accessing the channel, while all devices operating within the network are treated as peers. Operation over the beacon-enabled mode relies on the network synchronization, which is dictated by the coordinator, in the form of periodic beacon transmissions, defining the beacon intervals. Within a beacon interval during the super-frame interval 4 nodes can either compete for accessing the channel (slotted CSMA / CA) or to transmit their data in a contention-free manner, using pre-allocated Guaranteed Time Slots (GTS).

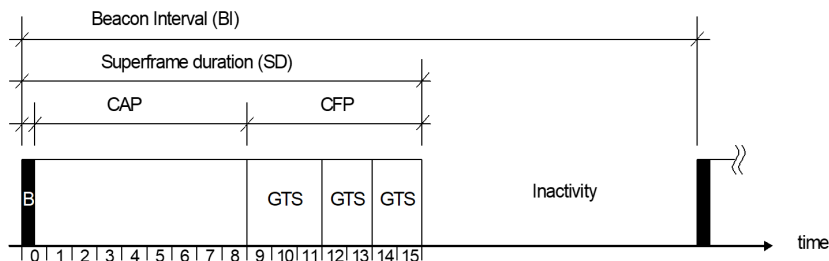


Figure 4: The structure of the IEEE 802.15.4 beacon interval [36].

Driven by its wide adoption, the standardization body of IEEE 802.15.4 has issued 5 major amendments (Table 2), either for further specifying PHY regulations or providing alternative MAC architectures. With regard to the smart water management arena, those of greater interest are

Table 2: The amendments of the IEEE 802.15.4 standard

Amendment	Release Date	Characteristics
IEEE 802.15.4a	2007	PHY Layer Extension to Chirp Spectrum Techniques and UWB systems
IEEE 802.15.4c	2009	Alternative PHY Extension to support one or more of the Chinese 314-316 MHz, 430-434 MHz, and 779-787 MHz bands
IEEE 802.15.4d	2009	Alternative PHY Layer Extension to support the Japanese 950 MHz Bands
IEEE 802.15.4e	2012	MAC sub-Layer amendment to address CSMA-CA unreliability
IEEE 802.15.4f	2012	Active Radio Frequency Identification (RFID) System PHY

IEEE802.15.4a and IEEE802.15.e. Specifically, IEEE802.15.4a [37] defines an extension for the PHY layer towards both Ultra-Wide Band (UWB) and Chirp Spread Spectrum (CSS) systems at the 2.4GHz ISM band, for addressing challenges associated to high-precision ranging capability, thereby targeting sensing and location mapping services over mobile/static sensors (e.g., leak or pollution detection using mobile sensors) [38]. While the UWB PHY specification is suitable for limited-range (< 10 m) communications at increased throughput (up to 27Mbps), the CSS PHY

specification is ideal for applications with more relaxed data rates demands (up to 1Mbps) at longer distances (500 m in open air). Considering in addition the robustness of CSS against disturbances such as noise and multipath fading, the IEEE 802.15.4a CSS PHY specification and respective products (e.g., Fig. 5) could provide an alternative for the communication backbone of smart water networks in at data rates that exceed the nominal speed of 250Kbps.



Figure 5: CSS PHY radio module by Nanotron Technologies® [39].

The IEEE 802.15.4e [40] features functional improvements for the MAC layer associated CSMA/CA limitations, such as unbounded delays, limited communication reliability, and no protection against interference/fading, thereby better supporting industrial applications [41]. Briefly, the IEEE802.15.4e considers five new MAC behavior schemes (Table 3) intended for various applications, ranging from tracking, large scale deployments, and process automation. Out of these MAC modes, the Time Slotted Channel Hopping (TSCH) has rapidly gained popularity for industrial applications, as it provides increased network capacity (multi-channel and channel hopping), high reliability, and predictable latency (time-slotted access). In a nutshell, TSCH exploits the number of available channels (e.g., 16 for a typical IEEE802.15.4 PHY Layer at 2.4GHz / DSSS) for representing a link between two communicating devices by a couple specifying the timeslot in the slotframe and the channel offset used by the devices in that timeslot. Therefore, the frequency  $f$  used for communication in the timeslot is expressed as a function  $F$  of the total number of timeslots elapsed since the start of the network, and the number of available channels. Notably, function  $F$  can be implemented as a lookup table. In addition, TSCH allows the existence of shared links, accessible by more than one transmitter. To reduce the possibility of repeated collisions over shared links, the standard defines a re-transmission back-off algorithm, which exploits the principles of the CSMA-CA mechanism.

**Expandability towards upper layers for industrial applications.** Due to its structural design, IEEE802.15.4 and its amendments have been extensively employed as the basis of integrated industrial network standards, including among others ISA100.11a, WirelessHART® [42], and, more recently, 6TiSCH by the Internet Engineering Task Force (IETF) [43].

This has been primarily powered by the design and integration of the 6LoWPAN, an IETF standard which enables the adoption of IPv6 addressing and respective functionalities over low-power, constrained-memory, IEEE 802.15.4 platforms [44]. Essentially, the 6LoWPAN allows long IPv6 packets (up to 1280 bytes) to fit into short IEEE 802.15.4 frames (at most 127 bytes). To this end, 6LoWPAN disregards sophisticated IPv6 functions to generate less complicated IPv6 functionality, while additionally considers two mechanisms, namely: (a) the compression of the IP headers, (b) the fragmentation and reassembly, so that multiple IEEE802.15.4 packets can make a complete IPv6 packet. The compression is based on stripping the IP packet headers to the absolute minimum (Fig. 6), while the fragmentation and reassembly additionally considers the routing mechanism; in case of mesh-under routing, fragments are reassembled at their final destination only, while in the case of route-over networks data packets are reassembled at every hop. Despite its usefulness, fragmentation essentially introduces additional overhead both within the network and each sensor node responsible for fragmenting/reassembling packets. Therefore, *practical guidelines on the use of 6LoWPAN indicate that small-sized payloads and the use of*

Table 3: The MAC modes of IEEE 802.15.4e standard

Mode	Key characteristics	Applications
Radio Frequency Identification Blink (BLINK)	Minimal frame containing ID • Association is not required • Aloha contention mechanism	Item and people identification, location, and tracking
Asynchronous multi-channel adaptation (AMCA)	Asynchronous multi-channel adaptation • Non-beacon enabled networks	Large-scale deployments for process automation/control, infrastructure monitoring
Deterministic and Synchronous Multi-channel Extension (DSME)	Extending number of GTS • Grouping multiple superframes together • Multi-channel operation • Beacon-enabled mode	Industrial and commercial applications with hard real-time and reliability requirements
Low Latency Deterministic Network (LLDN)	Star topology • Short data packets & superframes • Multi-channel operation and slotted CSMA-CA between FFDs • Grouped Acknowledgment	Factory automation & robotics with low latency requirements
Time Slotted Channel Hopping (TSCH)	Time-slotted access with multi-channel and channel hopping • Well suited for multi-hop peer-to-peer topology	Process automation incl. water/waste water treatments

header compression are essential for preserving an energy conservative industrial network.

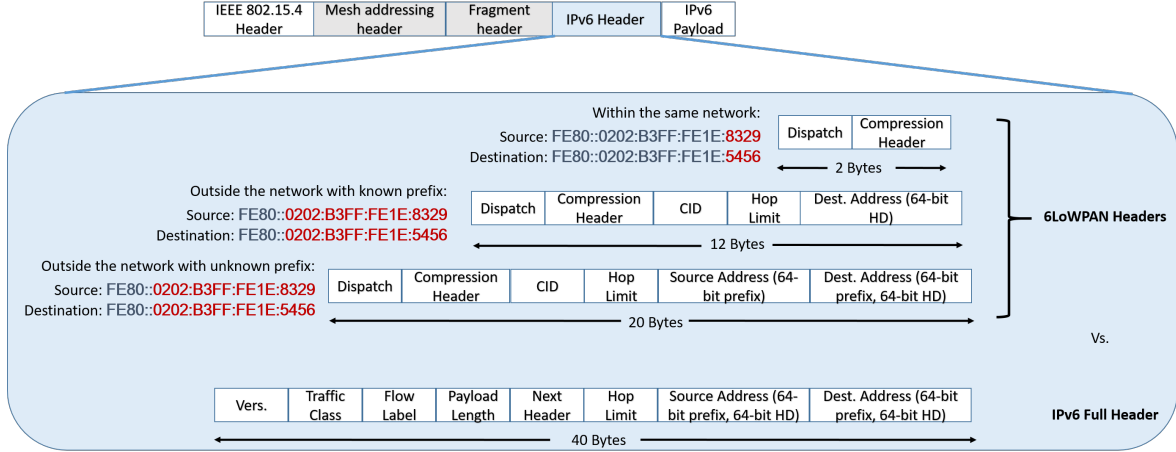


Figure 6: The IEEE802.15.4 frame format including 6LoWPAN compressed headers. The mesh networking and fragment header are only used in case of multi-hop topologies and packet fragmentation, respectively.

The 6LoWPAN has been employed as part of the ISA100.11a (2009) standard for the design of centralized networks, based on star, star-mesh, and mesh topologies. ISA100.11a relies on the IEEE802.15.4 PHY, while for the MAC layer it employs the TSCH mechanism. Routing capabilities are optional, while the standard provides flexible network implementation by allowing to optimize the stack parameters, at the expense of interoperability issues; in essence, ISA 100.11a promotes proprietary, non-interoperable designs in the specification, while implementation options are not fully specified (e.g., application interface for process control protocols)[45]. A counterpart of ISA100.11a is WirelessHART®, relies on the IEEE802.15.4/e, without the support of 6LoWPAN[42]. Much like ISA100.11a, WirelessHART yields a centralized network, providing the ability of creating scalable networks by the interconnection of multiple access points. Data transmissions are based on the combination of time division multiple access (TDMA) with channel hopping, thereby alleviating interference effects. In contrast to ISA100.11a, WirelessHart ensures the interoperability of the standard with previous and future releases of the HART protocol.

WirelessHART has been a field proven technology, which is however limited by its IPv6 incompatibility. To address this shortcoming, and additionally enable Internet connectivity for wireless, low-cost and computationally-constrained sensor- and actuator-enabled devices in industrial process monitoring and control applications, IETF proposed in 2013 the 6TiSCH integrated industrial protocol stack. 6TiSCH is the latest generation of protocols exploiting TSCH technology and considers an integrated protocol stack (Fig. 7(a)) [46, 43], which incorporates the IEEE802.15.4e TSCH, IETF 6LoWPAN [47], RPL [48], and CoAP [49]. Specifically, the IETF 6top Protocol [50], addresses the existing link scheduling limitations of the IEEE802.15.4e, by the means of defining a distributed scheduling policy. This policy allows neighbor nodes to negotiate for adding or removing “cells”, defined by the combination of available frequencies and the duration of network scheduling operation. The IEFTRPL Protocol is the IPv6 routing protocol for low-power wireless networks. RPL supports many-to-one traffic and it is suitable for a network topology where all information needs to reach a single destination (root). As such, RPL organizes the sensor/actuator nodes into a Destination Oriented Acyclic Graph (DODAG) (Fig. 8-top), which is essentially a tree

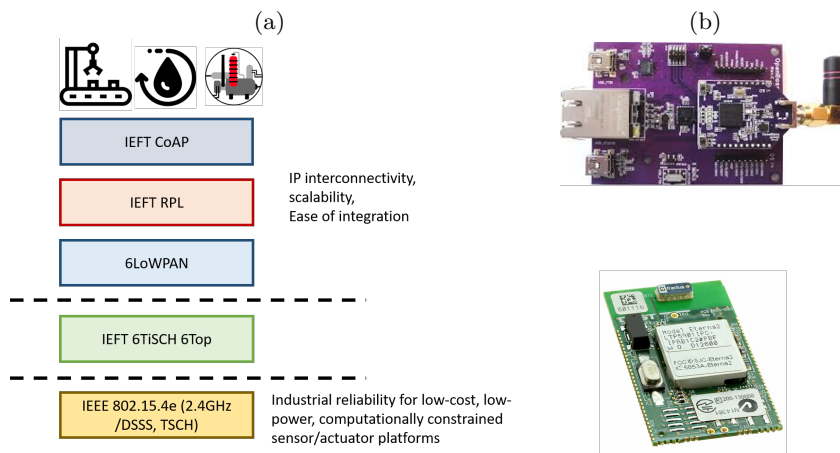


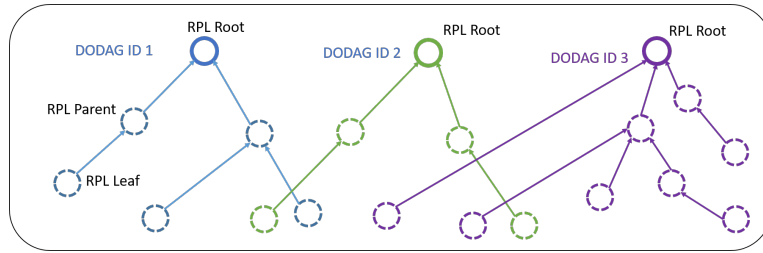
Figure 7: (a) The 6TiSCH protocol stack (adapted from [46, 43]), (b) 6TiSCH enabling modules: OpenMote<sup>TM</sup> (top), Analog Devices SmartIP<sup>TM</sup> (bottom).

routing topology, manifested by (a) the IPv6 address of the root, (b) the objective function defining the routing decisions, i.e. defining the next hop/parent towards the root node. The flexibility of RPL is based on the selection of the objective function for selecting the parent, and while the IEF standard defines both node- and link-metrics (Fig. 8-bottom), it also allows for network designers to define customized objective functions, e.g. [51, 52]. Ultimately, the IEF Constrained Application Protocol (CoAP), enables web-like interactions over low-power wireless devices, which can act both like a web-server and a web-browser. CoAP enables RESTful interactions with individual nodes, without the overhead of TCP and verbose nature of HTTP. Instead, it consists of a 4-byte header on top of UDP. As such, a CoAP-enabled node can publish its sensor readings onto a server on the Internet.

### 2.3 Long-range Technologies

Short range communications and respective industrial protocol stacks can be extremely beneficial in numerous applications, since they combine ease of deployment and low power consumption. Nevertheless, their adoption at larger scales is limited by their communication range. As a consequence, despite being more expensive, conventional cellular networks (e.g., GSM, GPRS, UMTS, LTE) are often employed to provide connectivity at large-scale industrial deployments (e.g., telemetry systems for water supply networks). Even so, these technologies are designed for traditional broadband services characterized by increased bandwidth demands, instead of low-rate, or even event-based data transmission of sensor readings.

These limitations on both short-range technologies and cellular networks have been the driving force for a new class of Low-Power, Wide-Area Networks (LPWAN). Typically, LPWAN complement short-range technologies in terms of infrastructure-less networks, and inherit the basic aspects of legacy cellular systems architecture (e.g., star topology) while stripping at the same time its most advanced features (e.g., user mobility and resources scheduling). Notably, while typically operating at the ISM unlicensed band, LPWAN can achieve expanded network connectivity that reaches 10-15km in rural areas and 2-5km in urban areas, at the expense of low data rates that do not exceed the magnitude of Kbps [53]. In all cases, the principle of increasing the communication range relies on the increase of the link budget, or equivalently, the signal-to-noise ratio (SNR) at the receiver.



RPL Objective Function Metrics		Node	Link / Network
IEFT Standard Defined	Hop Count	x	
	Node state & attributes objects (node workload)	x	
	Node energy object	x	
	Expected number of transmissions (ETX) per hop or over the entire route		x
	Link Quality Indicator		x
	Latency (maximum or over the entire route)		x
	Throughput		x
Customized	Expected longevity (energy of nodes and ETX)	x	x
	Stability index w.r.t. to routing tree attributes and maintenance		x
	Path loss metrics		x
	R-metric (reliability w.r.t. to successful packet reception at MAC sublayer)		x
	Q-metric (forward load balancing and power consumption during TX & RX)	x	

Figure 8: Top: The RPL Destination-Oriented Directed Acyclic Graphs. Depending on the address of the root node and the objective function, different RPL topologies can co-exist within the same area. Bottom: IEF/T standard and customized metrics for the RPL objective function.

The widely adopted spectrum handling techniques adopted to this end are either Spread Spectrum (SS) or Ultra-Narrow-Band (UNB). Briefly, SS techniques spread the energy of the signal over a wide band which effectively reduces the spectral power density of the signal, while Ultra-Narrow-Band UNB employs a narrow channel width to attain higher receiver sensitivity, which in turn increases the range achievable at the expense of reducing the achievable data rate [54].

Networks compliant to LWPAN are often based on proprietary solutions at the PHY and/or the MAC layer, resulting into enabling technologies linked with commercial vendors such as SIGFOX®, Ingenu®, and SemTech®. Specifically, the SIGFOX technology is a representative mature LPWAN proprietary technology with wide adoption in industrial applications, including the domain of smart water meters (e.g., Fig. 9-top). SIGFOX devices employ UNB wireless modulation at the Sub-GHz ISM band (868MHz in Europe, 902 in US), and unslotted ALOHA for accessing the transmission medium from the MAC sub-layer. In SIGFOX networks, nodes are organized into star topology, wherein the device initiates a transmission by sending three up-link packages in sequence on three random carrier frequencies. The base station will successful receive the package even if two of the transmissions are lost. SIGFOX networks are characterized by extremely low data rates (in the order to a 100bps) and payload length (12 bytes). Ingenu [55] offers a competitive LPWAN technology, featuring operation at the 2.4GHz band, hence offering worldwide availability, while employing Direct Sequence Spread Spectrum. As a result, Ingenu-based devices (e.g., Fig. 9-bottom) achieve data rates that reach up to 31Kbps. The Ingenu-based networks leverage the Random Phase Multiple Access RPMA® [56], which exploits a proprietary scheme based on Time Division Multiple Access for improving the achieved capacity in unscheduled (e.g., event-based) small data payloads.



Figure 9: SIGFOX® and Ingenu-RPMA® LPWAN commercial devices. Top: SIGFOX® : (a) The SIGFOX LPWA radio module, (b) Kamstrup’s MULTICAL® 21 smart water meter with SIGFOX communication, (c) smart digital inputs reader for remote meter control with special flat antenna for installation into manholes. Bottom: Ingenu-RPMA® : (d) The u-blox® radio module implementing the Ingenu LPWAN technology, (e) the KONWPT-N7 for water pressure monitoring featuring the Ingenu LPWAN technology, (f) the SG111 LPWAN RF Datalogger, a rugged battery powered industrial logger for smart water meter data routing, logging, alarm monitoring with Ingenu LPWAN technology.

In 2012 SemTech® introduced the LoRA™ technology, which leverages on CSS and GFSK modulation for long-range connectivity in different regions of the Sub-GHz ISM band (433/868Mz for Europe, 915MHz for US, and 430MHz for Australia). Much like SIGFOX, LoRA uses duty cycled transmissions, thereby limiting its data rates within 0.3Kbps-37.5Kbps, while achieving communication range of up to 15km in rural areas and 5 km in urban areas. One of the key characteristics of LoRA is the ability to use different combinations of essential PHY parameters (bandwidth, spreading factor<sup>1</sup>, coding rate<sup>2</sup>, and transmission power) for optimizing modulation, and thereby meeting the essential range and data requirements. The resulting configuration modes lead to different levels of sensitivity at the side of the receiver (e.g., Fig. 10, [57]), and thereby, offering different communication range and data rates. While the nominal transmission range of LoRA in urban and rural areas is extended in the order of km, independent empirical studies ([58, 59] and [60]) on the performance of LoRA technology in underground environments (specifically aired manholes with metallic lid) highlight the impact of the environment on the effective communication range achieved. Specifically, Kartakis et. al [58, 59], report that in experiments with the Welsh water supply networks, the actual transmission range varies between 315m (Mode 1 of Libellium® radio module) to 40m (Mode 10 Libellium® radio module), while *reliable communication (i.e., Packet Reception Ratio > 90%) is achievable at communication range  $\simeq 160m$* . Along similar lines, Cattani

<sup>1</sup>Spreading Factor: The number of chips utilized for the transmission by the SS mechanism. Typical values for LoRA  $\in \{2^6, \dots, 2^{12}\}$

<sup>2</sup>Error detection/correction mechanism, according to which the transmitter generates  $n$  bits of data for every  $m$  bits of useful information. Typical values for LoRA  $\in \{4/5, \dots, 4/8\}$

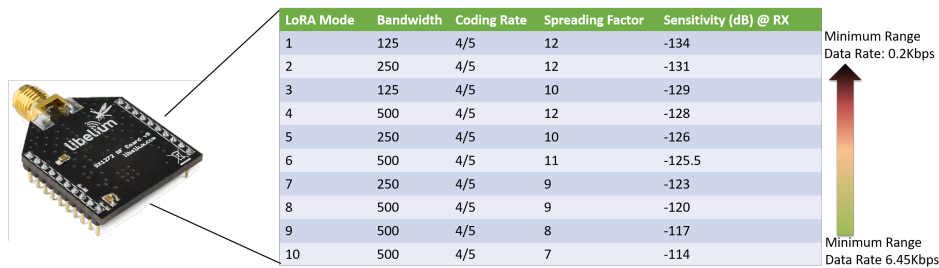


Figure 10: The LoRA™ radio module (868MHz) by Libellium® along with the re-configurable combinations of bandwidth, spreading factor, and coding rates, leading to different communication modes (adapted from [57]).

et. al [60] suggest that when nodes are at the edge of their communication range, using the fastest PHY setting and the highest transmission power is more efficient than selecting slower settings that maximize the link quality. Remaining key empirical observations for LoRA technology are summarized in Table 4.

While LoRA technology has been subject of extensive studies such the aforementioned, it has also been basis for the formulation of the LoRA Alliance™ [63], comprised of big industrial players in the arena of the Internet of Things (e.g., IBM, Microchip, Semtech), which in 2015, defined the LoRAWAN specification, an open protocol stack to support the proprietary PHY [64]. The LoRAWAN specification essentially defines the logical architecture of LoRA compliant networks; the different classes of LoRA end nodes; the respective types of data/control frames and frames formats; the rules for enabling symmetric cryptography across the LoRAWAN-compliant network. Briefly, LoRAWAN exploits the ALOHA MAC protocol for the access of the propagation medium. With regard to the logical architecture, the specification defines a star-of-stars topology, according to which the end devices are connected via a single-hop LoRa link to one or many gateways that, in turn, are connected to a common network server (NetServer) via standard IP protocols (Fig. 11(a)). The gateways are responsible for relaying messages between and the NetServer, while the end devices may associate to more than one gateways to get access to the network. To this end, each gateway can support up to nine LoRa channels, where each channel is defined by the combination of a specific sub-band and level of spreading factor. In addition to the topology, LoRAWAN specification categorizes the end devices, into three categories, namely Class A (*All*), Class B (*Beacon*), and Class C (*Continuously Listening*) (Fig. 12). Specifically, Class A devices allow for bi-directional communications, according to which, each uplink transmission is followed by two short optional, low-priority downlink receive windows, employing the ALOHA MAC rules. This Class A operation is the lowest power end-device system for applications that only require downlink communication from the server shortly after the end-device has sent an uplink transmission (e.g., monitoring and optional remote parameters reconfiguration). End-devices of Class B build on top of the functionality of Class A for opening extra receive windows at scheduled times, based on time synchronized beacon from the gateway (e.g., monitoring, and event-based actuation). Ultimately, end-devices in Class C are characterized by continuously open downlink communication with the NetServer, which is only deactivated during uplink communications. Class C end-devices offer more sophisticated options for downlink communication (e.g., periodic, high-priority actuation) at lower end-to-end latency and the expense of increased energy consumption.

While LoRA/LoRAWAN has started gaining wide adoption for providing industrial solutions in unlicensed bands, including water quality monitoring, e.g. Fig. 13, the 3rd Generation Partnership Project (3GPP) [65] published in 2016 the Narrow Band-Internet of Things (NB-IoT) standard,

Table 4: Summary of PHY settings and parameters for LoRA and their impact on communication performance (adapted from [59, 60, 61, 62]).

Parameter	Effects
Bandwidth	Higher bandwidths allow for transmitting packets at higher data rates (1kHz = 1kbps) but reduce receiver sensitivity and communication range
Spreading Factor	Big spreading factors increase the signal-to-noise ratio sensitivity, augmenting the communication range at the cost of longer packets and hence a higher energy expenditure.
Coding Rate	Larger coding rates increase the resilience to interference bursts and decoding errors at the cost of longer packets and a higher energy expenditure.
Transmission Power	Higher transmission powers reduce the signal-to-noise ratio at the cost of an increase in the energy consumption of the transmitter.
Payload size	The communication modules perform more reliably (i.e. up to 70%) with smaller packet/payload sizes (i.e. up to 10 bytes). Large amounts of transmitted data (e.g. more than 1MB) may lead to high energy consumption due to the long transmission time $\Rightarrow$ The split of information into relatively small chunks is necessary.
Duty cycle regulations for the ISM band	Small duty cycle (e.g. 1% for 868MHz band) combined with large spreading factor leads to enlarged over-the-air transmission time (e.g., 36 s/h) and thus longer off-period duration per LoRA node.
PHY setting (combination of bandwidth, spreading factor, coding rate)	At the edge of the communication range, using the fastest PHY setting and the highest transmission power is more efficient (in terms of data rate and power consumption) than selecting slower settings that maximize the link quality • The static predetermination of the PHY settings limits the scalability of the LoRA network ( $\sim$ 120 nodes per gateway in a Smart City scenario [61]).
Scalability & payload size	For small payload size (e.g., 10bytes) an increase of the network scale (e.g., 250 $\rightarrow$ 5000 nodes) leads to a decrease in the maximum throughput per node (e.g., 3670bytes/hour $\rightarrow$ 180bytes per hour) [62].

offering long-range coverage at the commercial bands of the EM spectrum. NB-IoT is an evolution of the LTE system and as such, it is operating at 832-862MHz for the downlink, 890-915MHz for the uplink. NB-IoT is not compatible with 3G but can coexist with GSM, GPRS and LTE, and can be supported with only a software upgrade on top of existing LTE infrastructure [54]. This line of technology for LPWAN aims at enabling deployment flexibility, long battery life, low device cost and complexity and signal coverage extension, which theoretically can support up to 50,000 end devices per cellular cell [66]. The reduction in cost and energy consumption is attempted by the means of reducing the data rate and bandwidth requirements, while simplifying the protocol design and mobility support. Notably, for a 164 dB coupling loss<sup>3</sup>, an NB-IoT based radio can

<sup>3</sup>Coupling loss: The loss that occurs when energy is transferred from one circuit, circuit element, or medium to another

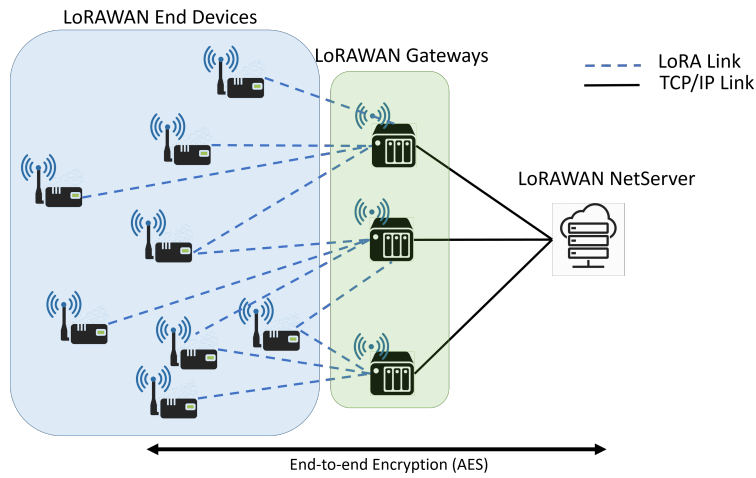


Figure 11: The LoRAWAN star-of-stars network topology.

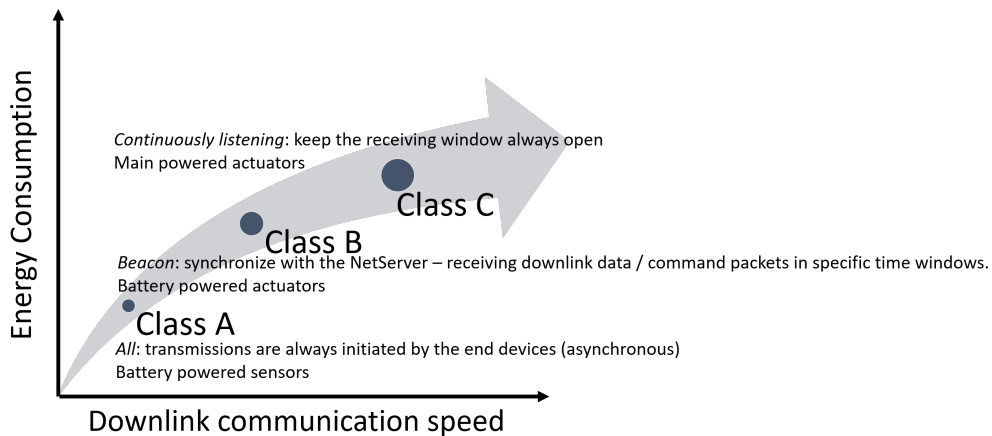


Figure 12: The LoRAWAN categorization of end nodes into Classes A, B, and C.

achieve a battery life of 10 years when transmitting 200 bytes of data per day on average. Opposed to LoRA/LoRAWAN, which considers a simplified protocol stack (Fig. 14(a)), the protocol stack defined for NB-IoT is designed as a new air interface for LTE [67] (Fig. 14(b)). Briefly, the protocol structure has been divided into control plane and user plane, while dedicated emphasis is given on defining the detailed mechanisms for L2-layer operations. For the control plane, the NB-IoT protocol stack considers a dedicated layer (Non-access Stratum, NAS) for authentication, security control, mobility management, and bearer management.

NB-IoT takes both advantages of 4G/5G technology (e.g., mobility, peak rate, and user experienced data transmission rate) as well as the low-power, low data-rate principles of LPWA. Empirical studies on the coverage capacity of SIGFOX, LoRA, and NB-IoT [68] also suggest that while SIGFOX (LoRA) exhibits optimized performance compared to LoRA (SIGFOX) in uplink (downlink)



Figure 13: The Libellium® smart sater end-node, implementing the LoRAWAN specification for monitoring water quality parameters.

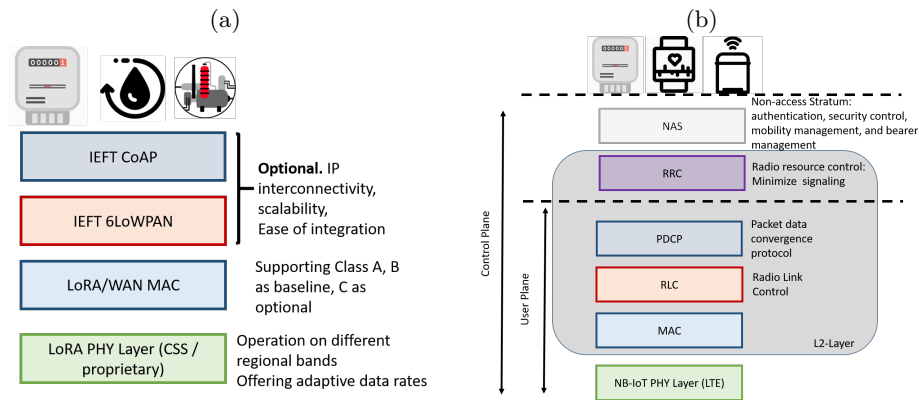


Figure 14: (a) The LoRAWAN protocol stack. (b) The NB-IoT protocol stack (adapted from [67]).

communication, NB-IoT outperforms these two technologies, having an 95%-tile uplink failure probability of less than 4%. These kind of studies, along with the easy of interoperability with mobile telephony operators (e.g., Vodafone ®) over LTE networks have been the driving force for a new line of NB-IoT radio modules employed in smart metering solutions (e.g., Fig. 15) for providing innovative solutions in the smart water arena<sup>4</sup>. Even so, the most important criticism against NB-IoT is associated to: (a) the cost of operating in licensed bands, which eventually increases the cost of the end-product, (b) the inability of NB-IoT to realize IoT applications that require acknowledging of all uplink data traffic unless the application implements some form of reliability mechanisms, thereby introducing increased application complexity and higher energy consumption. Figure 16 summarizes all key specifications and considerations for dominating LPWA technologies.

## 2.4 Industrial Applications

The discussion thus far highlights the potential of both short- and long-range wireless technologies for realizing the vision of smart water networks in a low-cost and easy-to-deploy fashion. Related

<sup>4</sup>[https://www.metering.com/industry-sectors/data\\_analytics/nb-iot-kamstrup-vodafone/](https://www.metering.com/industry-sectors/data_analytics/nb-iot-kamstrup-vodafone/) Kamstrup and Vodafone achieve 98% smart meter accuracy in NB-IOT pilot. Last accessed: June 2018.



Figure 15: The u-blox<sup>®</sup> radio module for NB-IoT (left), and the NUmeter<sup>™</sup> ultrasonic meter with fully integrated NB-IoT by Water Group PTY<sup>®</sup> (right).

research and engineering efforts indeed fully or partially employ the technologies outlined in the previous sections for addressing different aspects of smart water networks, ranging from leakage detection, to water quality monitoring and industrial treatment. In the following paragraphs we provide a brief overview representative practical works which has been actually deployed in relevant environments.

**Short Range Communications.** Stoianov et al. [69], pioneered this field of research by the means of Pipenet, which is considered one of the first underground platforms for leak detection in water distribution pipelines. The scope of this Pipenet was to collect hydraulic and acoustic/vibration data at high sampling rates and provide the essential algorithmic toolkit for leakage detection and isolation. From a network perspective, the project featured sensor nodes operating at 2.4GHz /Frequency Hopping SS (Bluetooth protocol) and a GPRS-data relaying mechanism to centralized hosts for performing leak detection. The monitoring system was deployed in Boston, MA, US in collaboration with Boston Water and Sewer Commission and it has been continuously operating for an extensive period (at least 12 months) in the form of small-scale field studies. Similarly, the authors in [70] designed and developed a multimodal Wireless Underground Sensor Network, featuring a customized IEEE 802.15.4-compliant platform for pipeline structural health monitoring. The emphasis was on non-invasive methods for monitoring the pressure of the water pipelines, based on Force Sensitive Resistor (FSR) technology. The platform has been tested and validated in laboratory and field trials, while emphasizing among others on the power consumption. EARNPIPE (2016) [71], is a more recent representative prototype in the arena of leakage detection and localization based short-range (IEEE802.15.4) technologies, coupled with Predictive Kalman Filter. Notably EARNPIPE invests on a clustering routing architecture for minimizing the power consumption over the network, combined with a decentralized architecture for detecting leaks over the heads of the network clusters. Shifting towards mobile architectures, TropiusNet [72] is a IEEE802.15.4-compliant prototype for autonomous pipeline monitoring. The novelty of TropiusNet relies on the automated in-field deployment and replacement of mobile sensors by releasing them from the water inlet, while leveraging both natural water flow propulsion inside pipes to carry sensor nodes, as well as coverage and connectivity algorithms for the final location of each released sensor node. As more sensor nodes are released and deployed, the system gradually builds an interconnected wireless sensor network covering the entire pipeline.

The use of short-range enabling technologies in the smart water arena has also been employed for industrial water treatment [73, 74] and sewage systems [75, 76]. Specifically, the authors in [73, 74] have designed and developed an integrated network platform based on the combination of IEEE802.15.4, IEF 6LoWPAN, IEF RPL (Fig. 17(a)) for the automated monitoring and control of the concentration of biofouling in reverse osmosis membranes, typically employed in

	SIGFOX	Ingenu	LoRA/LoRAWAN	NB-IoT
PHY Layer	UNB / 868MHz (Europe) 902MHz (North America)	RPMA® DSSS / 2.4GHz	CSS / EU: 433MHz & 868Mz (Europe), 915MHz (North America) 430Mz (Australia)	UNB / 832-862MHz (DL), 890-915MHz (UL) uplink
Data Rate	0.1Kbps (UL) – 0.6Kbps (DL)	15.6Kbps (UL) – 31Kbps (DL) <sup>2</sup>	0.5Kbps –37.5Kbps	20Kbps (UL)-250Kbps (DL)
Nominal Range / Coverage	10km (urban), 50 Km (rural)	15km (urban)	5km (urban), 15km (rural)	10km-15km (rural)
Topology	Star	Star, Tree	Star-of-stars	Star (Cellular)
MAC	Unslotted ALOHA	CDMA-like	Unslotted ALOHA	Cell-based, supporting Random Access Channel
Encryption	Not supported	AES 256	AES 128	LTE-based encryption layer
Maximum Payload Length	12 Bytes (UL) 8 Bytes (DL)	10 KBytes	256 Bytes	128 Bytes (UL) 85 Bytes (DL)
Peak current consumption	49mA <sup>1</sup>	245mA <sup>3</sup>	32mA	120/130mA
Over the air updates	Not supported	Supported	Supported	Supported
IP interoperability	Not supported	Not supported	Supported (through IEEE 6LoWPAN)	Supported (through LTE infrastructure and mobile operators)
Nominal nodes per gateway / cell	~10,000	~10,000	~10,000	~50,000
Deployment	Nationwide (multiple countries)	Private or nationwide Networks (strong presence in North America)	Private or nationwide Networks / wide adoption by LPWAN radio module vendors.	Nationwide networks / wide adoption by mobile operators
Range of applications	Industrial low-rate applications without QoS requirements.	Asset tracking, wearables, smart metering, smart cities	Industrial low-rate applications, smart metering, smart cities	Wearables / healthcare, smart metering, smart cities with increased QoS requirements
Considerations	<ul style="list-style-type: none"> <li>Extremely small payload &amp; data rate limits range of modern industrial applications (e.g., real-time control).</li> <li>Low duty cycle significantly limits effective scalability.</li> <li>Worse coverage probability than NB-IoT.</li> </ul>	<ul style="list-style-type: none"> <li>Operation in a noisy region of the EM spectrum / coexistence with WiFi networks.</li> <li>Increased current consumption w.r.t. remaining technologies NB-IoT.</li> </ul>	<ul style="list-style-type: none"> <li>Low duty cycle significantly limits effective scalability.</li> <li>Worse coverage probability than NB-IoT.</li> <li>Premature deployment based on early trials and sporadic deployments</li> </ul>	<ul style="list-style-type: none"> <li>Cost of licensed bands, increasing cost of end product.</li> <li>Increased current consumption w.r.t. LoRA</li> <li>Best-effort traffic. Realization of reliable links increases protocol complexity.</li> <li>Premature deployment based on early trials.</li> </ul>
Availability / maturity of commercial products for smart water networks	High	High	Medium	Low (recent standard)

- 1: @maximum TX power (+14dBm) Libellium SIGFOX Radio Module
- 2: offered by u-blox® portfolio of RPMA-based devices
- 3: @maximum TX power (+22dBm) u-blox® Nano-S100 RMPA Radio Module

Figure 16: Key technical specifications and considerations for LPWA technologies (SIGFOX, Ingenu, LoRA, NB-IoT).

desalination plants. From a network perspective, this platform is further employed for the design

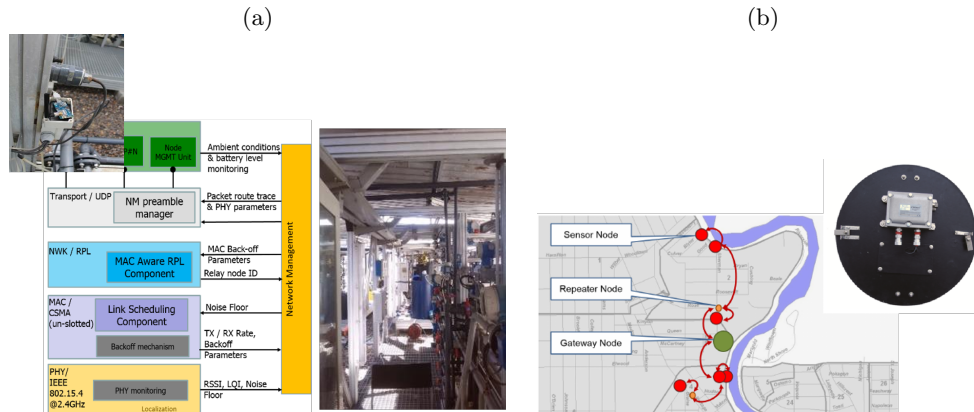


Figure 17: (a) The IEEE80215.4/6LoWPAN/RPL stack for water desalination and respective platform for deployment and operational environment [73, 74], (b) the architecture of the network and sensor node employed for the CSONet project [75, 76].

of the automated extraction of key network conditions that affect the performance of user-defined links in industrial water environments. Ultimately, the authors in [75, 76] propose CSONet, a large-scale and commercialized platform for the automated management of stormwater in sewer systems. CSONet, has been designed to minimize pollution to a nearby river which results from excess storm water entering the sewer system, and is comprised by 150 wireless short-range wireless sensor nodes (Fig. 17(b)), featuring proprietary technology operating at 900MHz / DSSS. The implementation of CSONet resulted in effective reductions of wet weather induced sewer overflows, while at the same time, enables visibility into the city’s sewer infrastructure.

**Long Range Communications.** Despite the strong presence of SIGFOX and Ingenu in the water market arena, the use of long-range communication technologies in the context of smart water networks has until recently relied primary in cellular and WiFi® technologies. A representative example is the Wireless Water Sentinel project in Singapore (WaterWiSe@SG) [77], which interconnected off-the-shelf water sensors for leak detection and burst events with the control centre of the city’s Public Utilities Board. The deployment considered 25 sensor nodes, featuring a Computer-on-Module, WiFi® communication, 2GB Storage disk, and a GPS, while the entire system operated remotely with a stand-alone browser-based interface. Similarly, in [78], GRPS-based telemetry has been employed for building a system for continuous monitoring and critical event detection in the intermittent water distribution network of the city of Hurghada, Egypt. Emphasis has been given to the design considerations for optimizing the node sensing and transmission scheduling, for reducing power and communication load.

Shifting towards state-of-art standards for long-range communications, the authors in [79] employed LoRAWAN for creating a smart water management system in Mori, India. The objective of the project was to monitor and improve the water quality in the region, by the means of providing real time information to the residents of Mori and the local authorities. To this end, a small-scale network, comprised of 7 LoRAWAN nodes has been deployed within the water supply network and linked commercial sensors for monitoring both flow as well as quality of the water. The network infrastructure has been complemented with cloud services for the collection, storage, and further processing of the received data in order to: (a) provide alert mechanisms for streamlining the water locks, and (b) deliver water data analytics services for domestic and irrigation use. Finally, in the

context of urban water infrastructures, Kartakis et al. in [59, 58] proposed a LoRA-based network for enabling the collection of 900 reliable pressure measurements every 15 minutes ( $\sim 1800$  bytes). Each node has been equipped with a 400mAh ( $\sim 5330$  Joules) battery and an energy harvester (i.e water pressure difference recharges the battery by 9 Joules per 15 minutes), for deployment in the Welsh water supply network in Cardiff, UK.

### 3 Modelling and Simulation

Water authorities, on a daily basis, striving to upgrade their networks and repair (or replace) damaged pipes, in an attempt to mitigate the effects of pipe bursts and water loss and to maintain the uninterrupted transport of water to their consumers. In doing so, WDNAs have in mind four guiding principles [80]:

- Keep the quality of the water at the highest possible standards,
- Improve their service to consumers,
- Operate networks cost-efficiently,
- Maintain networks cost-efficiently.

The use of new technologies and methods for monitoring, repairing and/or replacing aging infrastructure for the sustainable management of WDSs, is not enough. Nowadays, as technology is rapidly evolving, dynamic modeling of the WDSs behavior is increasingly gaining more importance, and the modeling of a network's deteriorating infrastructure conditions should be center-staged. In fact, managers of water systems are looking for methodologies, which are dynamically modeling a network's deterioration over time and proactively devising "replace or repair" strategies. The ultimate goal of water authorities is the maximization of their network's reliability and the minimization of the operational and management costs, through an intelligent and efficient assessment of their network and by use of mathematical and/or numerical models [80].

Thus, WDSs agencies are in need of a mathematical tool which would model and simulate a WDN behavior, and by use of such mathematical models the agencies would be able to not only monitor their networks in real time but they would also be provided with a decision support tool for taking maintenance actions [80].

#### 3.1 The EPANET ecosystem

In 1994, the US Environmental Protection Agency (EPA) released EPANET, which is an open source software for modeling hydraulic and quality dynamics of a water distribution system (WDS). EPANET is a research tool that enables understanding of the dynamics within water pipelines, taking into account bulk flow and pipe wall reactions [81]. It examines the geometric structure of the pipeline system along with a set of initial conditions (e.g. pipe roughness and diameter) and rules of how the system is operated, so that it can compute flows, pressures and water quality (e.g. disinfection concentrations and water age) throughout the network for a specific period of time.

EPANET utilizes the "gradient algorithm" for solving the hydraulic state-estimation at each time step [82]. For water quality the Finite Volume Method was originally utilized [83], however, a Lagrangian approach [84] was adopted in the following release of EPANET (EPANET v2.0). That version allowed the dynamic linking of EPANET with external software through its shared object library. In 2015, the Open Source EPANET Initiative was established (comprised of various academic, industrial and other stakeholders), to manage further development of the EPANET software. An updated software (EPANET v2.1) released in 2016, while the next major version [85] is currently under development.

EPANET, during the last 20 years, has been established as the defacto standard tool for both industry and academia areas. Water authorities are using it to simulate possible "what-if" scenarios for the operational behavior of their systems. Industry exploits EPANET's public-domain software license to develop new products and services for the water authorities. EPANET is considered an efficient research tool and during the last 2 decades it is used to evaluate novel algorithms in a

variety of challenges associated with WDSs, using realistic benchmark data. It is extensively used as a tool to facilitate research in topics such as network design optimization [86, 87], operational optimization [88] and sensor placement [89].

The fact that EPANET is an open source software allows researchers to expand its capabilities. At this direction, the water research community developed a number of extensions, add-ons as well as software based on the EPANET.

EPANET can be used in two ways: (a) as a standalone executable software, or (b) as a shared object library. As a standalone executable software, EPANET can be called through a standard shell (e.g. Command Line in Windows). As a shared object (e.g. Dynamic Link Library for Windows), it can be called through a programming interface by external software written in different programming languages (such as C/C++, Python, MATLAB and Visual Basic). The external software can make calls to specific EPANET functions, which modify system parameters, the time series and the simulation configuration.

Researchers are using programming languages, such as MATLAB®, to design and evaluate new methodologies and tools for the analysis of the WDSs behavior. MATLAB is a high-level programming environment used for data processing and analysis. It allows development of applications in different platforms, and it has a large number of sophisticated build-in applications for optimization, control, signal processing etc. MATLAB enables connection to external software libraries, which allows researchers to use tools and simulators developed originally in a different language, such as C or C++. There are three methods of interfacing EPANET with MATLAB:

- Direct calls to the EPANET library, through the build-in function of the programming tool. It requires the use of MATLAB's build-in methods for loading and calling library functions (i.e. using the `loadlibrary` and `calllib` functions).
- Use of "wrappers" (MATLAB methods that follow similar naming conventions as the EPANET functions) that handle the communication with the library internally. This is a higher-level of interfacing with the library, however, it requires the user to design custom data structures. For each EPANET function, a corresponding MATLAB function is required, and new algorithms need to be designed using those functions.
- Use of an Object-Oriented approach by defining a MATLAB Class, which provides a standardized way to handle the network structure, to call all functions as well as procedures using multiple functions, to simulate and in general to perform different types of analysis in the network, through the corresponding object.

Evolution of the EPANET during the last decade has been extensive and important for the research community [90]. A number of extensions have been released, which expand EPANET's capabilities. Such extensions are: (a) EPANET-MSX extension that allows simulation of the reaction and transport dynamics of multiple physical / chemical / biological parameters within a WDS [91], (b) EPANET-BAM that allows incomplete mixing in pipe junctions [92], (c) EPANET-PDX for pressure-driven hydraulic state estimation [93] and (d) EPANET-RTX (or Real-Time EPANET) which is open source software project to develop, distribute and share real-time analytical technologies [94].

Recently, effort was given in developing software for using EPANET through Object-Oriented Programming interfaces, in different programming languages, such as R [95] and Python [96]. A significant effort in utilizing Object-Oriented Programming to expand EPANET's capabilities was by van Zyl et al. (2003) [97], who introduced OOTEN. OOTEN is comprised of different classes with associated methods (for instance the Class, which describes water pipes, provides functions to return pipe parameters such as the diameter and length).

The EPANET-MATLAB Toolkit (v2.1) is an open-source software released under the European Union Public License (EURL), developed at the KIOS Research and Innovation Center of Excellence of the University of Cyprus. The Toolkit interfaces EPANET with MATLAB® to execute direct calls to the EPANET library, to modify and to create EPANET networks, to run multi-species simulations through EPANET-MSX, as well as to visualize the network [98]. The Sensor Placement (S-PLACE) Toolkit is a software for computing the locations of the contaminant sensors that should be installed in a WDS to reduce the impact risks. The S-PLACE Toolkit, which also is developed at the KIOS Research and Innovation Center of Excellence, has been designed to be user-friendly and suitable for both professional and the research community (Fig. 18). It is programmed in MATLAB utilizing the EPANET software library, with a modular software architecture to make it extensible [99].

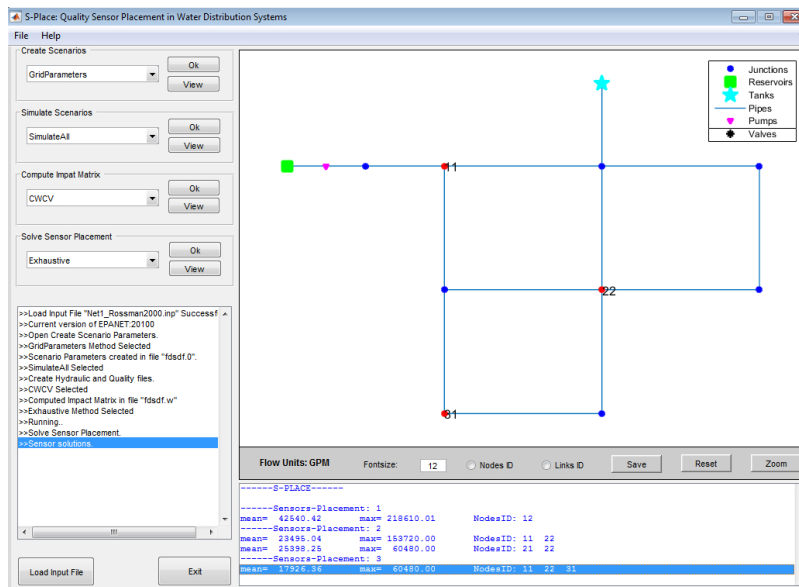


Figure 18: The S-PLACE Graphical User Interface

Another one product of the same research center is the dbpRisk software (Fig.19) . It is an open-source software platform for conducting simulation experiments in order to model the formation for disinfection by-product in drinking water distribution networks under various conditions and uncertainties. The goal is to identify the risk-level at each node location, contributing in the enhancement of consumer safety [100].

The US EPA, in partnership with Sandia National Laboratories, developed multiple water software tools to help support and management of WDSs. These tools are associated with:

- Network Models.
- Vulnerability Assessment.
- Sensor Placement Optimization.
- Event Detection.
- Source Inversion.
- Manual Sampling.

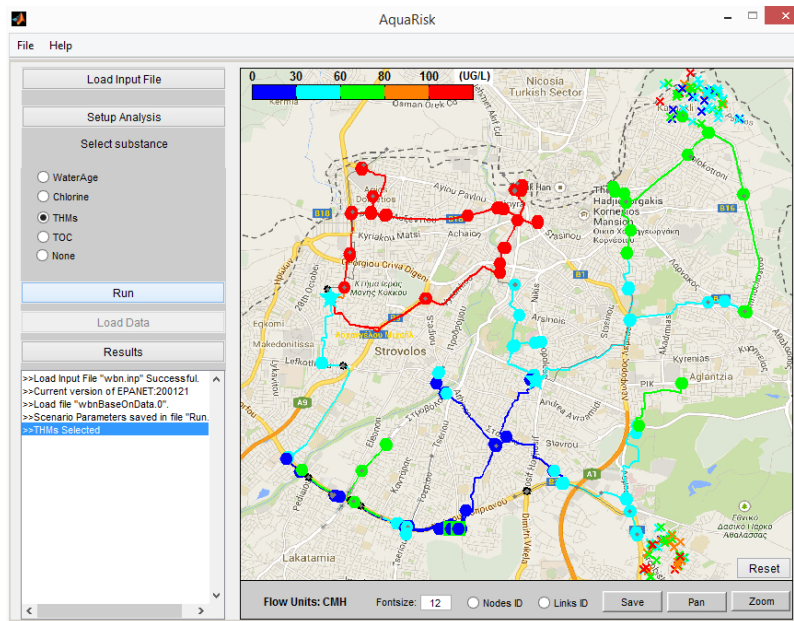


Figure 19: The dbpRisk Graphical User Interface

- Resilience.

### 3.2 Other Modelling Tools

A group of tools supports the design, implementation, and evaluation of contamination warning systems (CWS), which help build resilience to contamination incidents. CWS integrate multiple detection strategies to localize as quickly as possible a wide range of potential contamination incidents [94]. The TEVA-SPOT software comprises sensor placement optimization and Hydraulic / water quality simulation and vulnerability assessment tools. It helps to identify sensor locations in a WDS that minimize one or more objectives [101, 25, 102]. The CANARY is an event detection software that analyzes water quality sensor data in real time and alerting the operator when anomalous data is observed [103]. CANARY has been developed to provide both real-time, and off-line analysis tools to aid in the development of algorithms (which aim to provide event detection and need to be evaluated and configured properly), allowing developers to focus on the algorithms themselves, rather than on how to read in data and drive the algorithms [104]. The Water Security Toolkit (WST) is a suite of software tools that help provide the information necessary to help water utilities make good decisions in minimizing the impact on human health and the economic consequences caused by contamination incidents [94]. The WST assists in planning and evaluating response actions to terrorist attacks, natural disasters and traditional utility challenges, such as pipe breaks and poor water quality. It is consisted of hydraulic and water quality modeling software as well as optimization methodologies. The WST builds upon the simulation and optimization framework of TEVA-SPOT and adds several new features [105]. It is useful in identifying [94]:

- Sensor locations to detect contamination.
- Locations in the network at which the contamination was introduced.
- Hydrants to remove contaminated water from the distribution network.

- Locations in the network to inject decontamination agents to inactivate, remove or destroy contaminants.
- Locations in the network to take grab samples to confirm contamination or cleanup.
- Valves to close in order to isolate contaminated areas of the network.

The Water Network Tool for Resilience (WNTR) is an open source Python™ package designed to help water utilities investigate resilience of WDSs to hazards and evaluate resilience-enhancing actions. WNTR provides a flexible platform for modeling both disruptive incidents and repair strategies in WDSs. The primary modeling components in WNTR include (Klise et al., 2017):

- • Disaster models (e.g. prediction of ground movement after an earthquake)
- Fragility curves used to assign the probability of damage to network components
- Flexible controls to change the status and operation of network components
- Models to estimate leaks in the network
- PDD hydraulic simulation to model the network during low pressure conditions
- Resilience metrics to evaluate the effect of the disruption and repair strategies • Ability to perform Monte Carlo simulations.

### 3.3 Industrial Applications

To date there have been many efforts aimed at improving WDSs and several commercial software and products that target the monitoring, management and controlling of WDSs have been made commercially available. However, this huge effort has an important shortfall for it has not lead to an integrated approach, model or tool for the holistic management of WDNs. In addition, all available commercial tools concerning the management of WDNs have two major drawbacks: the high cost of ownership and the ownership of data. The purchase of such software is expensive and some of them require specialized knowledge that entails additional costs for the water authorities, which in most cases are not profitable organizations. Some of the available solutions are comprised of non-open source software, which requires processing of the data by the provider / creator of the software. This raises an important issue, as the water authorities manage confidential and sensitive data that should not be accessible by anyone outside the water authority [80].

MIKE URBAN is a GIS based modelling software that covers all water networks in the city, including WDSs, storm water drainage systems, and sewer collection in separate and combined systems. Typical applications of MIKE URBAN associated with WDSs are: (i) Master planning, (ii) System rehabilitation and pressure optimization, (iii) Leakage analysis and reduction, (iv) Fire flow analysis and (v) Water quality risk analysis [106].

WaterGEMS provides a decision-support tool for water distribution networks. The software models the WDS's behavior, its reaction to operational strategies and growing as population and demands increase. WaterGEMS has also the capability to simulate scenarios associated with fire flow and water quality as well as to analyze criticality and energy cost. WaterGEMS provides software tools for: (i) Intelligent planning for system reliability, (ii) Optimized operations for system efficiency and (ii) Reliable asset renewal decision support for system sustainability [107].

InfoWater is a GIS integrated WDS modeling and management software application. InfoWater enabling engineers and GIS professionals to work simultaneously on the same integrated platform. It offers direct ARCGIS integration enabling engineers and GIS professionals to work simultaneously

on the same integrated platform It allows command GIS analysis and hydraulic modeling in a single environment using a single dataset [108].

EDAMS Solutions platform addresses productivity enhancement and cost-efficiency from integrated commercial and technical management systems to data validation and the reduction and control of non-revenue water in Water Utilities. The EDAMS range of management systems covers the commercial, technical and planning functions of a Water Utility, and seamlessly integrates with SCADA, GIS and ERP to provide a coherent enterprise system solution. The main packages of the platform are: (i) GIS System, (ii) Billing and Customer Information, (iii) Maintenance Management Systems, (iv) Asset Management and Infrastructure Planning Systems and (v) Integrated Quality Management System [109].

KISTERS Group offers a combination of software tools and provides professional software solutions for the water industries. These software solutions are associated with: (i) Surface Water Hydrology, (ii) Groundwater Hydrology, (iii) Water Quality and Aquatic Ecosystems, (iv) Meteorology and Climatology, (v) Urban Water Systems and (vi) Resources Management [110].

Phoebe Innovations team specializes in various research and innovation topics linked to WDSs monitoring and control, focusing on event diagnosis. The mission of Phoebe Innovations is to: (a) design systems that reduce waste of resources and energy consumption, (b) provide a communication platform between researchers and industry and (c) offer high-impact solutions to the customers. Phoebe Innovations platform combines: (i) Cloud-based Software, (ii) Real-time State Estimation, (iii) Real-time Event Detection and (iv) Research Commercialization [111].

## 4 Data Acquisition and Processing

The Data Management Module (DMM) constitutes a core component of a SWN, which aims at better managing and analyzing data produced by the sensors or the models of the network. The main functionalities of a DMM include the collection and processing of measurements, as well as their high-level analysis for the detection and localization of abnormal events, in order to provide early warnings for performing corrective actions. In this section, we focus on the efficient data acquisition and processing in SWNs, whereas the accurate detection of abnormal behaviors is examined in Section 5.1.

As mentioned above, SWNs are subject to resource and computational constraints that make the efficient data acquisition and processing a challenging task. More specifically, the following problems will be addressed, that are of major importance for increasing the lifetime and analysis performance of our SWN: (i) reduction of telemetry cost, (ii) recovery of missing data, and (iii) time-synchronization of data streams for calculating pairwise correlations. The common characteristic of these problems is the necessity to fill in missing measurements. To this end, we employ state-of-the-art techniques, namely, *matrix completion* (MC) and *tensor completion* (TC), that have demonstrated increased performance in various application domains, in terms of recovering accurately the missing information.

In the case of SWNs, we discriminate between two main causes of missing data: (i) measurements are not acquired due to sensor malfunction, or not transmitted due to network failure; (ii) missing data positions are introduced artificially in order to increase the time resolution of a given data stream, or to synchronize distinct data streams acquired at different sampling frequencies. Fig. 20a illustrates the first case, where measurements are not acquired due to failures of the sensors (e.g. limited battery) or the network (e.g. scheduling issues). Specifically, the data are arranged in the form of a matrix, whose rows correspond to time slots and columns to sensors. That is, the  $ij$ th element of this matrix represents the measurement in the  $i$ th time slot acquired by the  $j$ th sensor. The second case is depicted in Fig. 20b, where, for instance, the sensors belong to two distinct groups, namely, those that are sampling with a period of one hour and those with a period of

two hours. Time synchronization of the sensors is required, such that the data vectors have the same length, prior to calculating their correlation. Furthermore, reduction of the telemetry cost is achieved indirectly for a single sensor by first sampling at a relatively low frequency and then performing temporal super-resolution to reconstruct the artificially introduced missing entries.

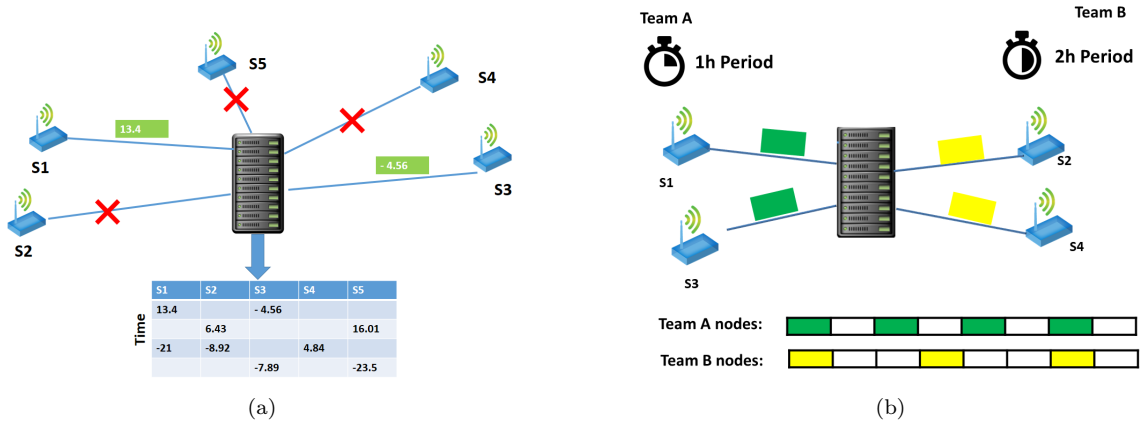


Figure 20: Occurrence of missing data due to: (a) sensors or network failure, (b) different sampling frequencies.

An alternative approach for reducing the cost of telemetry is to simultaneously acquire and compress the sensor data, thus decreasing significantly the volume of the transmitted information. This is exactly what *compressive sensing* (CS) does, which is an innovative framework that has revolutionized signal processing the recent years. In particular, the information conveyed by a signal of length  $N$  can be represented in a highly compact way by  $M$  appropriately generated random measurements<sup>5</sup>, where  $M \ll N$ . A necessary condition to guarantee accurate reconstruction is that the original signal is either sparse (or compressible) by itself or it can be sparsified in a suitable transform domain. Then, given the highly reduced set of  $M$  random measurements, the original signal can be reconstructed accurately by solving an appropriate optimization problem. The concept of CS applied to a SWN scenario is shown schematically in Fig. 21.

The subsequent sections overview the mathematical formulation and key properties of matrix/tensor completion techniques and compressive sensing, which constitute the core of our data acquisition and processing module.

#### 4.1 Missing Data Recovery and Temporal Super-resolution via Matrix Completion

As depicted in Fig. 20, a typical way to arrange the measurements acquired by multiple sensors is in the form of two-dimensional (2D) matrices. Due to various imperfections of the SWN, several measurements are often missing, yielding a sparse matrix whose entries must be reconstructed accurately before proceeding to further data analysis and decision making. Matrix completion provides an efficient algorithmic toolkit for reconstructing the missing entries of a partially observed matrix (ref. Fig. 22).

<sup>5</sup>We emphasize here the distinction between physical (sensor) measurements and random measurements generated in the framework of compressive sensing. In the former case, the measurements are acquired directly by the nodes of a network, whereas in the later, they are generated via an appropriate mathematical model.

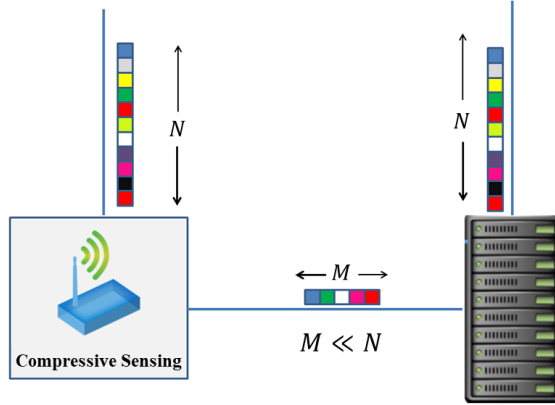


Figure 21: Reduction of telemetry cost using compressive sensing.

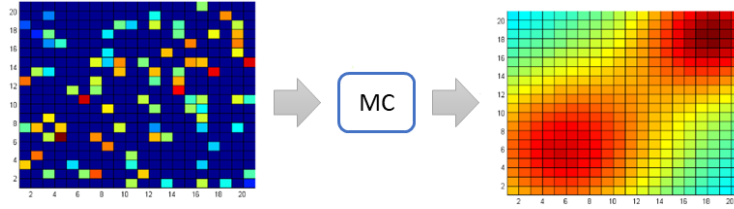


Figure 22: Schematic illustration of the MC process.

More specifically, let  $\mathbf{A}$  denote the  $N \times S$  matrix of measurements, with potentially missing entries, where  $N$  is the number of time instants and  $S$  the number of sensors. Moreover, let  $\Omega$  be the set of indices associated with the available entries of  $\mathbf{A}$ , that is, the measurement  $a_{ij}$  has been acquired if  $(i, j) \in \Omega$ , otherwise it corresponds to a missing value. A projection operator,  $P_\Omega$ , is defined accordingly as follows,

$$P_\Omega(\mathbf{A})_{ij} = \begin{cases} a_{ij}, & \text{if } (i, j) \in \Omega \\ 0, & \text{if } (i, j) \notin \Omega. \end{cases} \quad (1)$$

The redundancy of the measurements in  $\mathbf{A}$  can be expressed by the *rank* of the matrix. The rank of a matrix is defined as (a) the maximum number of linearly independent column vectors in the matrix, or (b) the maximum number of linearly independent row vectors in the matrix. Both definitions are equivalent. For a  $N \times S$  matrix, if  $N < S$ , then the maximum rank of the matrix is  $N$ . If  $N > S$ , then the maximum rank of the matrix is  $S$ . The rank of a matrix would be zero only if the matrix had no elements. If a matrix had even one element, its minimum rank would be one. If  $\text{rank}(\mathbf{A}) = r$ , then,  $\mathbf{A}$  can be expressed as the product of two matrices,

$$\mathbf{A} = \mathbf{U}\mathbf{R}^T, \quad (2)$$

where  $\mathbf{U}$  is  $N \times r$  and  $\mathbf{R}$  is  $S \times r$ . If there is the prior knowledge that  $\mathbf{A}$  is of low rank, then, it is possible to recover its missing entries by finding the lowest-rank matrix  $\mathbf{X}$ , if the rank of the completed matrix is known, which agrees with the given data. This matrix is obtained as the solution of the following optimization problem,

$$\min_{\mathbf{X} \in \mathbb{R}^{N \times S}} \text{rank}(\mathbf{X}) \quad \text{s.t.} \quad P_\Omega(\mathbf{X}) = P_\Omega(\mathbf{A}). \quad (3)$$

The matrix completion problem is in general NP-hard [112], but there are tractable algorithms that achieve exact reconstruction with high probability.

A number of assumptions on the sampling structure of the observed entries and the number of sampled entries are typically made to simplify the analysis and ensure that the problem is not underdetermined. First, in order to make the analysis more tractable, it is often assumed that the set  $\Omega$  with the indices of observed entries and fixed cardinality is sampled uniformly at random from the collection of all subsets of entries of cardinality  $|\Omega|$ . To further simplify the analysis,  $\Omega$  is constructed via Bernoulli sampling, that is, each entry is observed with probability  $p$ . Another commonly used simplification is to assume that the entries are sampled independently and with replacement. The second assumption refers to the estimation of a lower bound on the number of observed entries, in order to guarantee accurate recovery of the missing entries. Given that  $\text{rank}(\mathbf{A}) = r$ , there is an information theoretic lower bound on how many entries must be observed such that  $\mathbf{A}$  can be uniquely reconstructed. Assuming, without loss of generality, that  $N < S$ , at least  $2Sr - r^2$  entries must be observed for matrix completion to have a unique solution. Furthermore, there must be at least one observed entry per row and column of  $\mathbf{A}$ . Finally, assuming that  $r \ll \{N, S\}$ , which is valid for many practical applications, the lower bound on the number of observed entries required to prevent the problem of matrix completion from being underdetermined is at the order of  $Sr \log(S)$ . The third assumption for ensuring accurate reconstruction refers to the incoherence of  $\mathbf{A}$ . This is to ensure that the singular vectors of  $\mathbf{A}$  are not too sparse, in the sense that all coordinates of each singular vector are of comparable magnitude, instead of just a few coordinates having significantly larger magnitudes.

In the following, we overview the major methods for solving the optimization problem (3).

1. **Low-Rank Approximation:** This method seeks for the low-rank matrix  $\mathbf{X}$  that is closest to the original  $\mathbf{A}$  in terms of the sum-of-squares distance. The associated optimization problem is formulated as follows,

$$\min_{\mathbf{X} \in \mathbb{R}^{N \times S}} \|\mathbf{X} - \mathbf{A}\|_F^2 \quad \text{s.t.} \quad \text{rank}(\mathbf{X}) = r, \quad (4)$$

where  $\|\mathbf{X} - \mathbf{A}\|_F^2 = \sum_{i,j} (x_{ij} - a_{ij})^2$ . The above nonconvex problem can be solved efficiently by using the singular value decomposition (SVD) of  $\mathbf{A}$ ,

$$\mathbf{A} = \mathbf{U}\mathbf{\Sigma}\mathbf{V}^T = \sum_{k=1}^K \sigma_k \mathbf{u}_k \mathbf{v}_k^T, \quad (5)$$

where  $K = \min\{N, S\}$ ,  $\mathbf{U}$ ,  $\mathbf{V}$  are  $N \times K$  and  $S \times K$  matrices, respectively, with orthonormal columns, and  $\mathbf{\Sigma}$  is a diagonal  $K \times K$  matrix with the nonnegative singular values on its main diagonal sorted at decreasing order. The solution of (3) is based on the theory of Eckart-Young, according to which,

$$\mathbf{X} = \sum_{k=1}^r \sigma_k \mathbf{u}_k \mathbf{v}_k^T. \quad (6)$$

The procedure for calculating the above low-rank matrix corresponds to a thresholding operator which maintains the  $r$  largest singular values. By taking the Lagrangian of (3) we obtain the following regularized form,

$$\min_{\mathbf{X} \in \mathbb{R}^{N \times S}} (\|\mathbf{X} - \mathbf{A}\|_F^2 + \lambda \cdot \text{rank}(\mathbf{X})) , \quad (7)$$

where  $\lambda \in \mathbb{R}$  is a regularization parameter. Varying the value of  $\lambda$  yields a different solution to the above optimization problem. Given  $\lambda$ , a solution is obtained via (6) by first applying

a hard thresholding operator on the computed singular values,

$$\sigma = \begin{cases} \sigma_k, & \sigma_k \geq \gamma \\ 0, & \sigma_k < \gamma, \end{cases} \quad (8)$$

where  $\gamma = \sqrt{\lambda}$ , and then substituting in (6) those singular values (and the corresponding singular vectors) that exceed the threshold.

In some MC algorithms, hard thresholding is replaced by a soft thresholding operator, which shrinks the large singular values as follows,

$$\sigma = \begin{cases} \sigma_k - \gamma, & \sigma_k \geq \gamma \\ 0, & \sigma_k < \gamma. \end{cases} \quad (9)$$

This yields a gradual phasing out of the terms that just cross the threshold, which is preferable in the case of measurements corrupted by noise with small or moderate signal-to-noise ratio (SNR). On the other hand, in general, hard thresholding is better under strong SNR, but worse in intermediate SNR levels.

2. **Low-Rank Recovery and Nuclear Norm Minimization:** We will assume that rather than observing  $A$  directly we instead observe  $y = \mathcal{P}_N(A) + z$  where  $z$  represents noise and  $\mathcal{P}_N : R^{M \times N} \Rightarrow R^L$  is a linear measurement operator that acts on a matrix  $A$  by taking standard inner products against  $L$  pre-defined matrices  $\mathcal{P}_{N1}, \dots, \mathcal{P}_{NL}$  :

$$y_i = \langle A, \mathcal{P}_{Ni} \rangle + z_i = \text{trace}(\mathcal{P}_{Ni}^T A) + z_i = \sum_{m=1}^M \sum_{n=1}^N A[m, n] \mathcal{P}_{Ni}[m, n] + z_i \quad (10)$$

With the low-rank recovery problem where we are working from (possibly noisy) indirect observations,  $y \approx \mathcal{P}_N(A)$ .

The above soft thresholding operation becomes more computationally tractable by reformulating it in a variational framework. Specifically, when  $\gamma = \frac{\lambda}{2}$  the output of this operation is the solution of the following optimization problem,

$$\min_{\mathbf{X} \in \mathbb{R}^{N \times S}} (\|\mathbf{X} - \mathbf{y}\|_F^2 + \lambda \cdot \|\mathbf{X}\|_*), \quad (11)$$

where  $\|\mathbf{X}\|_*$  is the nuclear norm of  $\mathbf{X}$ , which is equal to the sum of the singular values of  $\mathbf{X}$ . Unlike the rank,  $\|\mathbf{X}\|_*$  is a convex function that is employed as a convex proxy of the rank in optimization problems. This relation is motivated by the fact that the rank represents the number of nonzero singular values, whereas the nuclear norm equals their sum. As such, the nuclear norm is used as a relaxation of the rank function. The problem in (11) is convex, thus any local minimum is the global minimum.

3. **Iterative Hard Thresholding:** Iterative hard thresholding (IHT) [113] is very similar to the proximal algorithms used to solve the above nuclear norm minimization problem. However, when the target matrix is of very low rank, IHT tends to converge extremely quickly. We introduce the adjoint of  $\mathcal{P}_N$  operator, which is defined as:

$$\mathcal{P}_N^*(w) = \sum_{i=1}^L w_i \mathcal{P}_{Ni} \quad (12)$$

The basic iteration of this method is as follows: From the current estimate  $\mathbf{X}_k$ , first we take a step in the direction of the gradient of  $\|\mathbf{X} - \mathbf{y}\|_2^2$ , and then we project onto the set of rank- $r$  matrices using the projection operator  $P_r$ ,

$$\mathbf{Y}_{k+1} = \mathbf{X}_k - \gamma_k \mathcal{P}_N^*(\mathcal{P}_N(\mathbf{X}) - \mathbf{y}) \quad (13)$$

$$\mathbf{X}_{k+1} = P_r(\mathbf{Y}_{k+1}) . \quad (14)$$

The  $P_r$  operator computes the top  $r$  left and right singular vectors and singular values; when  $r$  is small compared to  $N$  and  $S$ , this can be done in significantly less time than computing a full SVD and  $\gamma_k > 0$ .

4. **Alternating Projections:** The alternating projections algorithm is a memory-efficient technique, which stores the iterates in factorized form. The algorithm is characterized by a very simple formulation and easiness of interpretation: we seek for a  $N \times S$  matrix of rank  $r$  that is consistent with  $\mathbf{y}$ ,

$$\min_{\mathbf{X} \in \mathbb{R}^{N \times S}} \|\mathcal{P}_N(\mathbf{X}) - \mathbf{y}\|_2^2 \quad \text{s.t.} \quad \text{rank}(\mathbf{X}) = r , \quad (15)$$

This is equivalent to seeking for a  $N \times r$  matrix  $\mathbf{L}$  and a  $S \times r$  matrix  $\mathbf{R}$  whose product is consistent with  $\mathbf{A}$ , that is,

$$\min_{\mathbf{L} \in \mathbb{R}^{N \times r}, \mathbf{R} \in \mathbb{R}^{S \times r}} \|\mathcal{P}_N(\mathbf{L}\mathbf{R}^T) - \mathbf{y}\|_2^2 . \quad (16)$$

This optimization problem is still nonconvex, but by keeping  $\mathbf{L}$  or  $\mathbf{R}$  fixed, it is reduced to a simple least-squares problem. This motivates the following iterative scheme for solving the above optimization problem: Given the current estimates  $\mathbf{L}_k$  and  $\mathbf{R}_k$ , the solution is updated as follows,

$$\mathbf{R}_{k+1} = \arg \min_{\mathbf{R} \in \mathbb{R}^{S \times r}} \|\mathcal{P}_N(\mathbf{L}_k \mathbf{R}^T) - \mathbf{y}\|_2^2 \quad (17)$$

$$\mathbf{L}_{k+1} = \arg \min_{\mathbf{L} \in \mathbb{R}^{N \times r}} \|\mathcal{P}_N(\mathbf{L} \mathbf{R}_{k+1}^T) - \mathbf{y}\|_2^2 . \quad (18)$$

Each step involves solving a linear system of equations with  $rN$  or  $rS$  variables for which we can employ well-established numerical algorithms. The final solution tends to depend heavily on the initialization of  $\mathbf{L}$  and  $\mathbf{R}$ . The simplicity and efficiency of the alternating projections algorithm make it one of the most popular methods for large-scale matrix factorization, whilst it generally outperforms nuclear norm minimization, especially when the rank  $r$  is very small compared to  $N$  and  $S$ .

5. **Robust Principal Component Analysis:** Suppose we are given a large data matrix  $\mathbf{A}$ , for which we know that it may be decomposed as

$$\mathbf{A} = \mathbf{L} + \mathbf{S} , \quad (19)$$

where  $\mathbf{L}$  has low rank and  $\mathbf{S}$  is sparse. Furthermore, both components are of arbitrary magnitude. In addition, the low-dimensional column and row space of  $\mathbf{L}$ , and even their dimension, are unknown. Similarly, the number and locations of the nonzero entries of  $\mathbf{S}$  are also unknown. Thus the question is if it is possible to recover the low-rank and sparse components both accurately and efficiently.

In the general case of data corrupted by additive noise,

$$\mathbf{A} = \mathbf{L} + \mathbf{N} , \quad (20)$$

where  $\mathbf{N}$  is a small perturbation matrix, the classical principal component analysis (PCA) seeks the best, in an  $\ell_2$  sense, rank- $r$  estimate of  $\mathbf{L}$  by solving

$$\min_{\mathbf{L} \in \mathbb{R}^{N \times S}} \|\mathbf{A} - \mathbf{L}\|_2^2 \quad \text{s.t.} \quad \text{rank}(\mathbf{L}) \leq r . \quad (21)$$

As mentioned before, this problem can be efficiently solved via the SVD and enjoys a number of optimality properties when the noise  $\mathbf{N}$  is small and independent and identically distributed (i.i.d.) Gaussian.

PCA is arguably the most widely used statistical tool for data analysis and dimensionality reduction today. However, its sensitivity with respect to measurements corrupted by gross errors often puts its validity in jeopardy. Notice that a single grossly corrupted entry in  $\mathbf{A}$  could render the estimated low-rank matrix  $\hat{\mathbf{L}}$  arbitrarily far from the true  $\mathbf{L}$ .

To address this problem, an idealized version of robust PCA (RPCA) is considered in [114], in which the aim is to recover a low-rank matrix  $\mathbf{L}$  from highly corrupted measurements by solving a tractable convex optimization problem. Let  $\|\mathbf{A}\|_1 = \sum_{i,j} |a_{ij}|$  denote the  $\ell_1$  norm of  $\mathbf{A}$  seen as a long vector in  $\mathbb{R}^{N \times S}$ . Then, under rather weak assumptions, the principal component pursuit (PCP) estimate solving

$$\min_{\mathbf{L} \in \mathbb{R}^{N \times S}, \mathbf{S} \in \mathbb{R}^{N \times S}} \|\mathbf{L}\|_* + \lambda \|\mathbf{S}\|_1 \quad \text{s.t.} \quad \mathbf{L} + \mathbf{S} = \mathbf{A} , \quad (22)$$

exactly recovers the low-rank  $\mathbf{L}$  and the sparse  $\mathbf{S}$  components. Theoretically, this is guaranteed to work even if the rank of  $\mathbf{L}$  grows almost linearly in the dimension of the matrix, and the errors in  $\mathbf{S}$  are up to a constant fraction of all entries.

## 4.2 Missing Data Recovery and Temporal Super-resolution via Tensor Completion

In real-world applications, it is often necessary to store the measurements in higher-order structures, apart from 2D matrices. For instance, in the case of a SWN infrastructure, we typically have multiple sensors, which measure multiple modalities at different times. The acquired data can be arranged in the form of a tensor, which is considered as a generalization of scalars (zero-order tensors), vectors (first-order tensors) and matrices (second-order tensors). A 3D tensor, for example, may encode the sensors in its first dimension, the type of measurements (e.g. temperature, pressure, pH) in the second dimension, and the time in the third dimension.

For convenience, yet without loss of generality, in the following we focus on 3D tensors. Before defining the problem of tensor completion, we first introduce some basic functions. Specifically, by letting  $\mathcal{T} \in \mathbb{R}^{N \times S \times T}$  denote a third-order tensor, the following expression is obtained by employing the PARAFAC/CANDECOMP decomposition [115],

$$\mathcal{T} = \sum_{i=1}^J \lambda_i (\mathbf{a}_i \circ \mathbf{b}_i \circ \mathbf{c}_i) , \quad (23)$$

where  $\lambda_i \in \mathbb{R}$ ,  $i = 1, \dots, J$ , are normalization parameters and  $\mathbf{a}_i \in \mathbb{R}^N$ ,  $\mathbf{b}_i \in \mathbb{R}^S$ ,  $\mathbf{c}_i \in \mathbb{R}^T$  are the vector components. In such a decomposition,  $\mathbf{a}_i$ ,  $\mathbf{b}_i$ , and  $\mathbf{c}_i$  are treated as the columns of the factor matrices  $\mathbf{A} = [\mathbf{a}_1, \mathbf{a}_2, \dots, \mathbf{a}_J]$ ,  $\mathbf{B} = [\mathbf{b}_1, \mathbf{b}_2, \dots, \mathbf{b}_J]$  and  $\mathbf{C} = [\mathbf{c}_1, \mathbf{c}_2, \dots, \mathbf{c}_J]$ , whose outer product yields the original tensor  $\mathcal{T}$ . The number of terms,  $J$ , can be defined as the rank of the tensor and plays a pivotal role to tensor algebra.

To define formally the rank of a tensor we rely on simple, rank-1, tensors as the building blocks. In particular, a rank-1 (a.k.a. simple or decomposable) tensor is a  $K$ th-order tensor  $\mathcal{X}$  ( $K \in \mathbb{Z}^+$ ),

which can be written as the outer product of  $K$  vectors, that is,

$$\boldsymbol{\mathcal{X}} = \mathbf{a}^{(1)} \circ \mathbf{a}^{(2)} \circ \dots \circ \mathbf{a}^{(K)} . \quad (24)$$

Then, the rank of a tensor  $\boldsymbol{\mathcal{T}}$  is defined as the smallest number of rank-1 tensors whose summation generates  $\boldsymbol{\mathcal{T}}$ . It can be shown that, under mild conditions, the above tensor decomposition is unique for third- and higher-order tensors.

Reordering the elements of a tensor into a matrix simplifies subsequent matrix-based processing. Such a transformation, also called matricization or unfolding, is not unique, since different ways exist for stacking the horizontal, lateral and frontal slices of a tensor in either column-wise or row-wise arrays, as shown in Fig. 23.

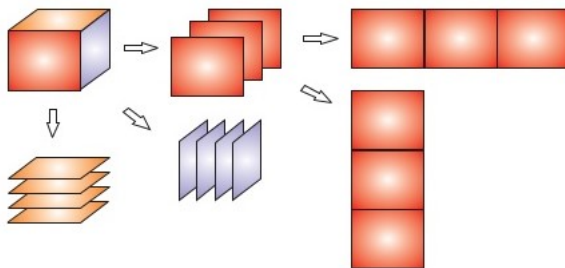


Figure 23: Matricization or unfolding of a higher-order tensor into a matrix or vector form.

A commonly used way for recovering missing entries in high-order tensors is first to reduce them to low-rank matrices via appropriate unfolding and then apply matrix completion techniques (ref. Section 4.1). As mentioned before, the process of unfolding is not unique and different unfoldings may result in significantly different ratios of high-magnitude over low-magnitude singular values. One should consider the matrix with the largest possible dimension, since such a matrix is typically characterized by limited degrees of freedom compared to its dimension.

Tensor completion (TC) techniques seek to estimate a low-rank tensor  $\boldsymbol{\mathcal{X}}$ , which agrees with the observed data  $\boldsymbol{\mathcal{T}}$ , as follows,

$$\min_{\boldsymbol{\mathcal{X}}} \|\boldsymbol{\mathcal{X}}\|_* \quad \text{s.t.} \quad P_{\Omega}(\boldsymbol{\mathcal{X}}) = P_{\Omega}(\boldsymbol{\mathcal{T}}) , \quad (25)$$

where  $P$  and  $\Omega$  denote a projection operator and the set of indices associated with the available measurements, respectively, as in the case of MC. However, the tensor-based optimization problem is much harder to be solved, since the tensor nuclear norm is not defined as the tightest convex relaxation of the tensor rank, as it was the case with matrices. Instead, the tensor nuclear norm is defined as the convex combination of the nuclear norms of all matrices unfolded along each of its modes, as follows,

$$\|\boldsymbol{\mathcal{X}}\|_* = \sum_{i=1}^n \alpha_i \|\mathbf{X}_i\|_* , \quad (26)$$

where  $\alpha_i \geq 0$ , with  $\sum_{i=1}^n \alpha_i = 1$ , and  $\mathbf{X}_i$  are the matrices in the unfolded representation of the tensor  $\boldsymbol{\mathcal{X}}$ . By combining (25) and (26) the TC problem is reformulated as follows,

$$\min_{\boldsymbol{\mathcal{X}}} \sum_{i=1}^n \alpha_i \|\mathbf{X}_i\|_* \quad \text{s.t.} \quad P_{\Omega}(\boldsymbol{\mathcal{X}}) = P_{\Omega}(\boldsymbol{\mathcal{T}}) . \quad (27)$$

A main drawback of the majority of methods used to solve (27) is that they do not exploit the low rank properties of all the dimensions of a tensor, but instead they utilize a single dimension. To

address this issue, the method of parallel matrix factorization (PMF) [116] has been introduced as an efficient alternative for solving the TC problem. PMF is characterized by a reduced computational complexity and improved performance, when compared against the solutions based on tensor unfolding. Focusing on the 3D case, we are interested in fully recovering a tensor  $\mathcal{T} \in \mathbb{R}^{N \times S \times T}$  from  $M \ll N \cdot S \cdot T$  measurements. Specifically,  $\mathcal{T}$  is unfolded across all of its modes to a set of matrix factors  $\mathbf{X}_n, \mathbf{Y}_n$ , such that  $\mathbf{T}_n \approx \mathbf{X}_n \mathbf{Y}_n$ , where  $n = 1, 2, 3$  indicates the corresponding mode. Introducing a common variable  $\mathcal{Z}$  to relate these matrix factorizations, we solve the following problem to recover  $\mathcal{T}$ ,

$$\min_{\mathbf{X}, \mathbf{Y}, \mathcal{Z}} \sum_{i=1}^3 \alpha_i \|\mathbf{X}_i \mathbf{Y}_i - \mathbf{Z}_i\|_F^2 \quad \text{s.t.} \quad P_\Omega(\mathcal{Z}) = P_\Omega(\mathcal{T}), \quad (28)$$

where  $\mathbf{X} = (\mathbf{X}_1, \mathbf{X}_2, \mathbf{X}_3)$ ,  $\mathbf{Y} = (\mathbf{Y}_1, \mathbf{Y}_2, \mathbf{Y}_3)$ , and  $\mathbf{Z}_i, i = 1, 2, 3$ , corresponds to the unfolding of the three-way tensor. The parameters  $\alpha_i$  are introduced in order to properly weight the contribution of each unfolding. A limitation of this method is that the tensor rank must be known in advance, which may not be the case in practice. In order to alleviate this issue, a rank-increasing scheme is applied, which starts from a tensor estimate of very low rank and increasing the rank gradually until the relative change of the singular values falls below a predefined threshold.

### 4.3 Reduction of Telemetry Cost Using Compressive Sensing

Let  $\mathbf{x} = [x_1, x_2, \dots, x_N]^T \in \mathbb{R}^N$  denote an observed discrete-time signal with real-valued elements. In the following, we assume that  $\mathbf{x}$  can be either  $s$ -sparse ( $s \ll N$ ) by itself, that is,  $|\{j \mid x_j \neq 0\}| \leq s$ , or sparse in some transform basis (a.k.a. *dictionary*)  $\Psi$ , such that  $\boldsymbol{\alpha} = \Psi \mathbf{x}$ , where  $\boldsymbol{\alpha} \in \mathbb{R}^{N'}$  is the  $s$ -sparse vector of transform coefficients. Notice that, in general,  $N' \geq N$ , since  $\Psi$  can be overcomplete [117]. In the subsequent analysis,  $\Psi$  and  $\Psi^T$  denote the analysis (direct) and synthesis (inverse) transforms, respectively.

In practice, the acquired signal is typically corrupted by observation noise, which is defined as a perturbation introduced to the true signal prior to its sampling. In the following, we adopt an *additive* model for the observation noise, that is,

$$\mathbf{x} = \mathbf{x}_0 + \mathbf{e}_o, \quad (29)$$

where  $\mathbf{x}_0 \in \mathbb{R}^N$  is the true noiseless signal and  $\mathbf{e}_o \in \mathbb{R}^N$  is the observation noise component.

Let  $A : \mathbb{R}^N \mapsto \mathbb{R}^M$  with  $M < N$  denote a sampling operator that maps a vector of  $N$  elements to a lower-dimensional vector of  $M$  *measurements*. The compressive sampling of  $\mathbf{x}$  is expressed by  $\mathbf{y} = A(\mathbf{x})$ , where  $\mathbf{y} \in \mathbb{R}^M$  is the vector of measurements.

In conventional compressive sensing (CS) systems the sampling operator  $A(\cdot)$  is a linear map. Considering the general case when the true signal is sparse in a transform basis  $\Psi$ ,  $\mathbf{x}_0 = \Psi^T \boldsymbol{\alpha}_0$ , the vector of measurements is constructed by taking linear projections onto the rows of a random matrix,

$$\mathbf{y} = \Phi (\Psi^T \boldsymbol{\alpha}_0 + \mathbf{e}_o) = \Phi \Psi^T \boldsymbol{\alpha}_0 + \mathbf{n}, \quad (30)$$

where  $\Phi \in \mathbb{R}^{M \times N}$  is a random *measurement matrix* and  $\mathbf{n} = \Phi \mathbf{e}_o \in \mathbb{R}^M$  is the projected noise.  $\Phi$  must satisfy specific conditions (e.g. the null space property and the restricted isometry property for  $\ell_1$ -norm minimization, and incoherence<sup>6</sup> with  $\Psi^T$ ) to guarantee the successful reconstruction of a sparse signal. The definition of the restricted isometry property (RIP) and the restricted isometry constant (RIC) is as follows (ref. [120] for more details):

<sup>6</sup>Although incoherence among  $\Phi$  and  $\Psi^T$  is a requirement for guaranteeing accurate sparse reconstruction [118], recent works have proven that for truly redundant dictionaries a no-incoherence restriction on the dictionary can still guarantee accurate sparse recovery [119].

**Definition (s-RIC):** The  $s$ -restricted isometry constant of  $\Phi$  is defined as the smallest positive quantity  $\delta_s$ , such that

$$(1 - \delta_s)\|\mathbf{v}\|_2^2 \leq \|\Phi\mathbf{v}\|_2^2 \leq (1 + \delta_s)\|\mathbf{v}\|_2^2 \quad (31)$$

holds  $\forall \mathbf{v} \in \mathcal{T}_s$ , where  $\mathcal{T}_s = \{\mathbf{v} \in \mathbb{R}^N \mid \|\mathbf{v}\|_0 \leq s\}$ . A matrix  $\Phi$  is said to satisfy a RIP of order  $s$  if  $\delta_s \in (0, 1)$ .

By setting  $\mathbf{A} = \Phi\Psi^T$  as the generic linear sampling operator, the true sparse coefficients vector  $\alpha_0$  can be recovered by solving, among other formulations, an  $\ell_1 - \ell_2$  constrained optimization problem of the form,

$$\min_{\alpha \in \mathbb{R}^{N'}} \|\alpha\|_1 \quad \text{s.t.} \quad \|\mathbf{y} - \mathbf{A}\alpha\|_2 \leq \varepsilon, \quad (32)$$

where  $\varepsilon > 0$  is a threshold depending on the noise level. Then, an estimate of the true signal is given by  $\hat{\mathbf{x}}_0 = \Psi^T \alpha_0^*$ . Several efficient optimization formulations have been proposed in the literature; for convenience and without loss of generality we consider the basis pursuit denoising (BPD) formulation in (32), which is solved effectively using, for instance, the orthogonal matching pursuit (OMP) algorithm [121].

Fig. 24 shows a schematic representation of the way CS will be applied in SmartWater2020's data processing module for reducing telemetry costs. Specifically, each sensor in the SWN acquires a vector of  $N$  data samples  $\mathbf{x}_i \in \mathbb{R}^N$ ,  $i = 1, \dots, C$ , where  $C$  is the number of sensors. Then, two options exist for the generation of  $M$  random measurements,  $\mathbf{y}_i \in \mathbb{R}^M$ , with  $M \ll N$ : 1) a distinct  $\Phi_i \in \mathbb{R}^{M \times N}$  is drawn for each sensor  $i$ , that is,  $\mathbf{y}_i = \Phi_i \mathbf{x}_i$ ,  $i = 1, \dots, C$ ; 2) all the sensors employ the same  $\Phi$ , that is,  $\mathbf{y}_i = \Phi \mathbf{x}_i$ , which is also available to the base station, where the reconstruction will take place. Then, the measurement vectors of highly reduced size,  $\mathbf{y}_i$ , are transmitted to a base station, where an optimization problem is solved to reconstruct the original vectors  $\mathbf{x}_i$ . Notice that the option 1) above does not induce any additional computational burden, since the extra amount of information each sensor has to send to the base station is only a seed (i.e., scalar) for the perfect regeneration of the corresponding  $\Phi_i$  using a random number generator.

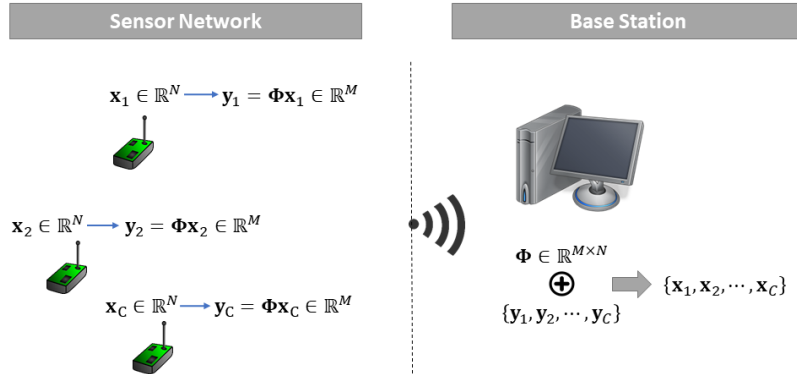


Figure 24: CS applied in SmartWater2020's data processing module for reducing telemetry costs (all sensors use the same measurement matrix  $\Phi$ ).

#### 4.4 Industrial Applications

The theoretical frameworks and algorithmic tools presented in the previous sections have been applied successfully in various distinct industrial applications, thus further motivating their use in the data management and analysis module envisioned by SmartWater2020. In the following, we

briefly review recent use cases that benefited from the above mentioned tools for data compression and recovery.

1. **Low-rank Matrix Completion for Sensor Data in Water Desalination Plants:** The framework of low-rank matrix completion was applied on data collected by a wireless sensor network installed in a water desalination plant [122]. This work examined the effect of matrix dimension, the number of sensors, and the impact of temporal super-resolution on reconstruction accuracy. It has been noticed that the reconstruction quality is governed by the percentage of information of the underlying data matrix and not by its size. Furthermore, the MC applied on a combination of individual measurements achieves improved accuracy when compared with a reconstruction of the values of each sensor individually, since it can fully utilize the potential correlations among the sensors. Finally, the reconstruction of missing data from a super-resolution perspective was examined, demonstrating that as the dimensionality of the data matrix increases and the fill ratio decreases, the MC-based reconstructed data preserve their smoothness and distribution to a great extent, compared with the initial full data matrix.
2. **Compressive Sensing and Tensor Completion in Cyber-Physical System:** In [123], CS and TC were applied on data acquired by the nodes of a cyber-physical system (CPS). Among other problems, this work investigated the effect of noise removal prior to the recovery of measurements which were either lost or intentionally not transmitted due to energy constraints. By examining a low-order matrix for detecting and removing rare errors via robust PCA, it was shown that the proposed method achieved accurate separation of the clean low-rank signal even in the presence of significant noise. Finally, the reconstruction performance from a subset of measurements was evaluated, when the measurements are stored in a tensor-like structure. A key remark was that a very realistic estimation of the original information can be performed even when half of the measurements are missing. Furthermore, the most significant features are preserved, even when a quarter of the measurements are available. Although increasing the sampling rate yields a more accurate reconstruction in both tensor and matrix modeling scenarios, the superiority of the tensor-based approach was highlighted, which achieved a nearly monotonically decrease of the reconstruction error, in contrast to the matrix-based cases, where the reconstruction error reached a plateau for several unfolding schemes.
3. **Compressive Sensing-based Scheduling in Wireless Sensor Networks:** In [124], a compressive sensing-based scheduling scheme was proposed that conserves energy by activating only a small subset of sensor nodes in each time slot to sense and transmit. Transmitting the minimum amount of data, while putting the rest of the sensor nodes in sleep mode, the energy efficiency can be improved significantly. The proposed algorithm was shown to outperform state-of-the-art approaches, in terms of energy consumption, network lifetime, and robustness to sensor node failures.
4. **Matrix/Tensor Completion for Industrial and Outdoor Environments Data:** In [125], the problem of recovering missing observations from environmental sensing platforms via MC and TC was examined. From the one hand, MC was employed to exploit inherent correlations within the data, in order to recover low-rank matrices from a substantially limited number of measurements. On the other hand, the use of TC was motivated by the fact that two-way matrices are unable to preserve the higher structural complexity needed for simultaneously encoding data from a variety of sources. An experimental evaluation was performed on two datasets of different sizes, demonstrating that TC achieves a reduced reconstruction error as the fill ratio increases, in contrast to the MC approach, where an increase in the fill ratio above 0.2 did not improve considerably the reconstruction performance.

## 5 Event Diagnosis

### 5.1 Extreme Event Detection

In an industrial setting, the distributed autonomous sensing envisioned by SmartWater2020 will be further exploited to produce intelligent reasoning over the acquired data by supporting advanced operations, such as querying, high-level analysis, and alerting. In particular, a high-level data management and analysis (HDMA) module is an integral part towards an efficient decision making. Typically, an HDMA component comprises of collaborating computational nodes, which observe and control distinct physical entities and dynamic phenomena. Rather than relying on single sensor stream statistics, such as average and standard deviation, which is the customary approach in most data analysis systems, an efficient HDMA module focuses on finding and extracting inherent information for detecting behavioral variations in the acquired data. This is crucial, especially in a SWN framework, since the accurate and timely detection of abnormal changes in sensor measurements will enable early actuation aiming at minimizing operational and maintenance costs, as well as reducing the environmental effects due to the loss of valuable water.

Usually, the sensor nodes do not handle any quality aspect of physical device data, but rather interface with a high-level representation of the sensed physical world. In practice, the recorded sensor data are often incomplete, imprecise, or even misleading, thus impeding the task of an accurate and reliable decision making. Motivated by this, a powerful HDMA system should also cope with what we call uncertain data. *Uncertainty-aware data management* [126] presents numerous challenges in terms of collecting, modeling, representing, querying, indexing and mining the sensor data. Since many of these issues are interrelated, we address them jointly wherever possible. In contrast to most of the existing industrial SWN platforms, a versatile HDMA module considers uncertainty as an additional source of information that could be valuable during data analysis and thus it should be preserved.

Another major functionality assigned to a modern data analysis system is to perform high-level operations, such as the *notification of extreme events* from raw sensor data. Since the detection of abnormal behavior is affected by the underlying uncertainty, incorporation of its estimated value is expected to yield more meaningful results. More specifically, widely used methods for extreme events detection can be enhanced by incorporating the inherent data uncertainty, yielding an integrated uncertainty-aware HDMA (U-HDMA) system capable of identifying, quantifying, and combining the individual uncertainties corresponding to the most significant sources of uncertainty for providing early warning notifications of extreme events.

On the other hand, extracting highly *correlated pairs of data streams* acquired by distinct sensors is another important issue. Doing so, we aim at revealing interrelations between seemingly independent physical quantities, or guaranteeing the validity of a detected extreme event. Whereas traditional statistical machine learning provides well-established mathematical tools for monitoring and analyzing multiple data streams by exploiting potential pairwise correlations [127, 128], their performance is limited when processing heterogeneous and uncertain data streams. More specifically, [129] studies the problem of maintaining data stream statistics over sliding windows, with the focus being only on single stream statistics, while [130] introduced an extension for monitoring the statistics of multiple data streams, but the computation of correlated aggregates is limited to a small number of monitored sensor streams. On the other hand, [131] introduced a successful data stream monitoring system, which enables the computation of single- and multiple-stream statistics. However, its performance diminishes in an industrial environment, since the sensor streams we manage describe dynamic phenomena, whose distribution is not known a priori. Such limitations of previous approaches can be overcome by designing an appropriate stream correlation engine based on a computationally efficient similarity function, which enables fast and accurate monitoring of pairwise correlations between time-synchronized, possibly big, sensor data streams.

Fig. 25 summarizes the main functionalities to be supported by our proposed U-HDMA module, namely, (i) uncertainty estimation, (ii) correlations extraction, and (iii) detection of extreme events.

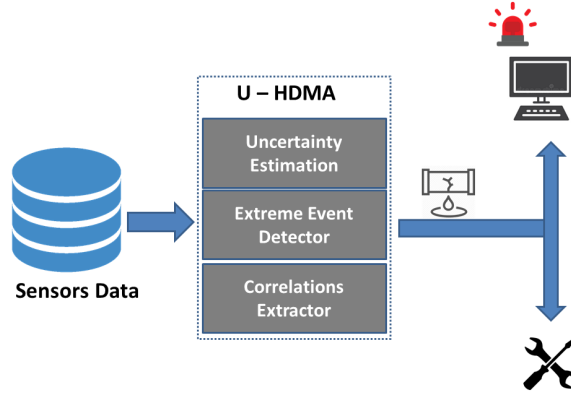


Figure 25: Building blocks of our uncertainty-aware high-level data analysis system.

### 5.1.1 Managing Uncertainty

In practice, the raw sensor data acquired by distinct sensors distributed across a SWN are often unreliable, imprecise, or even misleading. This yields results of unknown quality, which may impede the task of an accurate and reliable decision making. To this end, the notion of *measurement uncertainty* arises as an indicator of measurement quality. Speaking formally, the uncertainty is a *parameter associated with the result of a measurement, which characterizes the dispersion of the values that could reasonably be attributed to the measurand*, where a measurand refers to a quantity to be measured.

The underlying uncertainty may arise due to several distinct sources, such as, an incomplete definition of the observed quantities, sampling effects and interferences, varying environmental conditions, or hardware defections of the equipment. The effects of all these factors can be observed and quantified from the recorded sensor data only. For this purpose, a set of ordered steps need to be performed in order to obtain an estimate of the uncertainty associated with a measurement result. Fig. 26 presents the processing flow, which starts by identifying the measurands to be monitored and returns the overall estimated uncertainty.

Having specified appropriate measurands associated with our SWN application, such as temperature ( $^{\circ}\text{C}$ ) and pressure (bar), the next step is to identify the potential, most dominant, sources of uncertainty. To this end, the so-called *cause and effect* (or Ishikawa) diagram is exploited [132], which ensures comprehensive coverage, while helping to group similar sources and avoid double counting. Fig. 27 shows a typical cause and effect diagram for a temperature sensor. Its performance may be affected by several distinct factors, such as, its sensitivity and precision, calibration, and operating temperature. Furthermore, the accuracy of the acquired measurements depends also on the deployment density and location of the sensors, as well as on the sampling process. Possible misplacement or a very sparse time-sampling is expected to increase the uncertainty, especially when the monitored variables vary rapidly across time.

Towards assessing the underlying uncertainty component in a given raw sensor data stream we recall its distinction into two separate categories, namely, *type A* (aleatoric, statistical, or irreducible) and *type B* (epistemic, systematic, or reducible) uncertainty [133]. For instance, the physico-chemical properties of substances concentration, the operating conditions of the sensors and their manufacturing tolerances are typical examples associated with type A uncertainties, which

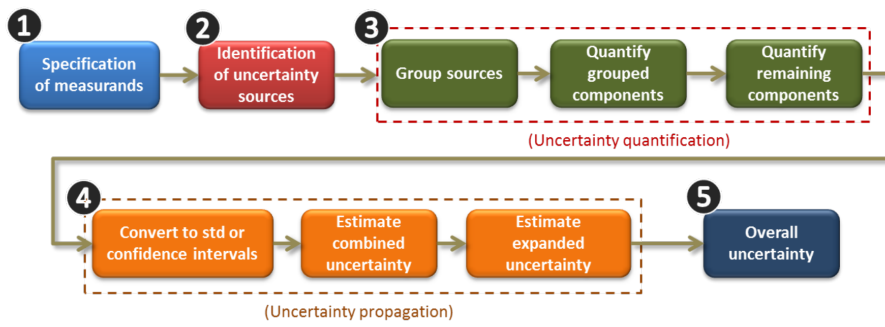


Figure 26: Flow diagram for uncertainty estimation in sensor data streams.

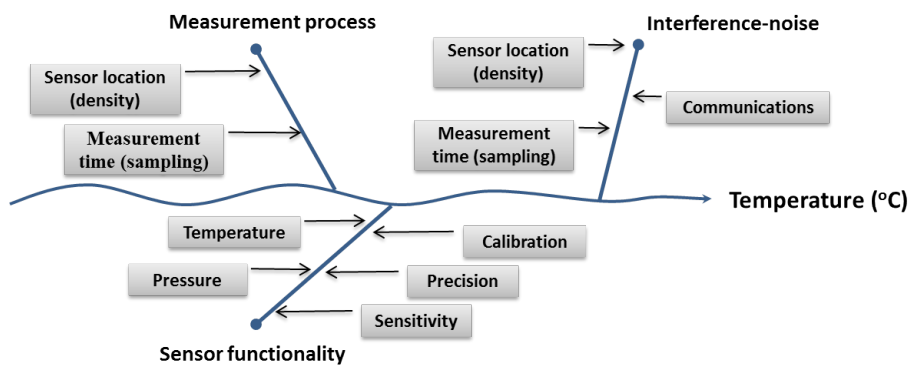


Figure 27: Cause and effect diagram for a temperature sensor.

cannot be reduced. On the other hand, the mathematical models, the calibration methods, and the inference techniques from experimental observations are typical sources of type B uncertainties, which can be reduced by improving the accuracy of our physical models or calibration methods.

Without going through much detail, in the following we introduce the main approaches for carrying out the steps 3 and 4 in Fig. 26. Specifically, uncertainties of type A are characterized by the estimated variances  $\sigma_i^2$ , which are obtained by statistical analysis of the measurements in the raw sensor streams. This is equivalent to obtaining a *standard uncertainty* from a probability density function derived from an observed frequency (empirical) distribution. Let  $\mathbf{y} = [y_1, \dots, y_N]$  be a vector of  $N$  sensor measurements, which correspond to a specific observed variable. Then, the standard uncertainty of  $\mathbf{y}$ , which is denoted by  $u(\mathbf{y})$ , is expressed in terms of the corresponding standard deviation  $\sigma_y$ , estimated directly from the observations  $y_i$ , as follows,

$$u(\mathbf{y}) = \frac{\sigma_y}{\sqrt{N}}. \quad (33)$$

For uncertainties of type B, the estimated “variance”  $s_j^2$  is obtained from an assumed probability density function based on our prior knowledge for the corresponding source of uncertainty, which may include: a) data from previous measurements; b) experience or knowledge of the properties of instrumentation and materials used; c) manufacturer’s specifications; and d) calibration data. In general, concerning type B uncertainties, the quantification is performed either by means of an external information source, or from an assumed distribution.

Typical assumptions for the prior distributions include the Gaussian (e.g. when an estimate is made from repeated observations of a randomly varying process, or when the uncertainty is given as a standard deviation or a confidence interval), the uniform (e.g. when a manufacturer’s specification, or some other certificate, give limits without specifying a confidence level and without any further knowledge of the distribution’s shape), and the triangular distribution (e.g. when the measured values are more likely to be close to a value  $\alpha$  than near the bounds of an interval with mean equal to  $\alpha$ ) [134]. For instance, if a manufacturer’s specification, or some other certificate, give limits in the form of a maximum range,  $y \pm \alpha$ , without any further knowledge of the distribution’s shape, then the estimated standard uncertainty is equal to  $u(\mathbf{y}) = \frac{\alpha}{\sqrt{3}}$ , while if the maximum range is described by a symmetric distribution then  $u(\mathbf{y}) = \frac{\alpha}{\sqrt{6}}$ .

Having expressed the individual uncertainties as standard uncertainties, the next step is to calculate the *combined standard uncertainty*. Although in practice there may exist correlations between the individual uncertainty sources, however, it is usually impossible to compute those correlations accurately. For this purpose, it is more convenient to rely on an assumption of independence between the individual uncertainty sources. In the following, let  $y = f(x_1, \dots, x_L)$  be an observed variable, which depends on  $L$  input variables  $x_l$  through a functional relation  $f(\cdot)$ . Then, the combined standard uncertainty of  $y$ , for independent input variables  $x_l$ ,  $l = 1, \dots, L$ , is given by

$$u_c(y) = \sqrt{\sum_{l=1}^L \left( \frac{\partial f}{\partial x_l} \right)^2 u^2(x_l)}, \quad (34)$$

where  $u(x_l)$  denotes the standard uncertainty of the input variable  $x_l$  (either of type A, or of type B), while the partial derivatives  $\frac{\partial f}{\partial x_l}$ , the so-called *sensitivity coefficients*, quantify how much the output  $y$  varies with changes in the values of the input variables  $x_l$ . It is also important to note that, before the evaluation of  $u_c(y)$ , we have to ensure that all the distinct standard uncertainties are expressed in the same units.

Finally, the combined standard uncertainty, which may be thought of as equivalent to one standard deviation, is transformed into an overall *expanded uncertainty*,  $U$ , which is the final output,

Table 5: Coverage factor as a function of confidence level for the Gaussian distribution

Coverage factor ( $k$ )	Confidence level (%)
$k = 1$	67%
$k = 1.96$	95%
$k = 2.576$	99%
$k = 2.3$	99.7%

via multiplication with a coverage factor  $k$ , that is,

$$U(y) = k \cdot u_c(y) , \tag{35}$$

where the value of  $k$  is determined by the desired confidence level of a Gaussian distribution, as shown in Table 5.

### 5.1.2 Uncertainty-aware Early Warning

Another major functionality assigned to a modern data analysis system is to perform high-level operations, such as the notification of extreme events from raw sensor data. Since the detection of abnormal behavior is affected by the underlying uncertainty, incorporation of its estimated value is expected to yield more meaningful results. More specifically, widely used methods for extreme events detection can be enhanced by incorporating the inherent data uncertainty, yielding an integrated uncertainty-aware HDMA (U-HDMA) system capable of identifying, quantifying, and combining the individual uncertainties corresponding to the most significant sources of uncertainty for providing early warning notifications of extreme events.

Extreme events can occur at any phase and time instant of the SWN infrastructure’s operation, which necessitates its continuous and efficient monitoring to achieve early detection of abnormal behavior. Although a typical SWN setting is generally intended to operate autonomously, however, in extreme events it is of high significance to anticipate the impact of the detected events by triggering appropriate actuators in time. To this end, designing fast and accurate extreme event detectors for providing *early warning notifications* is a strong demand in order to guarantee the smooth operation of our SWN.

Among the several approaches, which have been introduced in the literature, *extreme value theory* (EVT) provides efficient algorithmic tools to assess the probability of events that are more extreme than any previously observed. Two approaches are the most widely used in practice for extreme value analysis, namely, the method of *block maxima* (BMax) [135] and the method of *peaks-over-threshold* (POT) [136, 137]. Depending on the application, each method has its own advantages and limitations. For instance, BMax is easier to apply and theoretical assumptions are less critical in practice. However, estimation errors can be large for relatively small block sizes. On the other hand, POT yields more independent exceedances than BMax, along with tighter confidence intervals. Its main drawback is that an independence assumption is critical, which may not hold in practice, and also the choice of an appropriate threshold is somewhat ambiguous in practice resulting in a less easier implementation. Furthermore, in both cases, the detection of extreme events is based on the raw data without accounting for their underlying uncertainty. In addition, given our major requirement for providing timely notifications of abnormal behavior, the selected extreme events detection method must have a small computational complexity, without sacrificing the detection accuracy. The simplest approach to satisfy both requirements, that is, to exploit the inherent data uncertainty while being computationally efficient, is obtained by modifying an alternative widely used method, the so-called *compliance with operating limits* (COL).

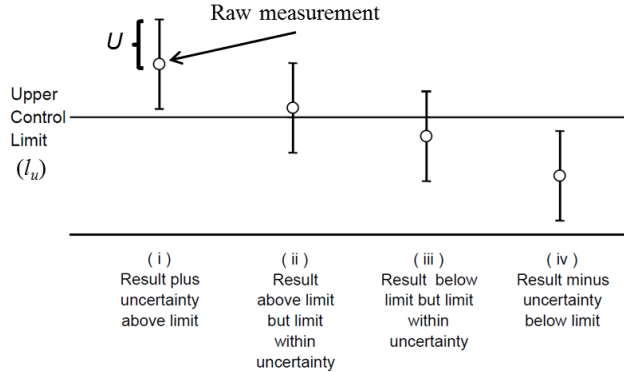


Figure 28: Compliance of uncertainty-augmented measurements with a predetermined upper operating limit.

Without loss of generality, in the following, we focus on the case of an upper operating limit, however, the same remarks are straightforward when compliance with a lower operating limit is required. More specifically, let  $l_u$  denote an upper operating limit dictated by a manufacturer or a specification standard. In addition, let  $\tilde{y} = y \pm U$  be a measurement augmented by its associated expanded uncertainty interval. In contrast to the typical COL method, for which only two cases exist when checking for compliance between the raw measurement  $y$  and the upper limit  $l_u$ , as shown in Fig. 28 there are two additional cases for its uncertainty-aware counterpart, hereafter denoted as U-COL. Specifically, the four possible cases of U-COL are as follows: (i) both the measurement and the expanded uncertainty interval are above the upper limit  $l_u$ ; (ii) the measurement is larger than  $l_u$  and the expanded uncertainty interval contains  $l_u$ ; (iii) the measurement is lower than  $l_u$  and the expanded uncertainty interval contains  $l_u$ ; and (iv) both the measurement and the expanded uncertainty interval are below  $l_u$ . Among them, only case (i) triggers clearly an alerting notification for the occurrence of an extreme event, while (iv) is the only one which is in compliance with the specifications. On the other hand, in cases (ii) and (iii) we cannot infer with absolute certainty whether an alert should appear or not. Nevertheless, in applications with profound social impacts, as is the case of reducing losses in a water supply network, a system operator should classify cases (ii) and (iii) as possible divergences from normal operation, and thus draw more attention on the associated monitored variables.

### 5.1.3 Fast Extraction of Data Stream Correlations

Fast and accurate identification of highly correlated pairs of data streams acquired by distinct sensors is another key functionality of a robust HDMA module. Doing so, we aim at revealing interrelations between seemingly independent physical quantities, or guaranteeing the validity of a detected extreme event. Nevertheless, the degree of “high correlation” is related to the specific application and the end-user, who has the flexibility to define how much strict this degree will be.

Extraction of pairwise correlations yields a partition of the set of available sensors into subsets of highly correlated sensors. This clustering facilitates the monitoring of the overall infrastructure by a system operator, who focuses only on a subset of sensors, where an abnormal behavior has been detected for at least one of its members. In the following, let  $\mathbf{x} \in \mathbb{R}^N$ ,  $\mathbf{y} \in \mathbb{R}^N$  be two sensor streams of length  $N$ , and  $\mathbf{x}_w = [x_{t_1}, \dots, x_{t_w}]$ ,  $\mathbf{y}_w = [y_{t_1}, \dots, y_{t_w}]$  be two time-synchronized windows of size  $w$ . The typical approach for extracting pairwise sensor stream correlations is by means of

the Pearson's correlation coefficient, which is defined by

$$\text{corr}(\mathbf{x}_w, \mathbf{y}_w) = \frac{\sum_{i=1}^w x_{t_i} y_{t_i} - w \bar{x}_w \bar{y}_w}{(w-1) \sigma_{x_w} \sigma_{y_w}}, \quad (36)$$

where  $\bar{x}_w, \bar{y}_w$  are the means of  $\mathbf{x}_w$  and  $\mathbf{y}_w$ , respectively, and  $\sigma_{x_w}, \sigma_{y_w}$  denote their corresponding standard deviations.

From a computational perspective, the main limitation is that the correlation coefficient has to be recalculated for each newly acquired measurement, which increases the computational burden, especially for big data streams or for a large number of sensors. To this end, a computationally efficient solution was proposed based on the use of the discrete Fourier transform (DFT). Working in a DFT framework, each sample  $x_{t_i}$  (similarly  $y_{t_i}$ ) can be expressed as a linear combination of exponential functions

$$x_{t_k} \approx \frac{1}{\sqrt{w}} \sum_{f=0}^{K-1} X_f e^{\frac{i2\pi f k}{w}}, \quad k = 1, \dots, w, \quad (37)$$

where  $X_f, f = 0, \dots, K-1$ , is the set of  $K$  DFT coefficients, with  $K < w$ . Doing so, the computation of the correlation coefficient in (36) is performed in terms of DFT coefficients. In our U-HDMA system we are interested in identifying and tracking highly correlated sensor pairs in an online fashion by also incorporating the estimated data uncertainty. Aiming at improving the computational performance of the DFT-based approach, while maintaining its accuracy, in our U-HDMA system the problem of extracting highly correlated pairs of sensors is translated into a problem of identifying highly *similar* sensors, where the similarity is measured by an appropriately designed function.

Let  $\mathbf{x}$  be the reference sensor stream and  $\{\mathbf{y}_1, \dots, \mathbf{y}_C\}$  the set of candidate streams. At the core of our fast and robust correlation extractor is an efficient *peak similarity* function. Given two windowed, yet time-synchronized, data streams  $\mathbf{x}_w, \mathbf{y}_{i,w}, i = 1, \dots, C$ , the corresponding expanded uncertainties  $U_{x_w}, U_{y_{i,w}}$  are estimated first. Then, the uncertainty-augmented windows are formed:  $\mathbf{x}_w^U = \mathbf{x}_w + U_{x_w}$  (or  $\mathbf{x}_w^U = \mathbf{x}_w - U_{x_w}$ ),  $\mathbf{y}_{i,w}^U = \mathbf{y}_{i,w} + U_{y_{i,w}}$  (or  $\mathbf{y}_{i,w}^U = \mathbf{y}_{i,w} - U_{y_{i,w}}$ ). After their normalization to mean zero and variance one,  $\hat{\mathbf{x}}_w^U$  and  $\hat{\mathbf{y}}_{i,w}^U$ , respectively, the  $M$ -sized ( $M \ll \frac{w}{2}$ ) truncated DFTs are computed,  $\hat{\mathbf{X}}_w^U = \mathcal{F}\{\hat{\mathbf{x}}_w^U\}$ ,  $\hat{\mathbf{Y}}_{i,w}^U = \mathcal{F}\{\hat{\mathbf{y}}_{i,w}^U\}$ . Finally, our *uncertainty-aware peak similarity* function is defined as

$$p_{sim,U}(\mathbf{x}_w, \mathbf{y}_{i,w}) = \frac{1}{M} \sum_{j=1}^M \left[ 1 - \frac{|\hat{\mathbf{X}}_{w;j}^U - \hat{\mathbf{Y}}_{i,w;j}^U|}{2 \cdot \max(|\hat{\mathbf{X}}_{w;j}^U|, |\hat{\mathbf{Y}}_{i,w;j}^U|)} \right], \quad (38)$$

where  $\hat{\mathbf{X}}_{w;j}^U$  denotes the  $j$ th element of  $\hat{\mathbf{X}}_w^U$  (similarly for  $\hat{\mathbf{Y}}_{i,w}^U$ ). Our U-HDMA system reports as *highly similar* those sensor pairs for which  $p_{sim,U}(\mathbf{x}_w, \mathbf{y}_{c,w}) > \epsilon_U$ . In order to account for the potential loss of information caused by the truncation of the set of DFT coefficients, as well as for the incorporation of the underlying uncertainties, special attention should be given on the selection of the threshold  $\epsilon_U$ . However, an automatic and adaptive rule to select an optimal threshold  $\epsilon_U$  is still an open question.

To illustrate the computational efficiency of  $p_{sim,U}$ , its performance is compared against the typical correlation coefficient and two state-of-the-art methods, namely, BRAID [138] and StatStream [131]. BRAID can handle data streams of semi-finite length, incrementally, quickly, and can estimate lag correlations with little error. On the other hand, StatStream resembles more the design principles of  $p_{sim,U}$  by finding high correlations among sensor pairs based on DFTs and a three-level time interval hierarchy. Fig. 29 compares the execution times of  $p_{sim,U}$  with the above three alternatives, as a function of the window size. The results reveal a significant improvement

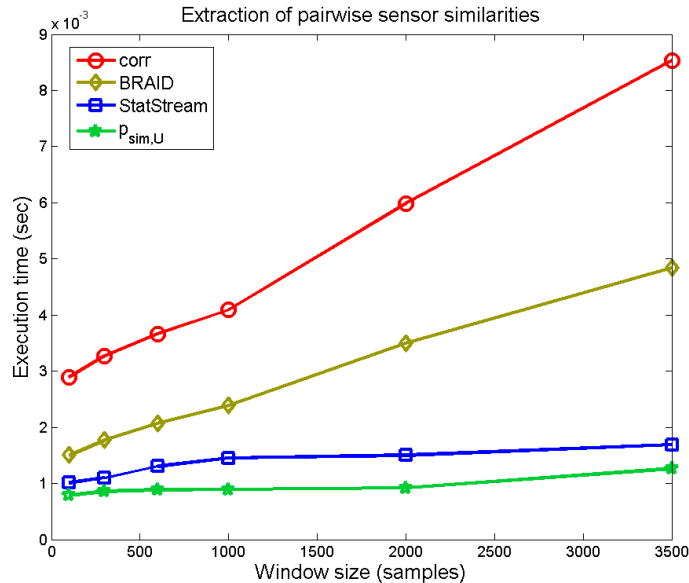


Figure 29: Comparison of execution times, as a function of the window size, between a) uncertainty-aware peak similarity ( $p_{sim,U}$ ), b) StatStream, c) BRAID, and d) correlation coefficient (corr).

in execution time achieved by  $p_{sim,U}$ , which is more prominent for higher window lengths. Most importantly, we observe that the execution time of  $p_{sim,U}$  remains almost constant over the whole range of selected lengths, in contrast to the naive (corr) and BRAID methods, whose execution times increase rapidly for increasing window length.

The BRAID algorithm, for which we set the correlation lag to zero, is characterized by gradual increase for increasing window size, since it employs all the values in the observed time interval. On the other hand, StatStream is based on a simple hash function of the mean of each sensor window. Keeping the integer part of the means, the data windows are mapped to appropriate cells in a grid structure. Doing so, only the correlations between neighboring cells are computed. The increased execution time of StatStream, compared to  $p_{sim,U}$ , is due to the hash function, which involves more computations for the mapping. It is expected though that the performance of StatStream could be enhanced by designing a more efficient hash function.

## 5.2 Leakage Event Detection

Water leaks in water distribution networks (WDN) can cause significant economic losses in fluid transportation and an increase on reparation costs that finally generate an extra cost for the final consumer. In many WDN, losses due to leaks are estimated to account up to 30% of the total amount of extracted water. Such burden is a very important issue in a world struggling to satisfy water demands of a growing population.

A selective literature review of transient-based leak detection methods was presented in [139]. These methods exploit the fact that any change in the physical (or propagation) structure of the pipe or system, such as a junction, constriction, expansion, blockage, roughness transition or leak imposes a wave reflection to an incoming transient signal, thus altering in some way a system's flow and pressure response. The localization of a leak is typically done via comparison of the pressure signal registered by monitoring devices relative to the signal that would be observed if the system

did not contain the leak or singularity. The second way in which a leak can be identified is through its role in pressure relief. As a high pressure wave passes, the leak causes some attenuation in the primary transient signal by permitting escape of some pressurized fluid.

Another review of leakage management related methods was presented by [19] and classify them as follows: (1) leakage assessment methods which are focusing on quantifying the amount of water lost; (2) leakage detection methods which are primarily concerned with the detection of leakage hotspots and (3) leakage control models which are focused on the effective control of current and future leakage levels. The review ends with the main conclusion that despite all the advancements made in the past, there is still a lot of scope and need for further work, especially in area of real-time models.

A leak magnitude estimation method is presented in [140] using continuous measurements of flow rates through the main supply line into a residential service zone are available during periods of low use. The sample mean and variance from the set of measured flow rates are computed as the set is truncated progressively from below. Trajectories of the sample statistics and their derivatives are plotted versus the level of data truncation. In the presence of leaks, these trajectories diverge from their expected theoretical path.

A methodology in [141] for evaluation of water losses is presented based on discrimination of physical losses in mains and service connections, and the volume of water consumed but not measured by meters. The water balance calculations consider that all non-measured consumption is an apparent loss. The methodology presumes that real losses in certain physical states of a network are a function of pressure, while apparent losses are a function of consumption patterns (i.e., domestic, industrial, institutional, etc.).

Covas et al., (2005) [142] investigate leakage detection and localization in pipe systems by means of the standing wave difference method (SWDM) used for cable fault location in electrical engineering. This method is based on the generation of a steady-oscillatory flow in a pipe system, by the sinusoidal maneuver of a valve, and the analysis of the frequency response of the system for a certain range of oscillatory frequencies (active fault detection?). A leak creates a resonance effect in the pressure signal with a secondary superimposed standing wave. The pressure measurement and the spectral analysis of the maximum pressure amplitude at the excitation site enable the identification of the leak frequencies and, consequently, the estimation of the leak approximate location.

The leak detection problem is formulated and solved in [143], as an inverse problem with unknown leak areas being the calibration parameters. A stochastic leakage detection methodology is developed and used. This methodology is based on the Shuffled Complex Evolution Metropolis (SCEM-UA) algorithm and is capable of estimating the posterior probability density functions of unknown leak areas in a single model run.

A model-based approach for sensor fault detection is used in [144] and a diagnosis strategy based on fuzzy residual analysis. Analytical redundancy is used to detect and isolate faults on sensors; specifically, parity functions are used to generate residuals; a parity function is an algebraic or a differential relationship based on a model process and observed measurements such that the measurement noise can be neglected. In the absence of fault, the residual is zero and when a fault occurs the residual takes a nonzero value. A theoretical matrix of fault signature is defined by coding with binary variables the occurrence of variables in the different residuals. This method relies upon the residuals fuzzification.

Morais et al. (2007) [145], propose a group decision-making model based on PROMETHEE V method to aim a leakage management strategy, which takes into account the points of view of four stakeholders, selecting feasible options, and considering the available budget as constraint. Thus, this strategy is the combination of options that will efficiently meet technical, socio-economic and environmental criteria to achieve sustainable development.

A steady-state network simulation model is presented in [146] using classical hydraulic repre-

sentation, pressure-driven demand and leakage at the pipe level, with aim to demonstrate a more realistic leakage analysis.

A complex hybrid model is presented in [147] based on a synergetic combination of deterministic and machine learning model components. State estimation is performed using a technique borrowed from machine learning, specifically a neuro-fuzzy approach. The quantification of the uncertainty of the input data (telemetry measures and demand predictions) can be achieved by means of robust state estimation. By making use of the mathematical model of the network, estimated states together with uncertainty levels, that is to say, fuzzy estimated states, for different anomalous states of the network can be obtained. These two steps rely on a theory-driven model. The final aim is to train a neural network (using the fuzzy estimated states together with a description of the associated anomaly) capable of assessing WSS anomalies associated with particular sets of measurements received by telemetry and demand predictions. This is the data-driven counterpart of the hybrid model.

Perez et al. (2011) [148] propose a leakage localization method based on the pressure measurements and pressure sensitivity analysis of nodes in a network. The same methodology is also described in [149]. Simulations of the network in the presence and the absence of leakage may provide an approximation of this sensitivity. A binary matrix is assumed as a signature matrix for leakages. A trade-off is identified between the resolution of the leakage isolation procedure and the number of available pressure sensors. To maximize the isolability with a reasonable number of sensors, an optimal sensor placement methodology, based on genetic algorithms. The sensor placement methodology was later described in [150].

Another methodology described in [151] and [152] performs leak detection, isolation and estimation computing residuals which are obtained comparing measured pressures (heads) in selected points of the network with their estimated values by means of a Linear Parameter Varying (LPV) model and zonotopes. The structure of the LPV model is obtained from the non-linear mathematical model of the network. The proposed detection method takes into account modelling uncertainty using zonotopes. The isolation and estimation task employs an algorithm based on the residual fault sensitivity analysis.

Gertler et al. (2010) [153] use pressure measurements and the application of principal component analysis to the fault diagnosis.

This team published a more detailed explanation of the model-based methodology for leak localization using pressure sensors and an application to a real network (Barcelona) in [154].

Islam et al. (2014) [155] propose an integrated framework for different kinds of faults in a network including water quality failures. The leakage detection and localization module uses many kind of data, such as traffic, temperature, soil type, pipe parameters as well as estimated hydraulic conditions to assess the possibility of a leakage at each pipe of the network.

A burst detection methodology is presented in [156] that utilizes sensor data in a district metered area using a data assimilation method (Kalman Filtering) and a hydraulic model. A sensitivity analysis was applied to evaluate the performance of various burst detection metrics under different conditions, and to identify appropriate thresholds for online burst detection using artificial generated burst events.

Romano et al. (2014) [157] present a methodology for the automated near-real-time detection of pipe bursts and other events that induce similar abnormal pressure/flow variations (e.g., unauthorized consumptions) at the district metered area (DMA) level. The new methodology makes synergistic use of several self-learning artificial intelligence (AI) techniques and statistical data analysis tools, including wavelets for denoising of the recorded pressure/flow signals, artificial neural networks (ANNs) for the short-term forecasting of pressure/flow signal values, statistical process control (SPC) techniques for short- and long-term analysis of the pipe burst/other event-induced pressure/flow variations, and Bayesian inference systems (BISs) for inferring the probability of a pipe burst/other event occurrence and raising corresponding detection alarms.

A methodology to detect leakages in a District Metered Area (DMA) with standard flow sensors to monitor the water inflow is proposed in [158]. The water inflow signal is normalized to remove yearly seasonal effects, and a leakage fault detection algorithm is presented, which is based on learning the unknown, time-varying, weekly periodic DMA inflow dynamics using an adaptive approximation methodology for updating the coefficients of a Fourier series; for detection logic the Cumulative Sum (CUSUM) algorithm is utilized.

An online fault detection approach for critical infrastructures based on a model-based fault diagnosis architecture for nonlinear uncertain discrete-time systems, with bounded modelling uncertainties is presented in [159]. A testbed has been developed (5 tank system), to emulate the operation and common faults of a critical infrastructure (i.e., a water supply system), as well as its interaction with a SCADA system.

A leak-detection and localization approach to be coupled with a calibration methodology that identifies geographically distributed parameters is proposed in [160]. The approach proposed consists in comparing the calibrated parameters with their historical values to assess if changes in these parameters are caused by a system evolution or by the effect of leakage. The geographical distribution allows unexpected behavior of the calibrated parameters (e.g., abrupt changes, trends, etc.) to be associated with a specific zone in the network.

### 5.3 Quality Event Detection

A drinking water distribution network (DWDN) is an interconnected collection of pipes, water sources and hydraulic control elements such as pumps, valves and tanks, that delivers to consumers water at the demanded quantity and pressure. Drinking water delivered to consumers should contain a small disinfectant residual in order to reduce the risk of human exposure to pathogens. A number of water utilities use chlorine for disinfection because it is inexpensive and effectively controls a number of disease-causing organisms. The regulation of chlorine concentration in drinking water, also referred to as water quality, requires chlorine injection stations. For monitoring chlorine concentration, chlorine sensors are used and regulation is performed either by a human operator, or automatically using real time sensor measurements and feedback control algorithms. Water quality monitoring and control is an important issue since customer complaints can occur if the disinfectant applied to the water is not regulated properly, but most importantly, in the case of a contamination event, thousands of people can be affected if not detected in time.

Water contamination warning systems (WCWSs) are typically deployed to monitor the quality of water. At the same time, wireless sensor networks (WSNs) have found extensive applications in monitoring physical or environmental conditions such as temperature, sound, pressure, etc. Therefore in this context, WCWSs have been one of the most recent embodiments of WSNs. The idea of a contamination warning system CWS has been highlighted by recent attention on making water distribution networks more robust against intentional contamination events. Several authors have demonstrated different detection algorithms in order to improve event detection in WDN. The contamination event detection approaches based on water quality measurements consist of two phases. The first phase is to set up the prediction model with the historical data as the training dataset. The second one is to determine the water quality by comparing the predicted values with the measurements. Various approaches have been proposed for addressing the problem of contamination detection, using single or multiple-type measurements which are analyzed separately or in combination, from one or more locations in the network, using model-based or model-free approaches.

In the threshold-based approaches, the threshold values are set through statistical models. Simplicity is the main advantage since raw data can be directly processed. The abnormal event detection with two thresholds were adopted in [161]. However, the threshold-based approaches cannot obtain the spatio-temporal feature of water quality data, which results in low accuracy and high false

positives of event detection. In the pattern matching approaches, the pattern is established and verified with water quality sensor readings to infer the contamination event [162]. Byer and Carlson assumed that the water quality parameters obey a Gaussian distribution. One statistical model was established to detect contamination events [163]. The statistical model detection methods cannot be used in the applications.

Learning-based methods can make inference of the possibility of contamination events based on the temporal and spatial correlation of water quality measurements [164, 165]. It was promising to make full use of the spatial and temporal correlation to detect contamination events.

Markov random fields (MRFs), Bayesian network (BN), dynamical BN, and SVM are common models in the WSNs with the high density. MRFs were adopted to model spatial context and stochastic interaction among observable quantities [166]. BN is considered as a means for unsupervised learning and anomaly detection in gas monitoring sensor networks for underground coal mines [164]. Perelman proposed a BN-based contamination event detection method to determine the event occurrence through estimating the possible locations of potential contaminants in WSNs [167]. One improved water-contamination events detection based on D-S theory was proposed to predict water quality parameters with on-line water quality sensors [168]. The contamination event detection algorithm based on principal component analysis (PCA) has been presented [169]. The PCA was applied to the normalized measurement. Then, the alarm index and the threshold of the alarm were obtained. In addition, a spatio-temporal model was adopted to detect the contamination events with water sensor networks [170]. A multiple type measurement approach at a single location was proposed in [163], where each parameter was compared to its three bounds. Control charts and Kalman filters have also been proposed in [171]. When multiple types of sensors are available, these can be used to compute distance metrics to detect contamination [172]. The probability of contamination events could be computed and compared to an adaptive threshold by utilizing a sequential Bayesian rule [173]. The estimation error of event detection was computed with respect to the measurements from a moving window [25]. Moreover, the S- placement toolkit [174] was used for computing at which locations to install contaminant sensors in water distribution systems to reduce the impact risks. Eliades and Polycarpou (2010) proposed a solution methodology for the sensor-placement problem by considering several risk-objectives including the state-space representation of the propagation and reaction dynamics, coupled with the impact dynamics describing the damage caused by a contamination under certain impact metrics. In addition, the US Environmental Protection Agency provides the event detection tool-CANARY [175] for time series analysis of multiple water quality parameters. Fluctuations in water distribution networks may cause significant variability, a Bayesian belief network was presented to infer the probability of contamination [176].

Based on the above analysis, most approaches for contamination event detection have been discussed via using single type water quality parameters. There are multiple components to indicate water quality in a WSN, such as free chlorine, EC, pH, temperature, TOC, and turbidity. Unfortunately, a single parameter of water quality cannot reflect the real water quality in a WSN. When a contamination event occurred, the observable values of multiple water quality parameters changed in a significant way. The contamination event detection methods based on single parameter may result in low detection accuracy and high false alarms. To improve the detection accuracy and reduce the false alarms, multiple parameters of water quality should be considered to make a decision with data fusion. Eliades et al. 2014, 2015 proposed a model-based method for contamination event detection using real-time concentration lower-bound estimations as well as multi-level thresholds, for enhancing detection and reducing detection delay while minimizing false positive alarms [177, 99]. Monte-Carlo simulations use the nonlinear model to obtain uncertainty bounds by randomly generating and evaluating a large number of parameter sets or realizations [177]. This approach is computationally intensive and even with a large number of simulations some extreme cases may not be covered. Koch and McKenna, 2011 proposed an approach for combining data from

multiple stations to reduce false background alarms [178]. By considering the location and time of individual detections as points resulting from a random space-time point process, Kulldorff's scan test can find statistically significant clusters of detections. Karami et al. 2012 investigated the application of hierarchical wireless sensor networks in water quality monitoring [179]. Adopting a hierarchical structure, the set of sensors were divided into multiple clusters where the value of the sensing parameter is almost constant in each cluster. The members of each cluster transmit their sensing information to the local fusion center (LFC) of their corresponding cluster, where using some fusion rule, the received information is combined, and then possibly sent to a higher-level central fusion center (CFC). A two-phase processing scheme is also envisioned, in which the first phase is dedicated to detection in the LFC, and the second phase is dedicated to estimation in both the LFC and the CFC. They focused on the problem of decision fusion at the LFC: proposing hard- and soft-decision maximum a posteriori (MAP) algorithms, which exhibit flexibility in minimizing the total cost imposed by incorrect detections in the first phase. Liu et al. [28] proposed a method for real-time contamination detection using multiple conventional water quality sensors. Eight sensors were used in the case study. Furthermore, they extended their work by determining how the number of sensors influences the detection performance and identifying the optimal combination of sensor deployment. Mao et al. 2017 [180] proposed M-STED that utilizes a back propagation neural networks model to estimate the relationships between water quality parameters in a WSN. The proposed M-STED can detect potential contamination events for temporary analysis of multivariate water quality time series with Bayesian sequential analysis.

The water industry increasingly requires the estimation of WDN hydraulic state variables, such as water flows and pressures, in order to operate water systems efficiently, provide better customer service and assess the system behavior in order to detect and isolate water leaks or other emergency events. State estimation is enabled by gathering sensor measurements of flows and pressures at certain locations of the network through a Supervisory Control and Data Acquisition (SCADA) computer system. Then, using a mathematical model of the network, the state at all locations is estimated. However, this is a challenging task due to the complexity and large area covered by water networks. Water outflow due to consumer demands is difficult to be measured accurately, as this would require a smart water meter at every residence. Thus, sensor measurements are scarce and the state estimation problem is under-determined. A common practice in WDN is to skeletonize the network by treating a group of consumers as a single demand point. It is then possible to use *pseudo-measurements*, which are demand estimates determined from population densities and historical data, to obtain an observable system configuration for state estimation [181]. Furthermore, modelling uncertainty is a cause of serious estimation errors. Pipe parameters, such as pipe roughness coefficients, are rarely known accurately. Even with an observable sensor configuration, model calibration is required a priori or during state estimation for the procedure to produce feasible solutions [182, 183].

In standard state estimation techniques, statistical characterization of sensor measurement error is needed to give more weight to measurements originating from more accurate sensors. Using the Weighted Least Squares method, the nodal demands are adjusted to fit the constraints imposed by the measurements and produce the most probable state estimate [184]. Another approach is to use the Kalman Filtering method to provide a solution for the network state [185]. The state estimate is computed using measurements with known statistical error characterization, which also allows the derivation of the variance of this estimate. The above methods can produce a point in state-space, a procedure which is referred to as *point state estimation* [186].

The assumption of a known statistical characterization of sensor measurement error can lead to a serious miscalculation of the state estimation error in WDN. This is due to the use of pseudo-measurements, which do not have a statistical characterization and in the best case their estimation error is defined by an upper and lower bound. The case is similar for pipe parameters (e.g. length, diameter, roughness coefficient), for which the most accurate description that can be given for the

error of the parameter value is an upper and lower bound.

An alternative approach uses bounds for the representation of measurement and model parameter uncertainty. In contrast to point state estimation methods, the use of bounded uncertainty can provide upper and lower bounds on the state variables. This method is referred to as *interval state estimation*. In many applications, such as leakage detection and contamination detection, the derivation of a range of possible values for the state of the WDN provides useful information for event and fault detection methodologies. Hydraulic state bounds can be used to generate bounds on chlorine concentration in the water network or other chemicals in the water, by taking into consideration the uncertainty on decay rate [187]. These bounded estimates can be used to detect water leakages and prevent catastrophic scenarios such as wide area water contamination.

The use of bounds for the representation of measurement uncertainty and their incorporation into the state estimation cost function for WDN was introduced in [188]. This idea was developed in [18] as the *set-bounded* state estimation problem. The process of calculating uncertainty bounds for state estimates caused by inaccuracies of input data is referred to as Confidence Limit Analysis and it was solved using different approaches, including Neural Networks [189], the Error Maximization method [190], the Ellipsoid method and Linear Programming [191]. These methods have the disadvantage of using a linear approximation of the water network model, which does not guarantee that the calculated bounds contain all possible solutions based on the uncertainty.

## 5.4 Industrial Applications

Intelligent event detection algorithms have been developed in various distinct industrial applications. The most relevant ones to SmartWater2020 are reviewed below.

1. **Intelligent Management of Singapore Water Resources:** In this project [192], a platform was designed for the intelligent management of Singapore waters. Specifically, the proposed platform (WaterWiSe) (ref. Fig. 30) monitors, detects, and predicts abnormal events that may be indicative of structural pipe failures, such as bursts or leaks. There are two general complementary strategies for dealing with pipe bursts and pervasive leakage problems, namely, 1) the development of condition assessment tools that can identify existing leaks or evidence of pipe deterioration and hence, support rational asset management programs, and 2) the design of monitoring systems that can detect and localize underground events or sources of long-term water losses, enabling timely mitigation and repair actions.

A basic component of WaterWiSe is the Integrated Data and Electronic Alerts System (IDEAS), which is responsible for data stream management, processing and alert notification. IDEAS is equipped with a set of analytics tools that are applied to data streams in order to detect abnormal events and provide location estimates. A complementary component is the Decision Support Tools Module (DSTM), which employs the sensor data streams as an input to decision support tools that model the water network as a set of demand zones. When data processing is completed, the water consumption can be predicted in a 24-hours rolling window, along with a detection of those pipes that will present a low or reversed flow, as well as the localization of areas with abnormally low or high pressure.

2. **Extreme Events Detection - Heraklion Smart City:** In this project [193], the uncertainty-aware high-level data analysis module presented above was exploited to produce early alerts for abnormal behaviors in a smart city application scenario. As shown in Fig. 31, the key functionalities of the system are related to a) the quantification of uncertainties in raw sensor streams, and b) the estimation of extreme events by incorporating the inherent data uncertainty.

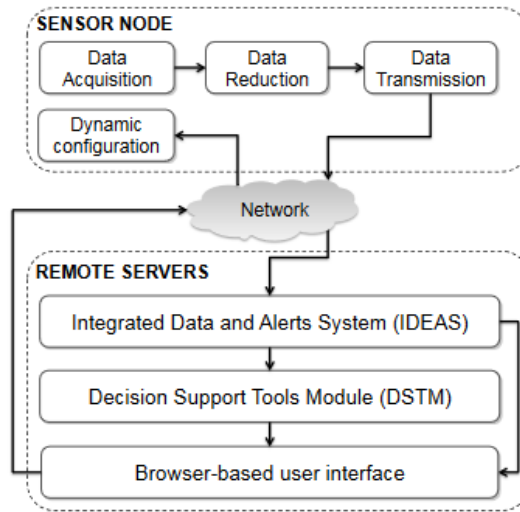


Figure 30: The architecture of the data processing platform of Singapore water management project (Image credits: [192]).

Specifically, the uncertainty quantifies the inherent imperfections in the acquired data. Then, driven by the demand of providing timely notifications of extreme events, the platform considers a modified version of the compliance-with-operating-limits method that incorporates the estimated uncertainty into the streaming data to detect the times when the observations exceed predefined upper or lower operational limits.

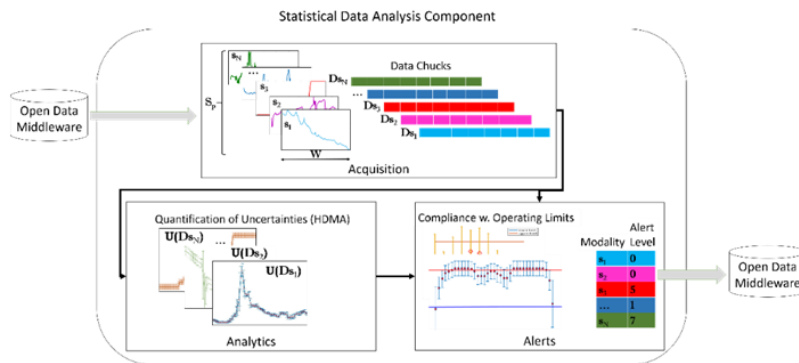


Figure 31: Uncertainty-aware high-level data analysis platform of the Heraklion Smart City project.

3. **Acoustic sensors** by Echologist (Fig. 32) are used for water loss management, leak detection, and pipe condition assessment, for a Transmission Main Leak Detection pilot survey [194]. Echologics' technology substantially reduces both electronic "white" noise as well as ambient background noise. Echologics apply in United Water New Jersey (UWNJ) acoustic sensors specifically developed for detecting leaks in large diameter mains, including sections of pipe where standard appurtenances were not available. With this technology leak detection service, gave the ability to UWNJ to quickly repair the leak avoiding potential failure.



Figure 32: Echologics acoustic sensors.

4. **Vibro-acoustic sensor monitoring** has been developed by TrunkMinder [195] (Fig. 33) with the ability to identify leaks including small emerging and emergent leaks that can be the precursor to a catastrophic failure, the immediate detection of bursts, the ability to record and analyze real-time operational conditions within their critical infrastructure and the ability to pinpoint leaks and bursts to within 1m on site. In order to determine the effectiveness of the technology a long term trial was arranged for TrunkMinder in a particularly challenging environment in London where there were previously surveyed leaks along a stretch of critical trunk main.
5. **A permanent leakage monitoring system** was provided by Gutermann [196] called ZoneScan ALPHA system (Fig. 34). This system comprises of correlating noise loggers, radio repeaters and ALPHA data collection modules. The noise loggers are deployed magnetically on valves and hydrants, the repeaters are installed on street lamps and the ALPHA were deployed on the top of a hill overlooking the town. The ALPHA collect the information from the loggers every day via the repeaters using radio communication and then send the data to the web host using GPRS. This system was employed in Eislingen in Southern Germany and provide immediate results notifying them of the location of all the leaks.
6. The first battery powered electromagnetic flow meter equipped with the GPRS wireless communication protocol were developed from ISOIL INDUSTRA [197]. They have installed hundreds of ISOIL FLOWIZ™ flow meters, mainly DN 100-250, with provision for the measurement of volumes, flow rates and pressures in Manila and Philippines. The meters installed



Figure 33: Trunkminder: Installation of head unit on trunk main.

permit the transfer of the captured data to a server over the Internet using dedicated software installed and managed through our local partner. The project has enabled the Water Authority to significantly reduce water losses compared to the previous situation.

7. **A real-time hydraulic model** was applied in Abu Dhabi in corporation with Schneider Electric, Abu Dhabi Water and Electricity Authority (ADWEA) [198]. The integrated system-Aquis, is consisting noise loggers and remote and automated meter readers. The system was capable of calculating water balances, optimizing chlorination, identify new bursts and prioritize the work on reducing the background leakage.
8. A new product for water monitoring, spectro:lyser, developed by S::can [199], that measures the entire absorption spectrum and is used by many drinking water providers all over the world as a key component in their raw water monitoring (Fig.35). The measured parameters include TSS, turbidity, NO<sub>3</sub>-N, COD, BOD, TOC, DOC, UV<sub>254</sub>, color, BTX, O<sub>3</sub>, H<sub>2</sub>S, AOC, temperature and pressure, depending on the application. Therefore, for water monitoring, a decentralized event detection system based on s::can's moni::tool, that continuously analyzes four spectral alarm parameters to detect changes resulting from untypical, possibly harmful, water quality events, have to be applied.
9. The Philadelphia Water Department (PWD) and Water Revenue Bureau serve the Greater Philadelphia region, implemented WISKI (Water Information Systems KISTERS) (Fig.36) as its OWQM data management system. Kisters [200] is a global software solutions and technology firm dedicated to effective long-term management of water resources. WISKI is



Figure 34: The ZoneScan monitoring system: (a) Loggers on a pipe, (b) Repeater set and (c) Alpha set

a N-Tier solution, Presentation Layer, Business Logic Layer and Data layer. All calculations are managed by the business logic layer (Time Series Manager) to provide a thin client and optimize the time for data processing. WISKI has the ability to store any time series data type with resolution down to a one second data raster.

10. Gestione Acque SpA in order to solve their problem to determine the correct amount of hypochlorite that would need to be dosed into the water, and ensure a reliable control of the hypochlorite dosing they applied Hach's colorimetric chlorine analysers [201]. Hach's CL17 Colorimetric Chlorine (Fig.37) new analysers have reliable readings even at low chlorine values, do not produce any signal drift and practically require no calibration after the first six months of use.

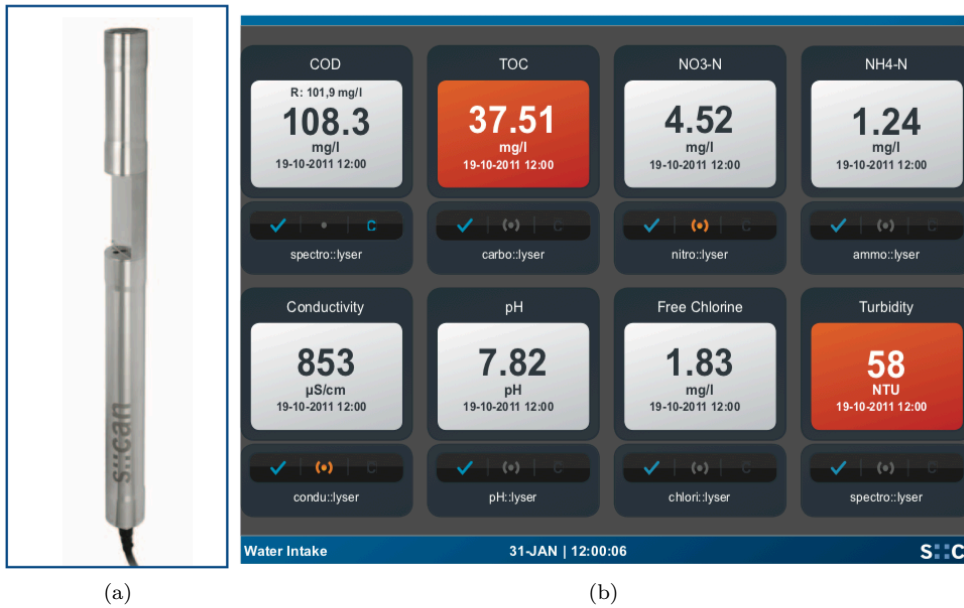


Figure 35: S::can's monitoring system: (a) Scan::Lyser and (b) S::can's monitoring tool

## 6 State-Estimation and Control

A water distribution network is the infrastructure responsible for delivering drinking water to consumers. Water enters the network after it has been collected from rivers, lakes, dams or underground sources and has been cleaned at treatment plants. Water distribution networks are comprised of pipes which are connected to storage tanks, reservoirs or other pipes using junctions, starting from the facilities of the water provider and reaching all the consumers. Water is supplied to consumers through various points in the network, namely the outflow nodes. Valves are usually installed to some of the pipes to reduce flow or pressure, or to isolate or close part of the network. Pumps deliver energy to the system by increasing the pressure at some locations. Both valves and pumps are considered as hydraulic actuators, which may be controlled through automated or manual feedback signals. Tanks which are connected to the network, fill or empty according to a time schedule or are regulated through feedback controllers. Demand is the water outflow due to consumer requests. Although such requests occur randomly throughout the day, in the macro-level they have some common characteristics, such as approximate periodicity or consumption patterns, which can be both learned and predicted.

In a water distribution network, hydraulic and quality parameters are usually measured through a Supervisory Control And Data Acquisition (SCADA) system. Hydraulic monitoring is quite common for water utilities, which measure flow and pressure at various points of the network in order to observe consumption behaviour and detect leaks. Quality monitoring, on the other hand, is more recent and involves performing mostly manual sampling or installing quality sensors at various locations, to determine the chemical concentrations of various chemical species such as chlorine (used for disinfection) or certain contaminants.



Figure 36: WISKI(Water Information Systems KISTERS) system.

## 6.1 Leakage Risk Estimation

Risk assessment tool of WDSs is a proactive management strategy that assists network owners to evaluate the condition of their network, to assess historical incident, real time measurements and risk of failure data so to prioritize the work / rehabilitation based on the inherent risks and the cost of action. WDN engineers will thus be able to prepare a proactive and organized service plan for their WDS. Furthermore, the network managers can use such a tool in cases where they have to: (1) decide the replacement or repair of a deteriorating network part and, (2) prioritize restoration of simultaneous leakage incidents. This, in turn, helps them to manage their networks in a more efficient way so they can minimize their operational and maintenance costs (Agathokleous 2015).

The need for vulnerability analysis is compounded by the importance of WDNs in our lives, as they constitute one of the primary "lifeline networks" of modern urban societies. It is thus imperative to develop knowledge and to devise methods for assessing their state of affairs and their vulnerability under both normal and abnormal operating conditions (Christodoulou et al. 2018). Furthermore, WDN vulnerability relates to water quality and the risks to the consumers' health, as natural or malicious threats to the WDN threaten the health and well-being of the citizens that the WDN serves. Pipe deterioration leads to pipe breakages, breakages lead to water loss and to infiltration of pathogens in the network, pathogens lead to water contamination, contamination leads to health threats for the population being serviced by the WDN (Christodoulou et al. 2018). Finally, WDN vulnerability is associated with the disruption of residential, commercial and industrial activities and the cause of severe direct and indirect economic losses which, in the case of indirect losses, are higher the more developed the society is. Direct losses relate to the cost of repair, while indirect losses relate to the way the economy is affected by the disruption of the lifeline (Christodoulou et al. 2018).

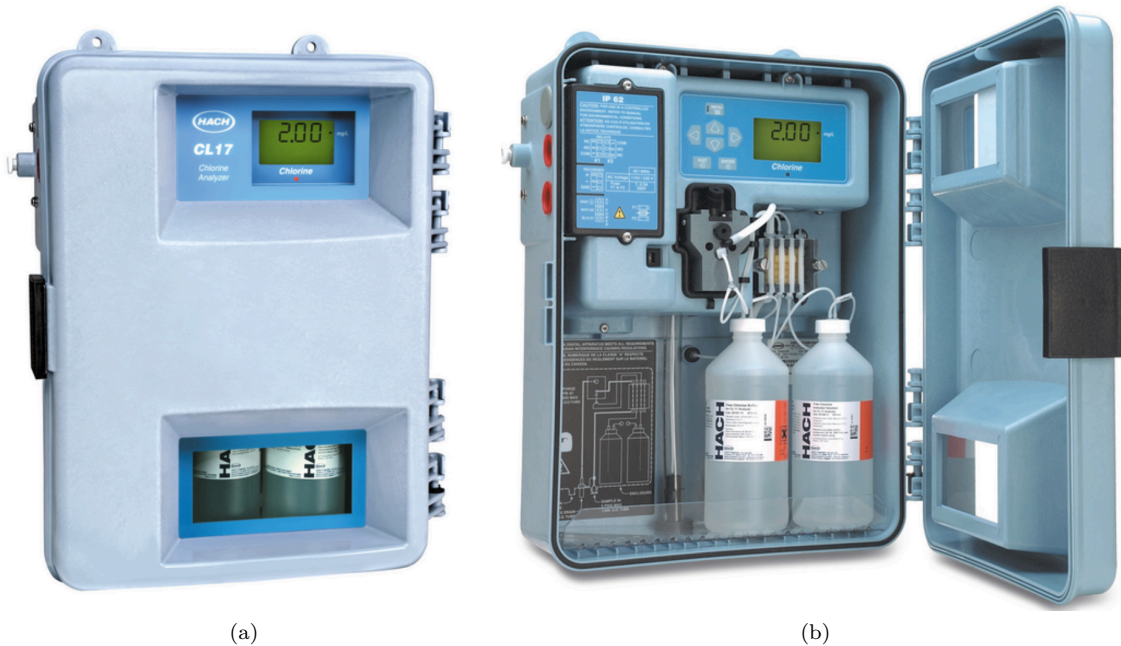


Figure 37: CL17 Colorimetric Chlorine Analyser

## 6.2 Hydraulic Dynamics

The hydraulic analysis problem in water distribution networks is defined as the problem of computing the hydraulic head at each junction and the flows at each pipe. To solve this problem, the topology of the network and pipe characteristics, the control inputs, as well as the demand at each node, need to be known. In general, structural information of the network is available by the water utilities; however, pipe characteristics may require field measurements, and nodal demands at each discrete can only be estimated using historical data and other hydraulic measurements available, if no online demand sensors are used by the utility to monitor each consumer.

In general, a set of ordinary differential equations can be used to describe the dynamic relation of water flow in pipes and the differences in the hydraulic heads [202]. However, in practice, approximation of the actual hydraulic dynamics are considered in discrete time, in steady state, and by using an iterative optimization algorithm (e.g. gradient descent), the heads and flows are computed, so that the conservation of mass and energy is satisfied, e.g. [203].

To establish the notation, consider a water distribution network composed of pipes, junctions and water storages. The topology of this network can be represented as a graph with edges corresponding to pipes, and nodes corresponding to junctions and water storages. At discrete time  $k$  with sampling time  $\Delta t$ , let  $d_i(k)$  be the consumer demand outflow at the  $i$ -th junction node, and let  $q_j(k)$  correspond to the flow in the  $j$ -th pipe connected to junction  $i$  ( $j \in \mathcal{A}_i$  where  $\mathcal{A}_i$  is the set of pipe indices which are connected to the  $i$ -th node, assuming that inflows have a positive sign and outflows have a negative sign). In accordance to the principle of mass conservation, the sum of all the pipe inflows and pipe outflows must equal to the demand (Kirchhoff's junction rule),

$$\sum_{j \in \mathcal{A}_i} q_j(k) = d_i(k).$$

Furthermore, in accordance to the principle of energy conservation, the flow-headloss relationship

across each link in the network must be balanced. Let  $h_i(k)$  be the *hydraulic head*, i.e. a measurement of water pressure expressed in length units, at the  $i$ -th node. For water moving from node  $j$  (higher head) to node  $i$  (lower head) with flow  $q_l(k)$  in the  $l$ -th pipe, the flow-headloss relationship is given by

$$h_j(k) - h_i(k) = f_h(q_l(k)) \quad (39)$$

where  $f_h(\cdot)$  is a nonlinear function, such that  $f_h(q_l(k)) = \alpha_r q_l(k)^{\alpha_f} + \alpha_m q_l(k)^2$ , which depends on the pipe resistance coefficient  $\alpha_r$ , the flow exponent  $\alpha_f$  and the minor loss coefficient  $\alpha_m$ . These parameters are computed using empirical methods; for example, by considering the *Hazen-Williams* headloss relation, the flow exponent is  $\alpha_f = 1.852$  and the resistance coefficient  $\alpha_r$  is calculated using a nonlinear function which takes as arguments the pipe diameter, the pipe length and a unitless roughness coefficient which depends on the pipe material and has been computed empirically. The minor loss coefficient  $\alpha_m$  is given empirically by the pipe fitting type [204]. Therefore, for a water distribution network, the set of hydraulic equations is constructed, and at each discrete time, a gradient optimization algorithm is solved using the current demand flows, control inputs and tank head [203].

Tanks are dynamic elements in the system and can be considered as nodes in the water distribution network; the head state of the  $i$ -th water tank node is given by

$$h_i(k+1) = h_i(k) + \frac{\sum_{j \in \mathcal{A}_i} q_j(k)}{f_{T_i}(h_i(k))} \Delta t,$$

where the tank head  $h_i(k)$  corresponds to the relative water level plus the tank elevation, and function  $f_{T_i}(\cdot)$  computes the cross-sectional area of the  $i$ -th tank at a certain height. Initial tank heads are typically known.

Currently, a number of off-the-shelf software are used to perform the hydraulic analysis in water distribution networks, such as the open-source EPANET [204]. To capture the time-variance of flows and pressure due to consumer water demands, these systems perform “extended-period simulations”, i.e. at discrete time  $k$ , solve the steady-state equations, compute the state of the dynamic elements in the network for  $k+1$  (i.e. the tanks), apply any control inputs and at discrete time  $k+1$ , repeat the procedure.

From a controls viewpoint, variations in demand flows are considered as time-varying disturbances, which affect flows in pipes and pressures throughout the network. In general, consumer demands are influenced by weather conditions, season, population growth, change of habits, even changes due to the response actions after a contamination. In practice, consumer demands are rarely measured online for each node; this information, however, is necessary to solve the hydraulic equations. Some information is acquired when water utilities measure the consumed water volume for a period of some months, for billing purposes. From those data, an average daily consumption demand could be calculated for each junction. Time varying consumer demands can be further estimated by using some flow measurements from within the network, and calculate water demand estimations.

Furthermore, in the hydraulic model discussed, we assume that some information of the system is known, such as the pipe characteristics, the initial tank levels and the pump flow/pressure equation. In addition, demands are assumed to be independent with respect to the pressure at the point of outflow; thus the hydraulic solver discussed is entirely demand-driven [205]. In some research, extensions to the demand-driven hydraulic model have been proposed, for pressure-driven analysis [146].

### 6.3 Quality Dynamics

Quality dynamics in water systems corresponds to the concentration of various contaminant or disinfectant substances, as well as other water chemical parameters, such as pH or turbidity; in this work, by water quality we refer to the concentration of some chemical substance in the water distribution system. Contaminants and disinfectants travel along the water flow within the pipe network, according to the advection and reaction dynamics. Advection is the transport mechanism of a substance in a fluid, which can be modelled as a hyperbolic partial differential equation and can be solved using various numerical methods [206]. Advection dynamics describes how a substance concentration propagates in space and time; reaction dynamics describes the change in the substance concentration due to decay, growth, or reaction with other substances. Advection and reaction dynamics are coupled to describe the quality dynamics. In addition, water quality in storage tanks is computed dynamically, and it depends on the inflows and their quality, the outflows, the tank volume and its quality.

#### 6.3.1 Advection Dynamics

When a substance enters a pipe in which water flows, the substance moves along with that flow. Inside a pipe, and by neglecting axial dispersion and the substance reaction dynamics, the first-order hyperbolic partial differential equation which describes the change in space and time of the substance concentration in water, is given by

$$\frac{\partial C(z, t)}{\partial t} + \frac{Q(t)}{a_P} \frac{\partial C(z, t)}{\partial z} = 0, \quad (40)$$

where  $C(z, t)$  is the substance concentration in water at continuous time  $t$  and at distance  $z$  along a certain pipe, with water flow  $Q(t)$  and cross-sectional area of the pipe  $a_P$ . The boundary conditions are given by  $C(z, 0) = C_t^0(z)$  and  $C(0, t) = C_z^0(t)$ .

In water distribution system quality modeling, two main methodologies have been considered for discretizing the set of hyperbolic partial differential equations describing the advection dynamics within the pipe network, the *Eulerian* and the *Lagrangian* approaches [83, 84, 204]. In general, the Eulerian schemes assume that the water moves between a fixed grid point (finite differences) or volume segments (finite volumes), with a constant time-step [83]; a finite volume methodology was used in EPANET version 1.1 [81]. On the other hand, the Lagrangian method considers variable-sized water segments, with a constant time-step, unless an event has occurred; the event-driven method is implemented in EPANET version 2.0 [84, 204].

Next paragraph provides more intuition to the formulation of a mathematical model describing the advection in water distribution systems, by presenting the *Finite Volume Method* [206]. This numerical method can be employed to approximate the set of hyperbolic partial differential equations which describe the advection dynamics. This requires to virtually segment all the pipes in the network, into a number of finite volume cells, while the Courant-Friedrichs-Lewy (CFL) condition is required for the convergence of the solution [206]. Consider a substance moving within a pipe which is segmented into a finite number of volume cells; for the  $i$ -th finite volume set, we define  $x_i(k)$  as the average concentration in that cell, such that

$$x_i(k) = \frac{1}{\Delta z} \int_{z_i}^{z_i + \Delta z} C(l, k\Delta t) dz,$$

where  $\Delta t$  is the length of a hydraulic discrete time-step, which is a design parameter and may depend on the available sensors,  $\Delta z$  is the width of a single cell and  $z_i$  is the distance of node  $v_i$  from the pipe inflow point. Both  $\Delta t$  and  $\Delta z$  are assumed to be fixed within a certain pipe.

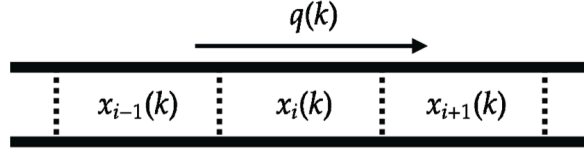


Figure 38: A pipe segmented into virtual finite volumes

### ***Numerical Approximation Schemes***

Various numerical approximation schemes can be used for solving the hyperbolic differential equation (40), such as the *leapfrog* or the *Lax-Wendroff*, which is second order accurate for smooth solutions [206]. Consider a pipe which is segmented into a number of finite volume cells, and the discrete flow  $q(k) = Q(k\Delta t)$ ; for the  $i$ -th finite volume which is not at the boundaries of the pipe, as in Fig. 38.

The *leapfrog* numerical scheme is given by

$$x_i(k+1) = x_i(k) - \lambda(k)(x_{i+1}(k) - x_{i-1}(k)),$$

and the *Lax-Wendroff* scheme is given by

$$x_i(k+1) = \frac{\lambda(k)}{2}[1 + \lambda(k)]x_{i-1}(k) + [1 - \lambda(k)^2]x_i(k) - \frac{\lambda(k)}{2}[1 - \lambda(k)]x_{i+1}(k),$$

where  $\lambda(k) = \frac{q(k)}{a_P} \frac{\Delta t}{\Delta z}$  is the Courant number, for  $a_P$  the cross-sectional area of the pipe; this must satisfy the CFL condition, i.e.  $\frac{|q(k)|}{a_P} \frac{\Delta t}{\Delta z} \leq 1$  for that pipe to guarantee stability in the solution[206]. The direction of the flow does not affect these specific approximations; however in the boundary cells we need to reformulate the equations to capture the network behaviour.

### ***Boundary Conditions***

Boundary conditions need special treatment, since, depending on the flow direction and the numerical method selected, the concentration of a finite volume outside the pipe may be needed for calculating the state. A technique is to virtually extent the pipe by adding *ghost cells* at the ends, with some virtual concentrations [206]. These cells will be used to compute the boundary states in the pipe. The choice of what values to place in these ghost cells is not related to the numerical solution methodology. At each new time-step, we know the internal states (or initial conditions) and apply a boundary condition procedure to determine the values of these virtual cells.

In the case of junctions, if the water flows from the last cell into the junction, then we consider that the ghost cell concentration  $x_i^+(k)$  has the same concentration as the  $i$ -th cell, i.e.  $x_i^+(k) = x_i(k)$ .

In the opposite case, we need to compute the concentration at the junction node, as a weighted sum of the concentrations which inflow. Let  $\mathcal{A}_i^+$  be the set of pipe indices which deliver water to the  $i$ -th node; we assume that all inflows have positive values.

However, if the water flows from the junction into the cell, we need to compute the overall concentration by considering the inflows; thus the overall concentration is given by the inflow-weighted sum of concentrations. Let  $x_{(T,j)}^+(k)$  be the outflow concentration of the pipe  $j \in \mathcal{A}_i^+$ .

The concentration at the  $i$ -th junction node is given by

$$x_i(k) = \left[ \sum_{j \in \mathcal{A}_i^+} q_j(k) x_{(T,j)}^+(k) \right] \cdot \left[ \sum_{j \in \mathcal{A}_i^+} q_j(k) \right]^{-1}, \quad (41)$$

as described in [204].

**Remark:** According to the Finite Volume method, the network must be segmented into a finite number of volume cells; the number of finite cells as well as the time step considered are crucial to guarantee stability in the approximation. In general for this method, assuming that the time step  $\Delta t$  does not change, it is considered that an optimization algorithm is solved at each discrete time, in order to compute a new  $\Delta z$  for each pipe. A different approach is to solve a nonlinear optimization problem in which a pre-determined number of finite volumes is distributed at each pipe, so that the minimum time step for which stability is guaranteed, is computed.

### 6.3.2 Reaction Dynamics

The reaction dynamics characterize how the concentration of one or more substances changes, when reacting, decaying or growing within a finite volume of water. Single-species reaction dynamics are widely used in research, to describe the rate of decay or growth of a substance [204]. Recently, there has been interest in modeling multiple-species reactions, which involves coupled sets of differential and algebraic equations, such that

$$\begin{aligned} \frac{dC(t)}{dt} &= f_R(C(t), C_A(t)) \\ 0 &= f_A(C(t), C_A(t)), \end{aligned}$$

where  $C(t) = C(t, 0)$  is the concentration of one or more chemical species,  $f_R(\cdot)$  is the function describing the concentration change rate,  $C_A(t)$  is a vector of algebraic variables and  $f_A(\cdot)$  is the algebraic function which describes the mass-balance relation [207].

#### *Reaction Models in Water Systems*

In most of the research, single-species reaction dynamics are considered. Let  $C(t)$  correspond to the concentration of a single substance within a finite water volume. Some typical reaction dynamics are:

- No reactions  $\frac{dC(t)}{dt} = 0$ , e.g. for fluoride
- Linear decay  $\frac{dC(t)}{dt} = -\kappa C(t)$ ,  $\kappa > 0$ , e.g. for radioactive materials
- Linear growth  $\frac{dC(t)}{dt} = \kappa C(t)$ ,  $\kappa > 0$ , e.g. for trihalomethanes

Linear decay in specific, is commonly used for modeling chlorine dynamics, even though the dynamics are more complex since they are coupled with the concentration of other substances reacting with chlorine. In the next subsection we present the dynamics of chlorine, one of the most common chemical substances used for disinfection in water distribution systems.

#### *Chlorine Reaction Modeling*

Chlorine is commonly used as a water disinfectant, due to its ability to deactivate various pathogen substances; in addition it has low cost and it is easy to store, transport and use [208].

Throughout the water distribution network, a detectable chlorine residual is required so that the various micro-organisms and chemical agents are below certain thresholds set by the World Health Organization and governments (e.g. at a minimum of  $0.2 \frac{mg}{L}$ ) [5].

When chlorine is injected into water (e.g. as gas), it produces hypochlorous acid (HOCl) and hypochlorite ion ( $ClO^-$ ), which react with natural organic matter floating in water or residing on the pipe/tank walls, disinfecting the drinking water. Chlorine reacts with organic compounds and other substances naturally present in the water flowing within the distribution networks and at the pipe walls.

The actual chlorine reaction dynamics in most of the cases are not known, and as a result, empirical models are utilized [209]. A common assumption in water research literature is that chlorine dynamics are first-order linear, such that  $\frac{dC(t)}{dt} = -\kappa C(t)$ , where  $C(t)$  is the chlorine concentration within a finite water volume and  $\kappa > 0$  is the reaction rate coefficient, which depends on the bulk reaction coefficient (initial water quality), the wall reaction coefficient (pipe material) and the mass transfer coefficient (chlorine transfer from bulk water to pipe walls) [204].

In practice, the chlorine reaction rate  $\kappa$  in some water volume is calculated off-line by using pipe condition information, and by measuring the concentration of a water sample in a bottle, at various time instances; since the dynamics are considered to be linear, the slope of the log-graph of the normalized concentration measured at each time step indicates an appropriate value for  $\kappa$ . It is important to note that this decay rate can be affected by exogenous parameters, such as temperature [204].

In order to provide a more accurate mathematical model of the chlorine dynamics in drinking water, a number of empirical studies have been conducted [208, 210, 211, 212]. Various chlorine reaction dynamics have been considered in research in addition to the first-order linear model, such as:

- the  $i$ -th power order,  $\frac{dC(t)}{dt} = -\kappa C^i(t)$ ,
- the first-order with a stable component  $\frac{dC(t)}{dt} = -\kappa(C(t) - \underline{C})$ , where  $\underline{C}$  is a concentration lower bound,
- the parallel first-order model,  $\frac{dC(t)}{dt} = -\kappa a_K C(t) - \kappa_0(1 - a_K)C(t)$ , where  $0 \leq a_K \leq 1$  is the percentage of the reacting chlorine concentration which decays with rate  $\kappa$  (fast reaction), whereas the remaining concentration decays with rate  $\kappa_0$  (slow reaction).

In some studies, the parallel first-order model was shown to better capture the chlorine dynamics [208], although the first-order linear in some studies adequately described the actual dynamics [210].

The above dynamics, however, do not consider explicitly the actual chemical reaction dynamics of chlorine with organic matter. Following an analytical methodology, the chlorine dynamics can be expressed as  $\frac{dC(t)}{dt} = -\kappa C(t) - \kappa_0 C^2(t)$ , where reaction rates  $\kappa, \kappa_0$  depend on the stoichiometry constants and the initial conditions of both chlorine and the reacting substance; in some studies this model was found to capture the dynamics of chlorine in drinking water with more accuracy than other models [212].

More comprehensive models have been proposed, based on the chemical characteristics for the reaction dynamics and the disinfection by-products in [213]. In addition, models describing chlorine reactions with contaminants (such as sodium arsenite and organophosphate) have been proposed [214, 215, 216].

### 6.3.3 Advection-Reaction Dynamics

The dynamic advection-reaction equations in pipes and tanks, which describe a water distribution system is described below.

### Quality Modeling in Pipes

By coupling the advection and reaction dynamics, a non-homogeneous equation is formulated describing the concentration change in time and space within a certain pipe, such that

$$\frac{\partial C(z, t)}{\partial t} + \frac{Q(t)}{a_P} \frac{\partial C(z, t)}{\partial z} = f_R(C(z, t)), \quad (42)$$

where  $C(z, t)$  is the substance concentration in water at continuous time  $t$  and at distance  $z$  along a certain pipe, with water flow  $Q(t)$  and a cross-sectional area of the pipe  $a_P$ ;  $f_R(\cdot)$  is the concentration change rate due to reactions.

To solve the advection-reaction equation numerically, we can use various methods, such as the single finite-difference *unsplit* method, or the *fractional step* method, which solves separately the advection and the reaction dynamics [206].

To illustrate the unsplit method, let's assume that the forward Euler method is used for discretization and that the reaction dynamics are described by linear decay (42); therefore the  $i$ -th finite volume state is given by

$$x_i(k+1) = x_i(k) - \lambda(k) [x_i(k) - x_{i-1}(k)] - \kappa x_i(k) \Delta t,$$

where  $\kappa > 0$  and  $0 < \lambda(k) < 1$ .

For the fractional step method, (42) is segmented into two parts,

$$\begin{aligned} \frac{\partial C(z, t)}{\partial t} + \frac{Q(t)}{a_P} \frac{\partial C(z, t)}{\partial z} &= 0, \\ \frac{dC(z, t)}{dt} &= -\kappa C(z, t); \end{aligned}$$

by using the second-order Runge-Kutta method for the standard differential equation and the Lax-Wendroff scheme for discretizing advection, the  $i$ -th finite volume is given by

$$\begin{aligned} x_i(k+1) = & \left[ \frac{\lambda(k)}{2} [1 + \lambda(k)] x_{i-1}(k) + [1 - \lambda(k)^2] x_i(k) - \right. \\ & \left. - \frac{\lambda(k)}{2} [1 - \lambda(k)] x_{i+1}(k) \right] (1 - \kappa \Delta t + \frac{1}{2} \kappa^2 \Delta t^2). \end{aligned}$$

In the advection-reaction algorithm implemented in EPANET 2.0, at each discrete time the reactions are performed to compute the new concentrations within each water segment; then advection of the segments is performed [204].

### Quality Modeling in Water Tanks

At least three types of tank models are considered in tank water quality modeling [204]:

- the continuous stirred-tank reactor (CSTR) model, at which the chemicals are perfectly mixed and uniformly spread;
- the plug-flow reactor model, at which there is no mixing of water between the different water parcels assumed to travel along the flow in the tank;
- the two-compartments mixing model, at which the tank is segmented into two perfectly mixed compartments.

The continuous stirred-tank reactor model is considered a reasonable assumption for various tanks [217, 204].

Let  $C(t)$  be the concentration in a water storage tank, which supplies water to a water distribution network. The water which fills the tank may be supplied from within the water distribution network, or it may be supplied from the treatment facilities through the transport system. For the CSTR, the quality concentration dynamics are given by

$$\frac{d}{dt}(V(t)C(t)) = Q_T^+(t)C_T^+(t) - Q_T^-(t)C(t) + f_R(C(t)),$$

where  $V(t)$  is the tank's volume,  $C_T^+(t)$  is the substance concentration of the water which flows into the tank,  $Q_T^+(t)$  is the tank inflow,  $Q_T^-(t)$  is the tank outflow, and  $f_R(C(t))$  a reaction term, such that if linear decay with reaction rate  $\kappa > 0$  is considered,  $f_R(C(t)) = -\kappa C(t)$ .

By using the forward difference scheme, the volume state  $v(k) = V(k\Delta t)$  at discrete time  $k$  is given by

$$v(k+1) = v(k) + (q_T^+(k) - q_T^-(k)) \Delta t,$$

where  $q_T^+(k) = Q_T^+(k\Delta t)$  and  $q_T^-(k) = Q_T^-(k\Delta t)$ . Let  $x(k) = C(k\Delta t)$  correspond to the water quality in the tank and let  $x^+(k) = C_T^+(k\Delta t)$  be the water quality of the water going into the tank with inflow  $q_T^+(k)$ , as depicted in Fig. ???. The tank water quality dynamics are given by

$$\begin{aligned} x(k+1) &= \frac{(q_T^+(k)x^+(k) - q_T^-(k)x(k)) \Delta t + v(k)x(k) - \kappa \Delta t x(k)}{v(k+1)} \\ &= \left[ \frac{q_T^+(k) \Delta t}{v(k+1)} \right] x^+(k) + \left[ \frac{v(k) - (q_T^-(k) - \kappa) \Delta t}{v(k+1)} \right] x(k) \end{aligned}$$

## 6.4 Quality Control

The feedback control problem in water systems can be defined as the problem of computing at each discrete time  $k$ , the input vector  $u(k)$ , for the pumps, valves as well as the concentration of the injected disinfectant at each booster station, so that the measured hydraulic and quality parameters in the output vector  $y(k)$  follow the reference signal vector  $r(k)$  specified for safe operation, computed using the  $f_u(\cdot)$  controller function.

In practice, due to the complex inter-dependencies between hydraulic and quality dynamics, the design of the hydraulic controller is typically considered independently from the quality controller [218, 219]. A schematic of the controllers is depicted in Fig. 39; the water distribution system is driven by unknown consumer demands which exhibit certain periodicity, and uncertainty; at certain locations within the distribution network, on-line flow and pressure sensors are installed and monitored through SCADA, as well as some quality sensors measuring various chemical parameters. In addition, manual sampling for laboratory examination is performed at certain locations. A hydraulic and a quality controller take the measurement outputs into consideration, as well as the desired hydraulic and quality specifications and any constraints, and compute an input signal which regulates the flows and pressures at valves and pumps, as well as concentration at the disinfectant boosters.

### 6.4.1 Hydraulic Faults

Hydraulic faults may correspond to leakages within the water distribution network or at tanks, to pipe bursts, to blocked pipes or to malfunctioning pumps and valves. In addition, we may

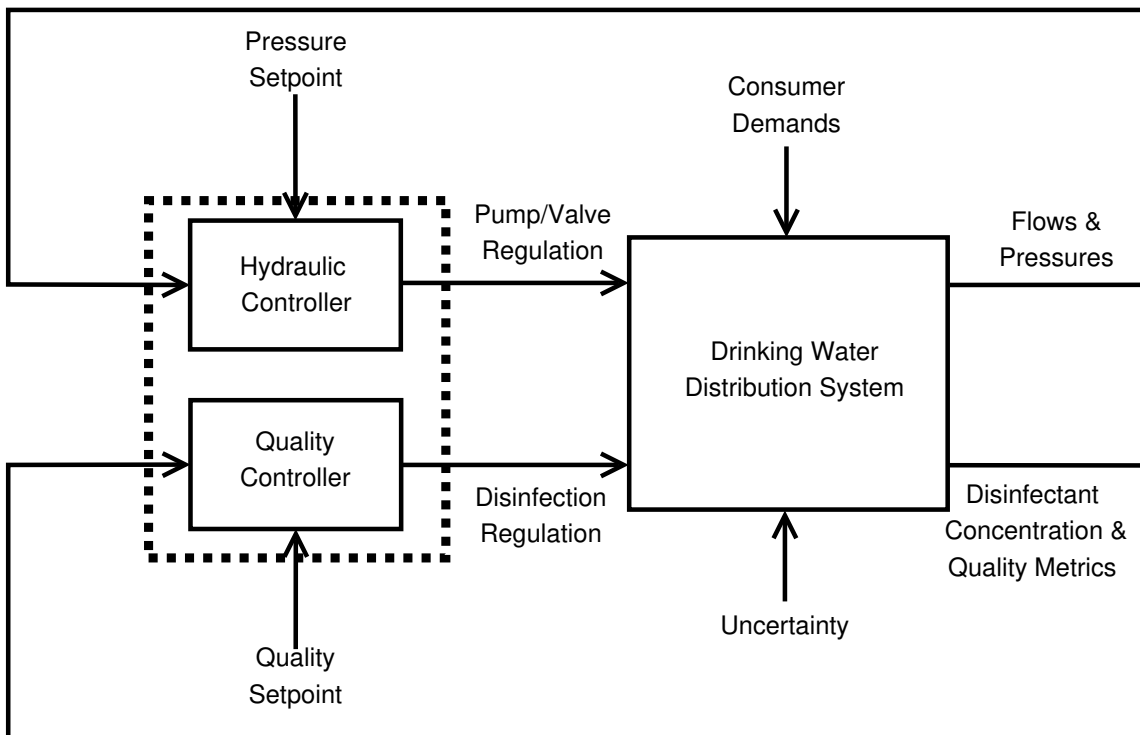


Figure 39: Controller for water distribution networks. Hydraulic and quality control are decoupled, but may exchange some information. The control objective is to regulate pressures and water quality so that they are within the desired bounds specified by the regulations.

consider as a hydraulic fault the unauthorized back-flow in the network using a pump for injecting contaminants.

Water loss may be due to a variety of reasons, such as leaks, theft or unauthorized use and faulty water meters. The largest portion of the water lost is due to leaks or breaks [8]. A break is an abrupt fault needing immediate action, and it is usually easy to isolate the location of the problem. On the other hand, leaks due to cracks at pipes, tanks or loose fittings can remain unnoticeable, are difficult to isolate and may cause significant water losses and escaping revenues. Some of these problems are prompted by the deterioration of the infrastructure, mainly due to age, or by high pressures. Water loss imposes an economic burden on the water utilities while reducing water supplies; furthermore it may cause quality faults. For example a crack in a pipe under certain circumstances can be the entry location for contaminants (e.g. organic matter).

Mathematical models which describe the leakage flow with respect to the pressure at the leakage location have been proposed in various empirical studies [220, 146]. Let  $\phi_h(k; h(k))$  be the hydraulic leakage fault, i.e. the flow due to leakage measured in  $\frac{m^3}{hr}$ , occurring at a node with head  $h(k)$ , at time  $k$ . Hydraulic faults can be modelled mathematically as

$$\phi_h(k; h(k)) = a_D [f_l(h(k))]^{a_E}, \quad (43)$$

where  $a_D > 0$  is a discharge coefficient,  $a_E \in [0.5, 2.5]$  is an exponent term which depends on the leakage type and  $f_l : \mathbb{R} \mapsto \mathbb{R}$  is an unknown function which maps the measured hydraulic head to the pressure at the leakage location (the pressure at the location where the leakage has occurred is usually not measured). In this model, both the discharge coefficient and the exponent term are unknown. However, empirical studies has shown that the exponent for small background leaks is  $a_E \approx 1.5$ , for larger leaks in plastic pipes is  $a_E \geq 1.5$  and for larger leaks in metal pipes is  $a_E \approx 0.5$ . In this work we consider the leakage fault model in simulating realistic leakage faults.

When a demand-driven hydraulic model is used, the leakage can be assumed as an additional time-varying demand, proportional to the corresponding nodal pressure/head; for the  $j$ -th node, the demand with a leakage fault is modelled as

$$d_j(k) = d_j^*(k) + \phi_h(k; h_j(k)),$$

where  $d_j^*(k)$  is the real consumption demand, and  $h_j(k)$  the nodal head. For modelling purposes, leakages which occur within a pipe are assigned as outflow from one of the adjusted nodes, which may be selected randomly.

#### 6.4.2 Quality Faults

Quality faults may occur due to the contamination of water by certain substances, usually chemical, biological or radioactive, which travel along the flow, and they may exhibit decay or growth dynamics. A contaminant substance can be injected into a network at any point by connecting a pump and forcing the outflow direction to reverse. The contaminant travels within the network, following the path of the carrier. Digestion of the contaminated water by consumers may affect the health of the served population; in addition, use of contaminated water in industrial production may cause economic losses.

Consider a water distribution network composed of pipes, junctions and water storage tanks. The topology of this network can be represented as a graph with edges corresponding to pipes, and  $N_m$  nodes corresponding to junctions and water storage tanks. For modeling purposes, each pipe in the network is *a priori* virtually segmented into a number of finite volume cells. Let  $N_n$  be the total number of all nodes and finite volume cells considered in the network. Let  $x_i(k)$  denote the average concentration of a certain contaminant at discrete time  $k$ , for  $i \in \{1, \dots, N_m, \dots, N_n\}$ . The vector

$x(k) = [x_1(k), \dots, x_{N_m}(k), \dots, x_{N_n}(k)]^\top$  is the state of the contaminant concentration dynamics. Let  $\mathcal{V}$  be the set of all node indices, such that  $\mathcal{V} = \{1, 2, \dots, N_m\}$ .

The advection-reaction equations [206] describing the propagation of a contaminant in a water distribution network can be expressed in a state-space formulation:

$$\begin{aligned} x(k+1) &= A(k)x(k) + f_R(x(k)) + F\phi(k), \\ y_c(k) &= Cx(k) \end{aligned} \quad (44)$$

where  $A(k)$  is an  $N_n \times N_n$  matrix which characterizes the advection dynamics and captures the network topology, and  $f_R : \mathbb{R}^{N_n} \mapsto \mathbb{R}^{N_n}$  is a function which describes the reaction dynamics of the contaminant. For  $N_m$  possible injection locations (i.e., at the nodes), let  $F$  be an  $N_n \times N_m$  matrix describing the locations of the injected contaminant. The function  $\phi : \mathbb{N}^+ \mapsto \mathbb{R}^{N_m}$  describes the change in the contaminant concentration due to a substance injection. The output vector  $y_c(k) \in \mathbb{R}^{M_s}$  corresponds to the state measurements, which are monitored using  $M_s$  online sensors.  $C$  is a binary output matrix,  $C \in \{0, 1\}^{M_s \times N_n}$ , such that the element  $(i, j)$  is  $C_{(i,j)} = 1$  when the  $i$ -th quality sensor measures the  $j$ -th state, and  $C_{(i,j)} = 0$  when there is no quality sensor installed.

We define a finite set  $\mathcal{E}$  of fault-location matrices  $E^j$ ,  $j = \{1, \dots, 2^{N_m}\}$ , given by

$$\mathcal{E} = \left\{ \left[ \begin{array}{ccc} E_{(1,1)}^j & & 0 \\ & \ddots & \\ 0 & & E_{(N_m, N_m)}^j \end{array} \right] \mid E_{(i,i)}^j \in \{0, 1\}, j = \{1, \dots, 2^{N_m}\} \right\}, \quad (45)$$

where  $E_{(i,i)} = 1$  corresponds to the case when a contaminant is injected at the  $i$ -th node  $i \in \mathcal{V}$ . For the  $i$ -th fault-location matrix  $E^i \in \mathcal{E}$ , we define the injected contaminant location matrix  $F$  given in (44) as  $F = [E^i \mid \mathbf{0}]^\top$ , where  $\mathbf{0}$  is an  $(N_n - N_m) \times N_m$  zero matrix;  $F$  is of dimension  $N_n \times N_m$ .

The function  $\phi(k) = [\phi_1(k), \dots, \phi_{N_m}(k)]^\top$  corresponds to the signals of the injected contaminant concentrations. These have a certain start time and duration, and are non-negative. The function  $\phi(k)$  can be represented through  $N_z$  linearly parameterized basis functions  $\zeta(k) = [\zeta_1(k), \dots, \zeta_{N_z}(k)]^\top$ , such as pulses or radial-basis functions. Therefore,  $\phi(k)$  is expressed as

$$\phi(k) = \Theta\zeta(k), \quad (46)$$

where  $\Theta \in \mathbb{R}^{N_m \times N_z}$ . The  $(i, j)$  element of  $\Theta$ , denoted as  $\Theta_{(i,j)}$ , represents the amplitude of the basis function  $\zeta_j(k)$  which is added to the state  $x_i(k)$ . Hydraulic dynamics are considered as approximately periodic (e.g. with a daily or weekly period) due to the periodic nature of consumer water demands. The basis functions are used to break up one hydraulic period into  $N_z$  time segments with possible overlaps, as in the case of radial basis functions. The motivation behind the use of a linearly parameterized form of the fault function, is that it simplifies the process of computing a finite set of fault parameter matrices, either through grid sampling or otherwise. This will be useful during the solution methodology for sensor placement (see Chapter 3).

From a practical viewpoint, the contaminant injection is measured in terms of the injected contaminant mass per unit time ( $\frac{mg}{min}$ ), while the state-space formulation is described in terms of contaminant concentration ( $\frac{mg}{L}$ ). The fault function  $\phi_i(k)$  affecting the  $i$ -th node can be expressed as a fraction of a contaminant mass injection rate ( $\frac{mg}{min}$ ) over the nodal inflows ( $\frac{L}{min}$ ).

## 6.5 Pressure Control

Most research works dealing with WDSs aims at optimizing the network management through actions associated with the real losses. Figure 40 illustrates the main factors that affecting real losses optimization, showing that the pressure management is one of the main parameters.

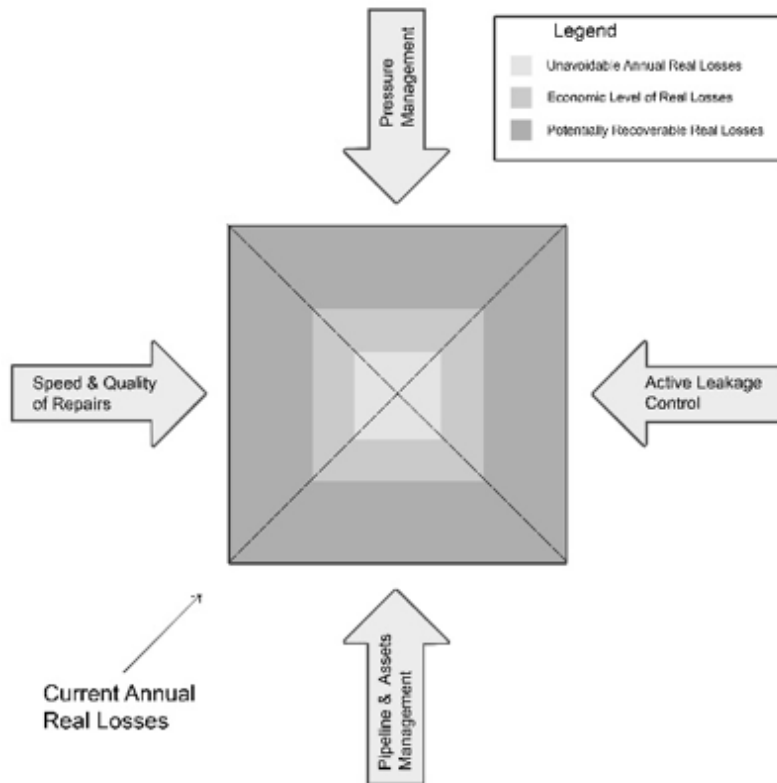


Figure 40: Leakage management [221]

For this reason, particular attention is given to the pressure control of WDSs and implementation of the District Metered Areas (DMAs) has been established (Fig. 41). DMAs are defined sections of the network that are comprised of separate regional water meters as well as of one entry / exit point. Water pressure within the pipelines of a DMA should be steady (about 3 bars). Therefore, there should not be large deviations in altitude within DMAs, especially in gravity-based networks. For cases where this is unavoidable, pressure reducing valves (PRVs) could be installed in order to ensure constant pressure across the DMA.

The importance of network pressure and the role of the valve control forces researchers to work in extent on this topic. The subdivision of WDSs into DMAs has been successfully applied in the pursuit of low-cost leak reduction methods by facilitating simplistic demand metering and pressure control [223]. The flow into these sectors can be measured and the pressure can be reduced to continuously maintain the minimum pressure requirements at a critical point. This practice has allowed an efficient leakage management, but it has severely reduced the redundancy in network connectivity [224] and water quality [225]. Recent work on WDSs with dynamically adaptive network topology [224] presents a hybrid mode of operation that integrates the benefits of leakage reduction and management provided by sectorised networks with the extra benefits of improved network connectivity, redundancy and resilience. Dynamically adaptive networks are segregated into small sectors during periods of low demand in order to maximize the detection and pre-localisation of leaks.

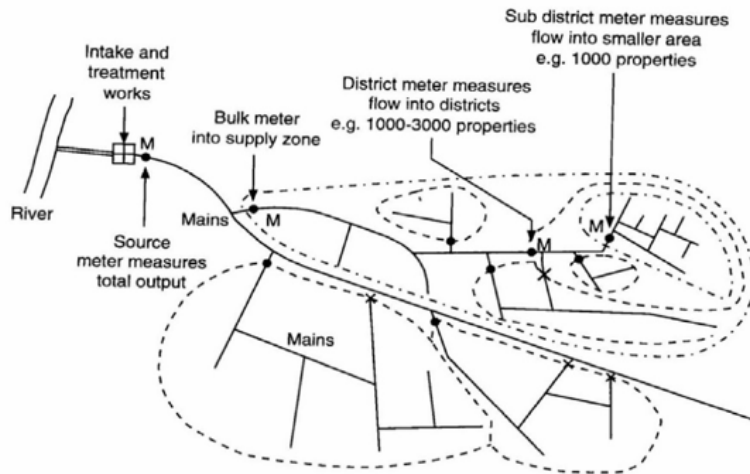


Figure 41: A typical arrangement of a WDN [222]

## 6.6 Industrial Applications

The research efforts for the development and deployment of WDN real-time monitoring systems had begun in the early 80's. Indicative is the research work by [188], who studied the development of a real-time monitoring model as a prerequisite of any form of online control. The development of a Wireless Sensor Network (WSN), focused on the monitored parameters, was also examined by the research activities of [226] and [227]. Furthermore, the architecture of the developed system and the efficiency of the sensors that will be implemented should also be examined, as discussed in the work by [228]. 'Project Neptune' [182] is a research work that targeted the development of a complete management system for the WDNs. The model is based on three pillars: the enhancement and upgrade of the WSN monitoring system, the development of tools for the management of pressure and energy (consumed by the system), and the development of an integrated DSS for the evaluation of rehabilitation strategies.

The Water-WiSe platform, presented in [229, 230], is an example of an integrated system comprised of wireless sensors for monitoring the WDN in real time. The Water-WiSe platform includes: (i) low cost WSN, (ii) leakage detection algorithms and (iii) real time data recordings to improve state estimation for the network.

Another industrial application is the software package developed by i2O water [231]. The i2O platform (Fig. 42) provides a suite of smart water network solutions that comprises: (i) Logging, Visualization and Alarms (dNET), (ii) Network Monitoring (iNET) and (iii) Advance pressure Management (oNET).

## 7 Discussion and Concluding Remarks

Based on the overview for the networking and communication technologies, well-established mathematical tools for WDN, data acquisition and processing, event diagnosis, state estimation and control and the representative industrial applications, the following discussion points can be extracted:

- Short-range enabling technologies offer an easy-to-deploy cost effective solution for battery operated nodes, which could be extremely beneficial for parts of the water network with



Figure 42: : i2O Platform [231]

minimum or no access to infrastructure (e.g., main power supply). This could be linked to short-term monitoring of specific aspects of the water network (e.g., exchanging laboratory-based quality sampling with on-site monitoring of quality parameters at designated regions);

- The provision of IP interoperability of short-range technologies through the means of the 6TiSCH industrial protocol stack is an important step towards providing scalable and cost-effective solutions in the smart water metering arena, easing the integration with designated control centers and abstracting heterogeneity at the level of the sensing infrastructure (e.g., through CoAP services);
- LoRA/LoRAWAN and NB-IoT are expected to empower long-range water sensing technologies, since opposed to short-range architectures, they require fewer intermediate components (e.g. bridging gateways), and thereby less complicated architectures. Even so, due to the increased power consumption they are preferred for deployments that will benefit from the existence of some infrastructure (e.g., access of main power supply or integration with photovoltaic cells). As such, long-range technologies for smart water networks, could be a feasible alternative solution for existing GRPR-based telemetry systems, suitable for long-term deployments and continuous monitoring / control of water parameters at relevant advanced metering infrastructures (e.g., pressure and flow monitoring).
- Epanet and other mathematical modeling tools, are capable to model and simulate a WDN behavior. WDNs agencies by using such mathematical tools are able to not only monitor their networks in real time but they would also be provided with a decision support tool for taking maintenance actions.
- In data acquisition and processing of SWNs, two main causes of missing data were introduced: (i) measurements are not acquired due to sensor malfunction, or not transmitted due to

network failure; (ii) missing data positions are introduced artificially in order to increase the time resolution of a given data stream, or to synchronize distinct data streams acquired at different sampling frequencies. These problems can be solved by using matrix completion, (MC) and tensor completion, (TC) that have demonstrated increased performance in various application domains.

- Event detection in WDN has been investigated by many authors and various approaches have been proposed for addressing the problem of leakage/contamination detection, using single or multiple-type measurements which are analyzed separately or in combination, from one or more locations in the network, using model-based or model-free approaches.
- The main challenges of water distribution networks, are related to *Monitoring* for event detection, and *Control* for efficient and fault-tolerant operation. For monitoring, utility operators may use sensors installed within the water distribution system, as well as manual sampling with utility employees, to determine the occurrence of events which may affect the normal operation of the system. By controlling the system actuators (such as pumps, valves), water utilities are able to supply sufficient quantity of water of good quality to consumers, while maintaining low pressures in order to reduce background leakages, reduce energy usage as well as reconfigure the system appropriately when an event occurs in order to reduce its impact. Moreover, utilities must make long-term planning ahead, to guarantee that the appropriate infrastructure is in place, in parallel with the development of the urban environment.

With regard to industrial applications:

- short-range deployments are preferred for research-oriented goals, for enabling the design of sophisticated (decentralized) algorithms (e.g., for leakage detection) and testing in field new sensing technology. By contrast, long-range deployments are preferred for system-wide studies with emphasis on end-to-end solutions for accessing water parameters, based on off-the-shelf sensors and centralized processing.
- several commercial software and products have been made commercially available for monitoring, management and controlling of WDSs, aiming at improving WDSs. However, all available commercial tools concerning the management of WDNs have two major drawbacks: the high cost of ownership and the ownership of data.
- intelligent event detection algorithms have been developed in various distinct industrial applications using platforms in order to monitor, detect and predict abnormal events. Important instruments for leak and quality detection are sensors, noise loggers, radio repeaters, flow meters and meters readers.
- real time monitoring models and wireless sensor networks in platforms are preferred for the development and deployment of WDN real-time monitoring systems.

## References

- [1] M. Bazilian, H. Rogner, M. Howells, S. Hermann, D. Arent, D. Gielen, P. Steduto, A. Mueller, P. Komor, R. S. Tol, and K. K. Yumkella, “Considering the energy, water and food nexus: Towards an integrated modelling approach,” *Energy Policy*, vol. 39, no. 12, pp. 7896–7906, 2011.
- [2] EPA, “Drinking Water Infrastructure Needs Survey and Assessment: Fifth Report to Congress,” U.S. Environmental Protection Agency, Tech. Rep., 2013.

- [3] R. M. Clark, S. Hakim, and A. Ostfeld, Eds., *Handbook of Water and Wastewater Systems Protection*. Springer, 2011.
- [4] B. Kingdom, R. Liemberger, and P. Marin, “The Challenge of Reducing Non-Revenue Water ({NRW}) in Developing Countries—How the Private Sector Can Help: A Look at Performance-Based Service Contracting,” World Bank, Dec. WSS Sector Board Discussion Paper 8, 2006.
- [5] World Health Organization, *Guidelines for drinking-water quality, Vol. 1, 3rd edition incorporating 1st and 2nd addenda*, 3rd ed. Geneva, Switzerland: World Health Organization, 2008.
- [6] European Commission, “Council Directive 98/83/EC of 3 November 1998 on the quality of water intended for human consumption,” Official Journal of the European Communities, pp. 32–54, 1998.
- [7] U.S. Government, “National primary drinking water regulations - Title 40, Code of federal regulations, Part 141 - Environmental Protection Agency (EPA),” 2002.
- [8] T. M. Walski and J. W. Male, in *Water distribution systems handbook*, L. W. Mays, Ed. McGraw-Hill New York, 2000, ch. Maintenannc, pp. 17.1–17.28.
- [9] P. S. Corso, M. H. Kramer, K. A. Blair, D. G. Addiss, J. P. Davis, and A. C. Haddix, “Cost of illness in the 1993 Waterborne Cryptosporidium outbreak, {Milwaukee, Wisconsin},” *Emerging Infectious Diseases*, vol. 9, no. 4, pp. 426–431, 2003.
- [10] J. Laine, E. Huovinen, M. J. Virtanen, M. Snellman, J. Lumio, P. Ruutu, E. Kujansuu, R. Vuento, T. Pitkänen, I. Miettinen, J. Herrala, O. Lepistö, J. Anttonen, J. Helenius, M. L. Hänninen, L. Maunula, J. Mustonen, and M. Kuusi, “An extensive gastroenteritis outbreak after drinking-water contamination by sewage effluent, {Finland},” *Epidemiology & Infection*, vol. 139, no. 07, pp. 1105–1113, 2011.
- [11] Safety Investigation Authority, “B2/2007Y Entry of treated waste water in to the drinking water network in Nokia on 28–30 November 2007,” 2009.
- [12] A. J. Whelton, L. McMillan, M. Connell, K. M. Kelley, J. P. Gill, K. D. White, R. Gupta, R. Dey, and C. Novy, “Residential Tap Water Contamination Following the Freedom Industries Chemical Spill: Perceptions, Water Quality, and Health Impacts,” *Environmental Science & Technology*, vol. 49, no. 2, pp. 813–823, 2015.
- [13] B. Charalambous, “Experiences in DMA redesign at the Water Board of Lemesos, Cyprus,” in *Proc. IWA Leakage*, 2005, pp. 403–413.
- [14] European Commission, “Critical Infrastructure Protection in the fight against terrorism,” 2004.
- [15] P. H. Gleick, “Water and terrorism,” *Water Policy*, vol. 8, no. 6, pp. 481–503, 2006.
- [16] W. S. Carus, *Bioterrorism and Biocrimes: The Illicit Use of Biological Agents since 1900*. Amsterdam, The Netherlands: Fredonia Books, 2002.
- [17] K. Wilhoit, “The SCADA That Didn’t Cry Wolf,” Trend Micro Incorporated, Tech. Rep., 2013.

- [18] M. A. Brdys and B. Ulanicki, *Operational control of water systems: structures, algorithms, and applications*. New York, USA: Prentice Hall, 1994.
- [19] R. Puust, Z. Kapelan, D. A. Savic, and T. Koppel, “A review of methods for leakage management in pipe networks,” *Urban Water Journal*, vol. 7, no. 1, pp. 25–45, feb 2010.
- [20] R. A. Stewart, D. Giurco, and C. Beal, “Hydroinformatics challenges and opportunities,” *Hydrolink*, no. 4, pp. 107–110, 2013.
- [21] A. Armon, S. Gutner, A. Rosenberg, and H. Scolnicov, “Algorithmic network monitoring for a modern water utility: a case study in Jerusalem,” *Water Science & Technology*, vol. 63, no. 2, pp. 233–239, 2011.
- [22] R. A. Stewart, R. Willis, D. Giurco, K. Panuwatwanich, and G. Capati, “Web-based knowledge management system: linking smart metering to the future of urban water planning,” *Australian Planner*, vol. 47, no. 2, pp. 66–74, 2010.
- [23] S. M. Amin, B. F. B. Wollenberg, S. Massoud Amin, and B. F. B. Wollenberg, “Toward a smart grid: power delivery for the 21st century,” *Power and Energy Magazine, IEEE*, vol. 3, no. 5, pp. 34–41, sep 2005.
- [24] H. Farhangi, “The path of the smart grid,” *IEEE Power and Energy Magazine*, vol. 8, no. 1, pp. 18–28, jan 2010.
- [25] R. Murray, T. Haxton, R. Janke, W. E. Hart, J. Berry, and C. Phillips, “Water quality event detection systems for drinking water contamination warning systems—development, testing, and application of CANARY,” U.S. EPA, Tech. Rep., 2010.
- [26] P. Zikopoulos, C. Eaton, and Others, *Understanding big data: Analytics for enterprise class hadoop and streaming data*. McGraw-Hill, 2011.
- [27] X. Wu, X. Zhu, G.-Q. Wu, and W. Ding, “Data mining with big data,” *IEEE Transactions on Knowledge and Data Engineering*, vol. 26, no. 1, pp. 97–107, 2014.
- [28] M. C. Vuran and A. R. Silva, “Communication through soil in wireless underground sensor networks—theory and practice,” in *Sensor Networks*. Springer, 2010, pp. 309–347.
- [29] A. R. Silva and M. C. Vuran, “Communication with aboveground devices in wireless underground sensor networks: An empirical study,” in *Communications (ICC), 2010 IEEE International Conference on*. IEEE, 2010, pp. 1–6.
- [30] B. Silva, R. M. Fisher, A. Kumar, and G. P. Hancke, “Experimental link quality characterization of wireless sensor networks for underground monitoring,” *IEEE Transactions on Industrial Informatics*, vol. 11, no. 5, pp. 1099–1110, 2015.
- [31] Z. Sun and I. F. Akyildiz, “Connectivity in wireless underground sensor networks,” in *Sensor Mesh and Ad Hoc Communications and Networks (SECON), 2010 7th Annual IEEE Communications Society Conference on*. IEEE, 2010, pp. 1–9.
- [32] Z. Sun, I. F. Akyildiz, and G. P. Hancke, “Dynamic connectivity in wireless underground sensor networks,” *IEEE Transactions on Wireless Communications*, vol. 10, no. 12, pp. 4334–4344, December 2011.
- [33] I. F. Akyildiz, Z. Sun, and M. C. Vuran, “Signal propagation techniques for wireless underground communication networks,” *Physical Communication*, vol. 2, no. 3, pp. 167 – 183, 2009.

- [34] Z. Sun and I. F. Akyildiz, “Channel modeling and analysis for wireless networks in underground mines and road tunnels,” *IEEE Transactions on communications*, vol. 58, no. 6, 2010.
- [35] IEEE Std 802.15.4, *Part 15.4: Wireless LAN Medium Access Control (MAC) and Physical Layer (PHY) Specifications for Low Rate Wireless Personal Area Networks (LR-WPANs)*, 2011.
- [36] J. Espina, T. Falck, A. Panousopoulou, L. Schmitt, O. Mülhens, and G.-Z. Yang, *Network Topologies, Communication Protocols, and Standards*. London: Springer London, 2014, pp. 189–236.
- [37] *IEEE Std 802.15.4a-2007: Amendment to 802.15.4-2006: Wireless Medium Access Control (MAC) and Physical Layer (PHY) Specifications for Low-Rate Wireless Personal Area Networks (LR-WPANs)*, IEEE Std., 2007.
- [38] E. Karapistoli, F.-N. Pavlidou, I. Gragopoulos, and I. Tsetsinas, “An overview of the ieee 802.15. 4a standard,” *IEEE Communications Magazine*, vol. 48, no. 1, 2010.
- [39] Nanotron, “Nanotron technologies,” <https://nanotron.com/EN/>.
- [40] *802.15.4e-2012 - IEEE Standard for Local and metropolitan area networks—Part 15.4: Low-Rate Wireless Personal Area Networks (LR-WPANs) Amendment 1: MAC sublayer*, IEEE Std., 2012.
- [41] D. De Guglielmo, G. Anastasi, and A. Seghetti, *From IEEE 802.15.4 to IEEE 802.15.4e: A Step Towards the Internet of Things*. Cham: Springer International Publishing, 2014, pp. 135–152.
- [42] H. Sun, C. Wang, and B. I. Ahmad, *From Internet of Things to Smart Cities: Enabling Technologies*. CRC Press, 2017.
- [43] D. Dujovne, T. Watteyne, X. Vilajosana, and P. Thubert, “6tisch: deterministic ip-enabled industrial internet (of things),” *IEEE Communications Magazine*, vol. 52, no. 12, pp. 36–41, 2014.
- [44] J. Olsson, “6lowpan demystified,” Tech. Rep.
- [45] M. Nixon and T. Round Rock, “A comparison of wireless hART and ISA100.11a,” Tech. Rep.
- [46] T. Watteyne, P. Tuset-Peiro, X. Vilajosana, S. Pollin, and B. Krishnamachari, “Teaching communication technologies and standards for the industrial IoT? use 6tisch!” *IEEE Communications Magazine*, vol. 55, no. 5, pp. 132–137, 2017.
- [47] C. Bormann, Z. Shelby, S. Chakrabarti, and E. Nordmark, *Neighbor Discovery Optimization for IPv6 over Low-Power Wireless Personal Area Networks (6LoWPANs)*, RFC 6775, Std. 6775, Nov. 2012.
- [48] *Routing Protocol for Low Power and Lossy Networks*, IETF Std., 2011.
- [49] *The Constrained Application Protocol (CoAP)*, IETF Std., 2014. [Online]. Available: <https://tools.ietf.org/html/rfc7252>
- [50] Q. Wang, X. Vilajosana, and T. Watteyne, *6top Protocol (6P)*, Internet Engineering Task Force Internet-Draft draft-ietf-6tisch-6top-protocol-11, Mar. 2018, work in Progress.

- [51] P. Di Marco, C. Fischione, G. Athanasiou, and P.-V. Mekikis, “Harmonizing mac and routing in low power and lossy networks,” in *Global Communications Conference (GLOBECOM), 2013 IEEE*. IEEE, 2013, pp. 231–236.
- [52] X. Liu, Z. Sheng, C. Yin, F. Ali, and D. Roggen, “Performance analysis of routing protocol for low power and lossy networks (rpl) in large scale networks,” *IEEE Internet of Things Journal*, vol. 4, no. 6, pp. 2172–2185, 2017.
- [53] M. Centenaro, L. Vangelista, A. Zanella, and M. Zorzi, “Long-range communications in unlicensed bands: The rising stars in the iot and smart city scenarios,” *IEEE Wireless Communications*, vol. 23, no. 5, pp. 60–67, 2016.
- [54] U. Raza, P. Kulkarni, and M. Sooriyabandara, “Low power wide area networks: An overview,” *IEEE Communications Surveys & Tutorials*, vol. 19, no. 2, pp. 855–873, 2017.
- [55] Ingenu-Inc., “Ingenu inc.” <https://www.ingenu.com/>.
- [56] I. Inc., “The making of rpma,” <https://www.ingenu.com/>, Tech. Rep., 2016.
- [57] Cooking-Hacks, “Libelium comunicaciones distribuidas s.l,” <https://www.cooking-hacks.com/>.
- [58] S. Kartakis, B. D. Choudhary, A. D. Gluhak, L. Lambrinos, and J. A. McCann, “Demystifying low-power wide-area communications for city iot applications,” in *Proceedings of the Tenth ACM International Workshop on Wireless Network Testbeds, Experimental Evaluation, and Characterization*. ACM, 2016, pp. 2–8.
- [59] S. Kartakis and J. McCann, *Communication Optimization and Edge Analytics for Smart Water Grid*. CRC Press, 2018, ch. 3.
- [60] M. Cattani, C. A. Boano, and K. Romer, “An experimental evaluation of the reliability of lora long-range low-power wireless communication,” *Journal of Sensor and Actuator Networks*, vol. 6, no. 2, p. 7, 2017.
- [61] M. C. Bor, U. Roedig, T. Voigt, and J. M. Alonso, “Do lora low-power wide-area networks scale?” in *Proceedings of the 19th ACM International Conference on Modeling, Analysis and Simulation of Wireless and Mobile Systems*. ACM, 2016, pp. 59–67.
- [62] F. Adelantado, X. Vilajosana, P. Tuset-Peiro, B. Martinez, J. Melia-Segui, and T. Watteyne, “Understanding the limits of lorawan,” *IEEE Communications Magazine*, vol. 55, no. 9, pp. 34–40, 2017.
- [63] Lora-Alliance, “Lora alliance,” <https://lora-alliance.org/>.
- [64] *LoRAWAN Specification v1.1*, LoRA Alliance TM Std., 2017.
- [65] 3GPP, “The 3rd generation partnership project,” <http://www.3gpp.org/about-3gpp/project-coordination-group-pcg>.
- [66] Y.-P. E. Wang, X. Lin, A. Adhikary, A. Grovlen, Y. Sui, Y. Blankenship, J. Bergman, and H. S. Razaghi, “A primer on 3gpp narrowband internet of things,” *IEEE Communications Magazine*, vol. 55, no. 3, pp. 117–123, 2017.
- [67] S. S. Rashmi, W. Yiqiao, and H. Seung-Hoon, “A survey on lpwa technology: Lora and nb-iot,” *ICT Express*, vol. 3, no. 1, pp. 14 – 21, 2017.

- [68] B. Vejlgaard, M. Lauridsen, H. Nguyen, I. Kovács, P. Mogensen, and M. Sørensen, “Coverage and capacity analysis of sigfox, lora, gprs, and nb-iot,” in *Proceedings of the IEEE 85th Vehicular Technology Conference, Sydney, Australia*, 2017, pp. 4–7.
- [69] I. Stoianov, L. Nachman, S. Madden, and T. Tokmouline, “Pipenet: A wireless sensor network for pipeline monitoring,” in *Proceedings of the 6th International Conference on Information Processing in Sensor Networks*, ser. IPSN ’07. New York, NY, USA: ACM, 2007, pp. 264–273.
- [70] A. M. Sadeghioon, N. Metje, D. N. Chapman, and C. J. Anthony, “Smartpipes: Smart wireless sensor networks for leak detection in water pipelines,” *Journal of Sensor and Actuator Networks*, vol. 3, no. 1, pp. 64–78, 2014.
- [71] F. Karray, A. Garcia-Ortiz, M. W. Jmal, A. M. Obeid, and M. Abid, “Earnpipe: A testbed for smart water pipeline monitoring using wireless sensor network,” *Procedia Computer Science*, vol. 96, pp. 285 – 294, 2016, knowledge-Based and Intelligent Information & Engineering Systems: Proceedings of the 20th International Conference KES-2016.
- [72] T. Tsung-Te Lai, W.-J. Chen, K.-H. Li, P. Huang, and H.-H. Chu, “Triopusnet: automating wireless sensor network deployment and replacement in pipeline monitoring,” in *Information Processing in Sensor Networks (IPSN), 2012 ACM/IEEE 11th International Conference on*. IEEE, 2012, pp. 61–71.
- [73] A. Panousopoulou and P. Tsakalides, “On graph-based feature selection for multi-hop performance characterization in industrial smart water networks,” in *2016 International Workshop on Cyber-Physical Systems for Smart Water Networks*, 2016, pp. 19–24.
- [74] A. Panousopoulou, M. Azkune, and P. Tsakalides, “Feature selection for performance characterization in multi-hop wireless sensor networks,” *Ad Hoc Networks*, vol. 49, pp. 70 – 89, 2016.
- [75] L. Montestruque and M. D. Lemmon, “Globally coordinated distributed storm water management system,” in *Proceedings of the 1st ACM International Workshop on Cyber-Physical Systems for Smart Water Networks*, ser. CySWater’15. New York, NY, USA: ACM, 2015, pp. 10:1–10:6.
- [76] L. Montestruque, *An Agent-Based Storm Water Management System*. CRC Press, 2018, ch. 6.
- [77] M. Allen, A. Preis, M. Iqbal, and A. J. Whittle, “Case study: a smart water grid in singapore,” *Water Practice and Technology*, vol. 7, no. 4, p. wpt2012089, 2012.
- [78] M. Afifi, M. F. Abdelkader, and A. Ghoneim, “An iot system for continuous monitoring and burst detection in intermittent water distribution networks,” in *Innovative Trends in Computer Engineering (ITCE), 2018 International Conference on*. IEEE, 2018, pp. 240–247.
- [79] M. Saravanan, A. Das, and V. Iyer, “Smart water grid management using lpwan iot technology,” in *Global Internet of Things Summit (GIoTS), 2017*. IEEE, 2017, pp. 1–6.
- [80] A. Agathokleous, “Sensor-based sustainable management of urban water distribution networks utilizing survival analysis modeling,” Thesis (Ph. D.), University of Cyprus, Nicosia, Cyprus, 2015.

- [81] L. A. Rossman, R. M. Clark, and W. M. Grayman, “Modeling chlorine residuals in drinking-water distribution systems,” *Journal of Environmental Engineering*, vol. 120, no. 4, pp. 803–820, 1994.
- [82] E. Todini and S. Pilati, “A gradient algorithm for the analysis of pipe networks,” in *Computer applications in water supply: vol. 1—systems analysis and simulation*. Research Studies Press Ltd., 1988, pp. 1–20.
- [83] L. A. Rossman, P. F. Boulos, and T. Altman, “Discrete volume-element method for network water-quality models,” *ASCE Journal of Water Resources Planning and Management*, vol. 119, no. 5, pp. 505–517, 1993.
- [84] L. A. Rossman and P. F. Boulos, “Numerical methods for modeling water quality in distribution systems: A comparison,” *ASCE Journal of Water Resources Planning and Management*, vol. 122, no. 2, pp. 137–146, 1996.
- [85] L. A. Rossman, “Epanet 2: users manual,” 2000.
- [86] M. M. Eusuff and K. E. Lansey, “Optimization of water distribution network design using the shuffled frog leaping algorithm,” vol. 129, no. 3, pp. 210–225.
- [87] D. A. Savic, “Genetic algorithms for least-cost design of water distribution networks,” vol. 123, no. 2, pp. 67–77.
- [88] E. Van Zyl Jakobus, D. A. Savic, and G. A. Walters, “Operational optimization of water distribution systems using a hybrid genetic algorithm,” vol. 130, no. 2, pp. 160–170.
- [89] A. Ostfeld, J. G. Uber, E. Salomons, J. W. Berry, W. E. Hart, C. A. Phillips, J.-P. Watson, G. Dorini, P. Jonkergouw, Z. Kapelan, F. di Pierro, S.-T. Khu, D. Savic, D. Eliades, M. Polycarpou, S. R. Ghimire, B. D. Barkdoll, R. Gueli, J. J. Huang, E. A. McBean, W. James, A. Krause, J. Leskovec, S. Isovitsch, J. Xu, C. Guestrin, J. VanBriesen, M. Small, P. Fischbeck, A. Preis, M. Propato, O. Piller, G. B. Trachtman, Z. Y. Wu, and T. Walski, “The battle of the water sensor networks (BWSN): A design challenge for engineers and algorithms,” vol. 134, no. 6, pp. 556–568.
- [90] E. Salomons, S. Hatchett, and D. G. Eliades, “The EPANET open source initiative.”
- [91] F. Shang, J. G. Uber, and L. A. Rossman, “EPANET multi-species extension software and user’s manual,” p. 115.
- [92] C. K. Ho and S. S. Khalsa, “EPANET-BAM: Water quality modeling with incomplete mixing in pipe junctions.”
- [93] C. Siew and T. T. Tanyimboh, “Pressure-dependent EPANET extension,” vol. 26, no. 6, pp. 1477–1498.
- [94] R. Murray, K. Klise, C. Phillips., and L. Walker, “Systems Measures of Water Distribution System Resilience,” U.S. Environmental Protection Agency, Cincinnati, OH, USA, DOCUMENT (PUBLISHED REPORT/REPORT), 2015.
- [95] B. J. Eck, “An r package for reading EPANET files,” vol. 84, pp. 149–154.
- [96] D. Steffelbauer and D. Fuchs-Hanusch, “OOPNET: An object-oriented EPANET in python,” vol. 119, pp. 710–718.

- [97] J. Van Zyl, J. Borthwick, and A. Hardy, “OTEN: An object-oriented programmers toolkit for epanet,” in *Supplementary Proceedings of International Conference on Advances in Water Supply Management*. Imperial College, p. 7.
- [98] G. Eliades, M. Kyriakou, S. Vrachimis, and M. Polycarpou, “Epanet-matlab toolkit: An open-source software for interfacing epanet with matlab.”
- [99] D. Eliades, M. Kyriakou, and M. Polycarpou, “Sensor placement in water distribution systems using the s-PLACE toolkit,” vol. 70, pp. 602–611.
- [100] M. Kyriakou, D. G. Eliades, and M. M. Polycarpou, “dbpRisk: Disinfection by-product risk estimation,” in *Critical Information Infrastructures Security*, C. G. Panayiotou, G. Ellinas, E. Kyriakides, and M. M. Polycarpou, Eds. Springer International Publishing, vol. 8985, pp. 57–68.
- [101] Berry Jonathan, Hart William E., Phillips Cynthia A., Uber James G., and Watson Jean-Paul, “Sensor Placement in Municipal Water Networks with Temporal Integer Programming Models,” *Journal of Water Resources Planning and Management*, vol. 132, no. 4, pp. 218–224, Jul. 2006.
- [102] U.S. Environmental Protection Agency, “Adaptation Strategies Guide for Water Utilities,” Feb. 2015.
- [103] D. B. Hart and S. A. McKenna, “User’s Manual for CANARY\_version 4.3.2,” U.S. Environmental Protection Agency, Cincinnati, Ohio, U.S.A., Manual, Sep. 2012.
- [104] Hart David, McKenna Sean A., Klise Katherine, Cruz Victoria, and Wilson Mark, “CANARY: A Water Quality Event Detection Algorithm Development Tool,” *World Environmental and Water Resources Congress 2007*.
- [105] K. Klise, J. Sirola, D. Hart, C. Phillips., T. Haxton, R. Murray, R. Janke, T. Taxon, C. Laird, A. Seth, G. Hackebeitl, S. McGee, and A. Mann, “Water Security Toolkit - User Manual Version 1.2,” U.S. Environmental Protection Agency, Cincinnati, Ohio, U.S.A., Manual, Aug. 2014.
- [106] Mike-Urban, “MIKE URBAN-DHI Group,” 2018.
- [107] WaterGEMS-Bentley, “WaterGEMS-Bentley,” Nov. 2014.
- [108] InfoWater, “InfoWater-Innovyze,” 2018. [Online]. Available: <http://www.innovyze.com/products/infowater/>
- [109] H. E. Ltd, “EDAMS-Hydro-Comp,” 2018. [Online]. Available: <http://www.edams.com/>
- [110] Kisters, “Water Solutions-KISTERS,” 2018. [Online]. Available: <https://water.kisters.de/en/>
- [111] Phoebe, “Phoebe Innovations Platform-Phoebe R&I,” 2018. [Online]. Available: <http://phoebeinnovations.com/>
- [112] M. Hardt, R. Meka, P. Raghavendra, and B. Weitz, “Computational limits for matrix completion,” in *JMLR: Workshop and Conference Proceedings*, vol. 35, 2014.
- [113] J. Tanner and K. Wei, “Normalized iterative hard thresholding for matrix completion,” *SIAM Journal on Scientific Computing*, vol. 35, no. 5, pp. 104–125, 2013.

- [114] E. J. Candes, X. Li, Y. Ma, and J. Wright, “Robust principal component analysis,” *J. ACM*, vol. 58, no. 3, pp. 11:1–11:37, Jun. 2011.
- [115] A. Phan, P. Tichavsky, and A. Cichocki, “CANDECOMP/PARAFAC decomposition of high-order tensors through tensor reshaping,” *IEEE Transactions on Signal Processing*, vol. 61, no. 19, pp. 4847–4860, 2013.
- [116] Y. Xu, R. Hao, W. Yin, and Z. Su, “Parallel matrix factorization for low-rank tensor completion,” *Inverse Problems and Imaging*, vol. 9, no. 2, pp. 601–624, 2015.
- [117] S. Mallat, *A Wavelet Tour of Signal Processing: The Sparse Way*. 3rd Ed., Academic Press, 2009.
- [118] E. Candes, J. Romberg, and T. Tao, “Robust uncertainty principles: Exact signal reconstruction from highly incomplete frequency information,” *IEEE Transactions on Information Theory*, vol. 53, no. 2, pp. 489–509, 2006.
- [119] E. J. Candes, Y. Eldar, D. Needell, and P. Randall, “Compressed sensing with coherent and redundant dictionaries,” *Appl. Comput. Harmonic Anal.*, vol. 31, no. 1, pp. 59–73, Jul. 2011.
- [120] E. J. Candes, “The restricted isometry property and its implications for compressed sensing,” *C. R. Acad. Sci. Paris, Ser. I*, vol. 346, pp. 589–592, 2008.
- [121] J. Tropp and A. Gilbert, “Signal recovery from random measurements via orthogonal matching pursuit,” *IEEE Transactions on Information Theory*, vol. 53, no. 12, pp. 4655–4666, Dec. 2007.
- [122] S. Savvaki, G. Tsagkatakis, A. Panousopoulou, and P. Tsakalides, “Application of matrix completion on water treatment data,” 2015.
- [123] G. Tzagkarakis, G. Tsagkatakis, D. Alonso, C. Asensio, E. Celada, A. Panousopoulou, P. Tsakalides, and B. Beferull-Lozano, *Signal and Data Processing Techniques for Industrial Cyber-Physical Systems*, ser. Cyber-Physical Systems: From Theory to Practice, D. B. Rawat, J. Rodrigues, and I. Stojmenovic (Eds.). USA: CRC Press, 2015.
- [124] R. Du, L. Gkatzikis, C. Fischione, and M. Xiao, “Energy efficient sensor activation for water distribution networks based on compressive sensing,” *IEEE Journal on Selected Areas in Communications*, vol. 33, no. 12, pp. 2997–3010, Dec. 2015.
- [125] M. Giannopoulos, S. Savvaki, G. Tsagkatakis, and P. Tsakalides, “Application of tensor and matrix completion on environmental sensing data,” 2017.
- [126] A. Aggarwal, *Managing and Mining Uncertain Data*. Springer, 2009.
- [127] T. Thanh, P. Liping, D. Yanlei, M. Andrew, and L. Anna, “CLARO: Modeling and processing uncertain data streams,” *The VLDB Journal*, vol. 21, no. 5, pp. 651–676, 2012.
- [128] M. Yeh, K. Wu, P. Yu, and M. Chen, “PROUD: a probabilistic approach to processing similarity queries over uncertain data streams,” 2009.
- [129] M. Datar, A. Gionis, P. Indyk, and R. Motwani, “Maintaining stream statistics over sliding windows,” 2002.
- [130] J. Gehrke, F. Korn, and D. Srivastava, “On computing correlated aggregates over continual data streams,” 2001.

- [131] Y. Zhu and D. Shasha, “StatStream: Statistical monitoring of thousands of data streams in real time,” 2002.
- [132] K. Ishikawa and J. Loftus, *Introduction to Quality Control*. Tokyo: 3A Corporation, 1990.
- [133] I. Farrance and R. Frenkel, “Uncertainty of measurement: A review of the rules for calculating uncertainty components through functional relationships,” *Clinical Biochemist Reviews*, vol. 33, no. 2, pp. 49–75, 2012.
- [134] B. Taylor and C. Kuyatt, “Guidelines for evaluating and expressing the uncertainty of NIST measurement results,” NIST Technical Note 1297, Aug. 1994.
- [135] E. J. Gumbel, *Statistics of Extremes*. Courier Dover Publications, 2004.
- [136] J. Pickands, “Statistical inference using extreme order statistics,” *The Annals of Statistics*, vol. 3, no. 1, pp. 119–131, 1975.
- [137] L. De Haan and A. Ferreira, *Extreme Value Theory: An Introduction*. Springer, 2006.
- [138] Y. Sakurai, S. Papadimitriou, and C. Faloutsos, “BRAID: Stream mining through group lag correlations,” 2005.
- [139] A. F. Colombo, B. Lee, and W. Karneya, “A selective literature review of transient-based leak detection methods,” *J. Hydro-environment Res.*, vol. 2, no. 4, pp. 212–227, apr 2009.
- [140] S. G. Buchberger and G. Nadimpalli, “Leak Estimation in Water Distribution Systems by Statistical Analysis of Flow Readings,” *J. Water Resour. Plan. Manag.*, vol. 130, no. 4, pp. 321–329, jul 2004.
- [141] J. Almandoz, E. Cabrera, F. Arregui, E. Cabrera, and R. Cobacho, “Leakage Assessment through Water Distribution Network Simulation,” *J. Water Resour. Plan. Manag.*, vol. 131, no. 6, pp. 458–466, nov 2005.
- [142] R. H. Covas, D. and D. A. A.B., “Standing Wave Difference Method for Leak Detection in Pipeline Systems,” *J. Hydraul. Eng.*, vol. 131, no. 12, pp. 1106–1116, dec 2005.
- [143] R. Puust, Z. Kapelan, D. Savic, and T. Koppel, “Probabilistic Leak Detection in Pipe Networks Using the SCEM-UA Algorithm,” in *Water Distrib. Syst. Anal. Symp. 2006*. Reston, VA: American Society of Civil Engineers, mar 2006, pp. 1–12.
- [144] J. Ragot and D. Maquin, “Fault measurement detection in an urban water supply network,” *J. Process Control*, vol. 16, no. 9, pp. 887–902, oct 2006.
- [145] D. C. Morais and A. T. de Almeida, “Group decision-making for leakage management strategy of water network,” *Resour. Conserv. Recycl.*, vol. 52, no. 2, pp. 441–459, dec 2007.
- [146] O. Giustolisi, D. Savic, and Z. Kapelan, “Pressure-Driven Demand and Leakage Simulation for Water Distribution Networks,” *J. Hydraul. Eng.*, vol. 134, no. 5, pp. 626–635, may 2008.
- [147] J. Izquierdo, P. Lopez, F. Martinez, and R. Perez, “Fault detection in water supply systems using hybrid (theory and data-driven) modelling,” *Math. Comput. Model.*, vol. 46, no. 3-4, pp. 341–350, aug 2007.
- [148] R. Perez, V. Puig, J. Pascual, J. Quevedo, E. Landeros, and A. Peralta, “Methodology for leakage isolation using pressure sensitivity analysis in water distribution networks,” *Control Eng. Pract.*, vol. 19, no. 10, pp. 1157–1167, oct 2011.

- [149] R. Perez, V. Puig, J. Pascual, A. Peralta, E. Landeros, and L. Jordanas, “Pressure sensor distribution for leak detection in Barcelona water distribution network,” *Water Sci. Technol. Water Supply*, vol. 9, no. 6, p. 715, dec 2009.
- [150] M. Casillas, V. Puig, L. E. Garza-Castano, and A. Rosich, “Optimal Sensor Placement for Leak Location in Water Distribution Networks Using Genetic Algorithms,” *Sensors*, vol. 13, no. 11, pp. 14 984–15 005, nov 2013.
- [151] J. Vento and V. Puig, “Leak Detection and Isolation in Pressurized Water Pipe Networks using Interval LPV Models,” 2009, pp. 36–41.
- [152] J. Blesa, V. Puig, J. Saludes, and J. Vento, “Leak Detection, Isolation and Estimation in Pressurized Water Pipe Networks using LPV Models and Zonotopes,” *IFAC Proc. Vol.*, vol. 43, no. 14, pp. 36–41, sep 2010.
- [153] J. Gertler, J. Romera, V. Puig, and J. Quevedo, “Leak detection and isolation in water distribution networks using principal component analysis and structured residuals,” in *2010 Conf. Control Fault-Tolerant Syst.* IEEE, oct 2010, pp. 191–196.
- [154] R. Perez, G. Sanz, V. Puig, J. Quevedo, M. A. Cuguero Escofet, F. Nejjari, J. Meseguer, G. Cembrano, J. M. Mirats Tur, and R. Sarrate, “Leak Localization in Water Networks: A Model-Based Methodology Using Pressure Sensors Applied to a Real Network in Barcelona [Applications of Control],” *IEEE Control Syst.*, vol. 34, no. 4, pp. 24–36, aug 2014.
- [155] M. S. Islam, R. Sadiq, M. J. Rodriguez, H. Najjaran, A. Francisque, and M. Hoorfar, “Water distribution system failure: a framework for forensic analysis,” *Environ. Syst. Decis.*, vol. 34, no. 1, pp. 168–179, mar 2014.
- [156] I. Okeya, Z. Kapelan, C. Hutton, and D. Naga, “Online Burst Detection in a Water Distribution System Using the Kalman Filter and Hydraulic Modelling,” *Procedia Eng.*, vol. 89, pp. 418–427, jan 2014.
- [157] M. Romano, Z. Kapelan, and D. A. Savić, “Automated Detection of Pipe Bursts and Other Events in Water Distribution Systems,” *J. Water Resour. Plan. Manag.*, vol. 140, no. 4, pp. 457–467, apr 2014.
- [158] D. G. Eliades and M. M. Polycarpou, “Leakage fault detection in district metered areas of water distribution systems,” *J. Hydroinformatics*, vol. 14, no. 4, p. 992, oct 2012.
- [159] C. Heracleous, E. E. Miciolino, R. Setola, F. Pascucci, D. G. Eliades, G. Ellinas, C. G. Panayiotou, and M. M. Polycarpou, “Critical Infrastructure Online Fault Detection: Application in Water Supply Systems,” in *Int. Conf. Crit. Inf. Infrastructures Secur.* Springer, 2016, pp. 94–106.
- [160] G. Sanz, R. Perez, Z. Kapelan, and D. Savic, “Leak Detection and Localization through Demand Components Calibration,” *J. Water Resour. Plan. Manag.*, vol. 142, no. 2, p. 04015057, feb 2016.
- [161] S. J. Yim and Y. H. Choi, “Fault-tolerant event detection using two thresholds in wireless sensor networks,” in *2009 15th IEEE Pacific Rim International Symposium on Dependable Computing*, Nov 2009, pp. 331–335.
- [162] W. Xue, Q. Luo, and H. Wu, “Pattern-based event detection in sensor networks,” *Distrib. Parallel Databases*, vol. 30, no. 1, pp. 27–62, Feb. 2012.

- [163] D. Byer and K. H. Carlson, “Expanded summary: Real-time detection of intentional chemical contamination in the distribution system,” *Journal (American Water Works Association)*, vol. 97, no. 7, pp. 130–133, 2005.
- [164] X. R. Wang, J. T. Lizier, O. Obst, M. Prokopenko, and P. Wang, “Spatiotemporal anomaly detection in gas monitoring sensor networks,” in *Wireless Sensor Networks*, R. Verdone, Ed. Berlin, Heidelberg: Springer Berlin Heidelberg, 2008, pp. 90–105.
- [165] L. Uusitalo, “Advantages and challenges of bayesian networks in environmental modelling,” *Ecological Modelling*, vol. 203, no. 3, pp. 312 – 318, 2007.
- [166] D. Piao, P. G. Menon, and O. J. Mengshoel, “Computing probabilistic optical flow using markov random fields,” in *Computational Modeling of Objects Presented in Images. Fundamentals, Methods, and Applications*, Y. J. Zhang and J. M. R. S. Tavares, Eds. Cham: Springer International Publishing, 2014, pp. 241–247.
- [167] L. Perelman and A. Ostfeld, “Bayesian networks for source intrusion detection,” *Journal of Water Resources Planning and Management*, vol. 139, no. 4, pp. 426–432, 2013.
- [168] D. Hou, H. He, P. Huang, G. Zhang, and H. Loaiciga, “Detection of water-quality contamination events based on multi-sensor fusion using an extended dempster–shafer method,” *Measurement Science and Technology*, vol. 24, no. 5, p. 055801, 2013.
- [169] C. Kühnert, T. Bernard, I. M. Arango, and R. Nitsche, “Water quality supervision of distribution networks based on machine learning algorithms and operator feedback,” *Procedia Engineering*, vol. 89, pp. 189 – 196, 2014, 16th Water Distribution System Analysis Conference, WDSA2014.
- [170] Y. Mao, X. Chen, and Z. Xu, “Real-time event detection with water sensor networks using a spatio-temporal model,” in *Database Systems for Advanced Applications*, H. Gao, J. Kim, and Y. Sakurai, Eds. Cham: Springer International Publishing, 2016, pp. 194–208.
- [171] D. Hou, S. Liu, J. Zhang, F. Chen, P. Huang, and G. Zhang, “Online monitoring of water-quality anomaly in water distribution systems based on probabilistic principal component analysis by uv-vis absorption spectroscopy,” *Journal of Spectroscopy*, vol. 2014, p. 9, 2014.
- [172] D. Kroll and K. King, *Laboratory and Flow Loop Validation and Testing of the Operational Effectiveness of an On-line Security Platform for the Water Distribution System*, 2006.
- [173] J. Arad, M. Housh, L. Perelman, and A. Ostfeld, “A dynamic thresholds scheme for contaminant event detection in water distribution systems,” *Water Research*, vol. 47, no. 5, pp. 1899 – 1908, 2013.
- [174] D. G. Eliades and M. M. Polycarpou, “A fault diagnosis and security framework for water systems,” *IEEE Transactions on Control Systems Technology*, vol. 18, no. 6, pp. 1254–1265, Nov 2010.
- [175] R. Murray, T. Haxton, S. McKenna, D. Hart, K. Klise, M. Koch, E. Vugrin, S. Martin, M. Wilson, and V. Cruze, “Water quality event detection systems for drinking water contamination warning systems - development, testing, and application of canary,” *US Environmental Protection Agency, Office of Research and Development, National Homeland Security Research Center, Cincinnati, Ohio, USA*, 2010.

- [176] S. Murray, M. Ghazali, and E. A. McBean, “Real-time water quality monitoring: Assessment of multisensor data using bayesian belief networks,” *Journal of Water Resources Planning and Management*, vol. 138, no. 1, pp. 63–70, 2012.
- [177] D. G. Eliades, D. Stavrou, S. G. Vrachimis, C. G. Panayiotou, and M. M. Polycarpou, “Contamination event detection using multi-level thresholds,” in *Proceedings of 13th Computing and Control for the Water Industry Conference, CCWI 2015*, vol. 119, no. 1, 2015, pp. 1429–1438.
- [178] M. W. Koch and S. A. McKenna, “Distributed sensor fusion in water quality event detection,” *Journal of Water Resources Planning and Management*, vol. 137, no. 1, pp. 10–19, 2011.
- [179] E. Karami, F. M. Bui, and H. H. Nguyen, “Multisensor data fusion for water quality monitoring using wireless sensor networks,” in *2012 Fourth International Conference on Communications and Electronics (ICCE)*, Aug 2012, pp. 80–85.
- [180] Y. Mao, H. Qi, P. Ping, and X. Li, “Contamination event detection with multivariate time-series data in agricultural water monitoring,” *Sensors*, vol. 17, no. 12, 2017.
- [181] C. J. Hutton, Z. Kapelan, L. Vamvakeridou-Lyroudia, and D. A. Savic, “Dealing with uncertainty in water distribution system models: A framework for real-time modeling and data assimilation,” *Water Resources Planning and Management*, vol. 140, pp. 169–183, 2014.
- [182] D. A. Savic, Z. S. Kapelan, and P. M. Jonkergouw, “Quo vadis water distribution model calibration?” *Urban Water Journal*, vol. 6, pp. 3–22, 2009.
- [183] D. Kang and K. Lansey, “Demand and roughness estimation in water distribution systems,” *Water Resources Planning and Management*, vol. 137, pp. 20–30, 2011.
- [184] J. W. Davidson and F. J. C. Bouchart, “Adjusting nodal demands in SCADA constrained real-time water distribution network models,” *Journal of Hydraulic Engineering*, vol. 132, pp. 102–110, 2006.
- [185] D. S. Kang, M. Pasha, and K. Lansey, “Approximate methods for uncertainty analysis of water distribution systems,” *Urban Water Journal*, vol. 6, pp. 233–249, 2009.
- [186] J. H. Andersen, R. S. Powell, and J. F. Marsh, “Constrained state estimation with applications in water distribution network monitoring,” *International Journal of Systems Science*, vol. 32, pp. 807–816, 2001.
- [187] S. G. Vrachimis, D. G. Eliades, and M. M. Polycarpou, “The backtracking uncertainty bounding algorithm for chlorine sensor fault detection,” in *Proceedings of 13th Computing and Control for the Water Industry Conference, CCWI 2015*, vol. 119, no. 1, 2015, pp. 613–622.
- [188] A. Bargiela and G. D. Hainsworth, “Pressure and flow uncertainty in water systems,” *Water Resources Planning and Management*, vol. 115, no. 2, pp. 212–229, 1989.
- [189] B. Gabrys and A. Bargiela, “Integrated neural based system for state estimation and confidence limit analysis in water networks,” in *Proceedings of European Simulation Symposium ESS’96*, 1997, pp. 398–402.
- [190] C. T. Arsene, D. Al-Dabass, and J. Hartley, “Confidence limit analysis of water distribution systems based on a least squares loop flows state estimation technique,” in *Proceedings of 2011 UKSim 5th European Symposium on Computer Modeling and Simulation*. IEEE, 2011, pp. 94–101.

- [191] A. Bargiela, W. Pedrycz, and M. Tanaka, "A study of uncertain state estimation," *IEEE Transactions on Systems, Man, and Cybernetics Part A: Systems and Humans.*, vol. 33, no. 3, pp. 288–301, 2003.
- [192] A. Whittle, M. Allen, A. Preis, and M. Iqbal, "Sensor networks for monitoring and control of water distribution systems," 2013.
- [193] "Building a smart city ecosystem for third party innovation in the city of heraklion."
- [194] Echologics, "United water new jersey discovers large leak on 42-inch water main with echologics transmission main leak detection service," Echologics, 6295 Northam Drive, Unit 1 Mississauga, ON L4V 1W8 Canada, Tech. Rep.
- [195] Trunkminder, "Thames water," Syrinix, UK, Syrinix Ltd, Hethel Engineering Centre Chapman Way, Hethel, Norwich, Tech. Rep.
- [196] Gutermann, "Permanent leakage monitoring is the fastest way to reduce leakage," Guter-mann, Gutermann AG-Sihlbruggstrasse 140, 6340 Baar, Switzerland, Tech. Rep.
- [197] Isoil, "Installing flow meters in asia," Isoil, soil Industria SpA, Via F.lli Gracchi, 27 I-20092 Cinisello Balsamo (MI) Italy, Tech. Rep., 2006.
- [198] S. Electric, "Managing scarce water integrated use of new technologies helps abu dhabi water and electricity authority (adwea) manage water resources much more efficient." Schneider Electric, Tech. Rep.
- [199] S. M. GmbH, "Early warning system monitors bratislava's water supply, ground water monitoring." scan Messtechnik GmbH, Brigittagasse 22-24 1200 Vienna, Austria, Tech. Rep.
- [200] Kisters, "Philadelphia water department online water quality monitoring project." Kisters, North America Inc. 1520 Eureka Road, Suite 102 Roseville, CA 95661, Tech. Rep.
- [201] Hach, "Disinfection in drinking water: Choosing the right chlorine analyser for your application." Hach, Hach Company, P.O. Box 389 Loveland, Colorado 80539-0389, Tech. Rep., 2015.
- [202] K. Lansey and L. W. Mays, *Water distribution systems handbook*. McGraw-Hill New York, 2000, ch. Hydraulics of Water Distributino Systems, pp. 4.1–4.29.
- [203] E. Todini and S. Pilati, "A gradient algorithm for the analysis of pipe networks," in *Proceedings of International Conference on Computer Applications for Water Supply and Distribution*, 1987.
- [204] L. Rossman, *EPANET 2 Users Manual*, National Risk Management Research Laboratory, Office of Research and Development, U.S. Enviromental Protection Agency, Cincinnati, OH 45268, 2000.
- [205] E. Todini and S. Pilati, "A gradient method for the analysis of pipe networks," in *Proc.of Computer Applications for Water Supply and Distribution*, 1987.
- [206] R. LeVeque, *Nonlinear Conservation Laws and Finite Volume Methods*. Berlin, Germany: Springer, 1998, pp. 1–159.
- [207] F. Shang, J. Uber, and M. Polycarpou, "Input-output model of water quality in water distribution systems," in *Water Resources 2000*, R. H. Hotchkiss and M. Glade, Eds., vol. 104, no. 40517. ASCE, 2000, pp. 215–215.

- [208] J. Vasconcelos, L. Rossman, W. Grayman, P. Boulos, and R. Clark, “Kinetics of Chlorine Decay,” *Journal American Water Works Association*, vol. 89, no. 7, pp. 54–65, 1997.
- [209] F. Hua, J. R. West, R. A. Barker, and C. F. Forster, “Modelling of chlorine decay in municipal water supplies,” *Water Research*, vol. 33, no. 12, pp. 2735 – 2746, 1999.
- [210] J. C. Powell, J. R. West, N. B. Hallam, C. F. Forster, and J. Simms, “Performance of various kinetic models for chlorine decay,” *ASCE Journal of Water Resources Planning and Management*, vol. 126, no. 1, pp. 13–20, 2000.
- [211] R. M. Clark, L. A. Rossman, M. Sivaganesan, and K. M. Schenck, *Controlling Disinfection By-Products and Microbial Contaminants in Drinking Water*. USEPA, Cincinnati, 2002, ch. Modeling chlorine decay and the formation of disinfection by products (DBPS) in drinking water.
- [212] D. L. Boccelli, M. E. Tryby, J. G. Uber, and R. S. Summers, “A reactive species model for chlorine decay and thm formation under rechlorination conditions,” *Water Research*, vol. 37, no. 11, pp. 2654–2666, Jun. 2003.
- [213] S. McKenna, B. Waanders, C. Laird, S. Buchberger, Z. Li, and R. Janke, “Source location inversion and the effect of stochastically varying demand,” in *Proc. of World Water and Environmental Resources*, 2005, pp. 1–10.
- [214] K. A. Umberg, “Performance evaluation of real-time event detection algorithms,” Master’s thesis, University of Cincinnati, 2006.
- [215] M. Dodd, N. Vu, A. Ammann, R. Kissner, H. Pham, M. Berg, and U. von Gunten, “Kinetics and mechanistic aspects of As (III) oxidation by aqueous chlorine, chloramines, and ozone: Relevance to drinking water treatment,” *Environ. Sci. Technol*, vol. 40, no. 10, pp. 3285–3292, 2006.
- [216] Q. Zhang and S. Pehkonen, “Oxidation of diazinon by aqueous chlorine: kinetics, mechanisms, and product studies,” *J. Agric. Food Chem*, vol. 47, no. 4, pp. 1760–1766, 1999.
- [217] L. A. Rossman, “The EPANET Programmer’s Toolkit for Analysis of Water Distribution Systems,” in *ASCE 29th Annual Water Resources Planning and Management Conference*, 1999, pp. 39–48.
- [218] M. Polycarpou, J. Uber, Z. Wang, F. Shang, and M. Brdys, “Feedback control of water quality,” *IEEE Control Systems Magazine*, vol. 22, no. 3, pp. 68–87, June 2002.
- [219] Z. Wang, M. Polycarpou, J. Uber, and F. Shang, “Adaptive control of water quality in water distribution networks,” *IEEE Transactions on Control Systems Technology*, vol. 14, no. 1, pp. 149–156, 2006.
- [220] T. Walski, W. Bezts, E. Posluszny, M. Weir, and B. Whitman, “Understanding the Hydraulics of Water Distribution System Leaks,” 2004.
- [221] M. Farley and S. Trow, *Losses in water distribution networks: a practitioner’s guide to assessment, monitoring and control*. London: IWA, 2003.
- [222] R. Pilcher, S. Hamilton, H. Chapman, D. Field, B. Ristovski, and S. Stapely, “Guidance notes on leak detection and repair,” 2007.

- [223] T. Jamasb and M. Pollitt, “Security of supply and regulation of energy networks,” *Energy Policy*, vol. 36, no. 12, pp. 4584–4589, Dec. 2008.
- [224] R. Wright, E. Abraham, P. Pappas, and I. Stoianov, “Control of water distribution networks with dynamic DMA topology using strictly feasible sequential convex programming: WATER DISTRIBUTION NETWORKS WITH DYNAMIC TOPOLOGY,” *Water Resources Research*, vol. 51, no. 12, pp. 9925–9941, Dec. 2015.
- [225] H. Armand, I. Stoianov, and N. Graham, “Investigating the Impact of Sectorized Networks on Discoloration,” *Procedia Engineering*, vol. 119, pp. 407–415, 2015.
- [226] B. Farley, J. B. Boxall, and S. R. Mounce, “Optimal Locations of Pressure Meters for Burst Detection,” in *Water Distrib. Syst. Anal. 2008*. American Society of Civil Engineers, apr 2009, pp. 1–11.
- [227] J. Koelbl, D. Martinek, P. Martinek, C. Wallinger, D. Fuchs-Hanusch, H. Zangl, and A. Fuchs, “Multiparameter Measurements for Network Monitoring and Leak Localising.” Cape Town, SA: International Water Association, Apr. 2009, pp. 1–8.
- [228] D. D. Ediriweera and I. W. Marshall, “Monitoring water distribution systems: understanding and managing sensor networks,” *Drinking Water Engineering and Science*, vol. 3, no. 2, pp. 107–113, Sep. 2010.
- [229] M. Allen, A. Preis, M. Iqbal, S. Srirangarajan, H. B. Lim, L. Girod, and A. J. Whittle, “Real-Time In-Network Distribution System Monitoring to Improve Operational Efficiency,” *Journal AWWA*, vol. 103, no. 7, pp. 63–75, Jul. 2011.
- [230] A. J. Whittle, M. Allen, A. Preis, and M. Iqbal, “Sensor Networks for Monitoring and Control of Water Distribution Systems.” Hong Kong: The Hong Kong Polytechnic University, Dec. 2013, pp. 1–13.
- [231] i2O-i2O Water, “i2o-i2o Water,” 2018. [Online]. Available: <https://en.i2owater.com/solutions/>